Airborne SAR Interferometry

- Prof. Stefano Perna

Università degli Studi di Napoli Parthenope

IR0000032 – ITINERIS, Italian Integrated Environmental Research Infrastructures System
(D.D. n. 130/2022 - CUP B53C22002150006) Funded by EU - Next Generation EU PNRR-Mission 4 “Education and Research” - Component 2: “From research to business” - Investment 3.1: “Fund for the realisation of an integrated system of research and innovation infrastructures”

Finanziato dall'Unione europea NextGenerationEU

Ministero dell'Università e della Ricerca

Italiadomani

SUMMARY

Synthetic Aperture Radar (SAR)

Geometry

SAR Raw Data

Geometric Resolution

SAR focusing

SAR Interferometry (InSAR)

DInSAR

An Airborne InSAR experiment

Synthetic Aperture Radar (SAR)

All-weather and night&day observation capability

- **Passive** sensors use solar radiation (light) or the one emitted by the observed object as source of illumination. Typically they operate in the **optical** or **infrared**.

- **Active sensors** have their own source of illumination. Typically they operate in the **microwave**.

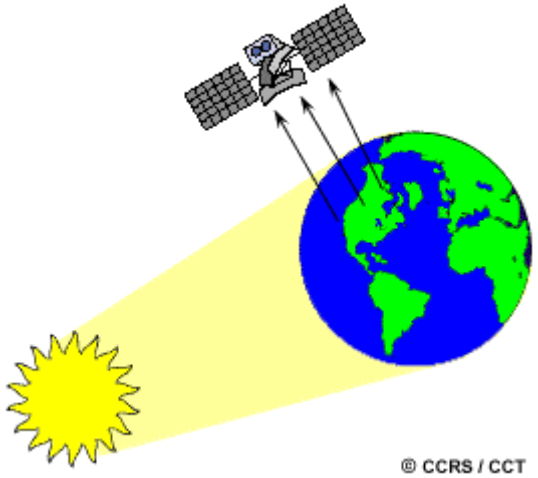

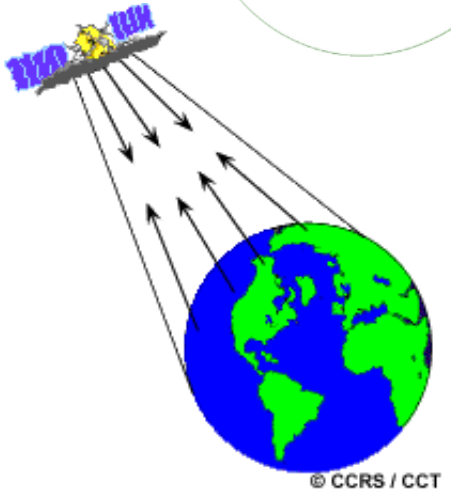

Synthetic Aperture Radar (SAR)

All-weather and night&day observation capability

Optical image

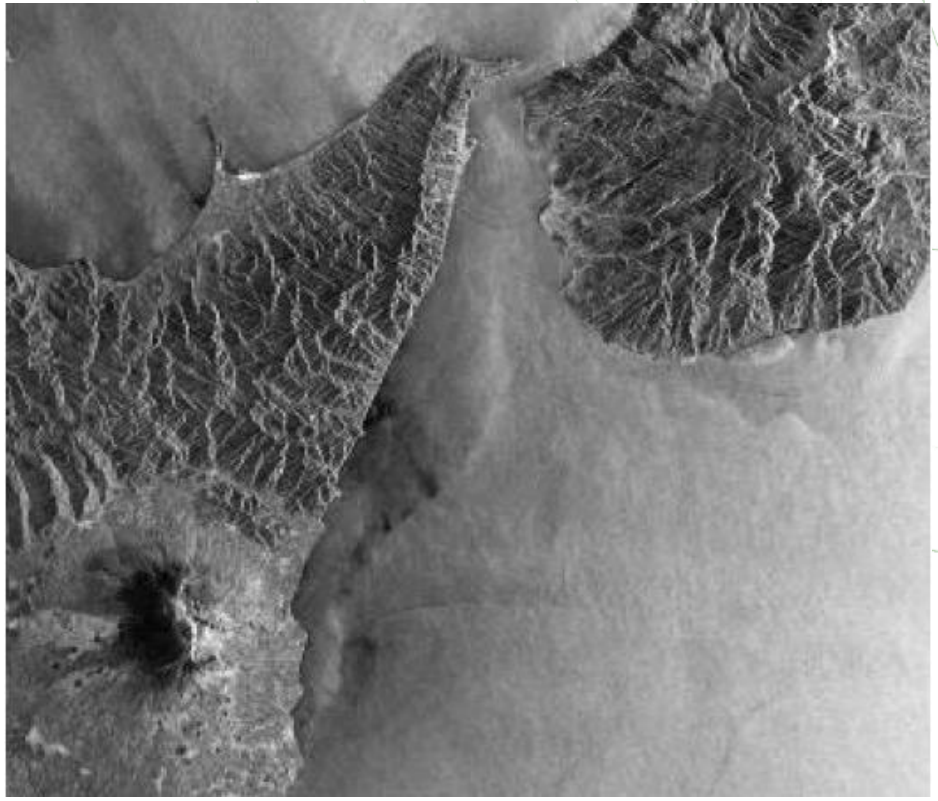

Radar (SAR) image

same acquisition time

Synthetic Aperture Radar (SAR)

All-weather and night&day observation capability

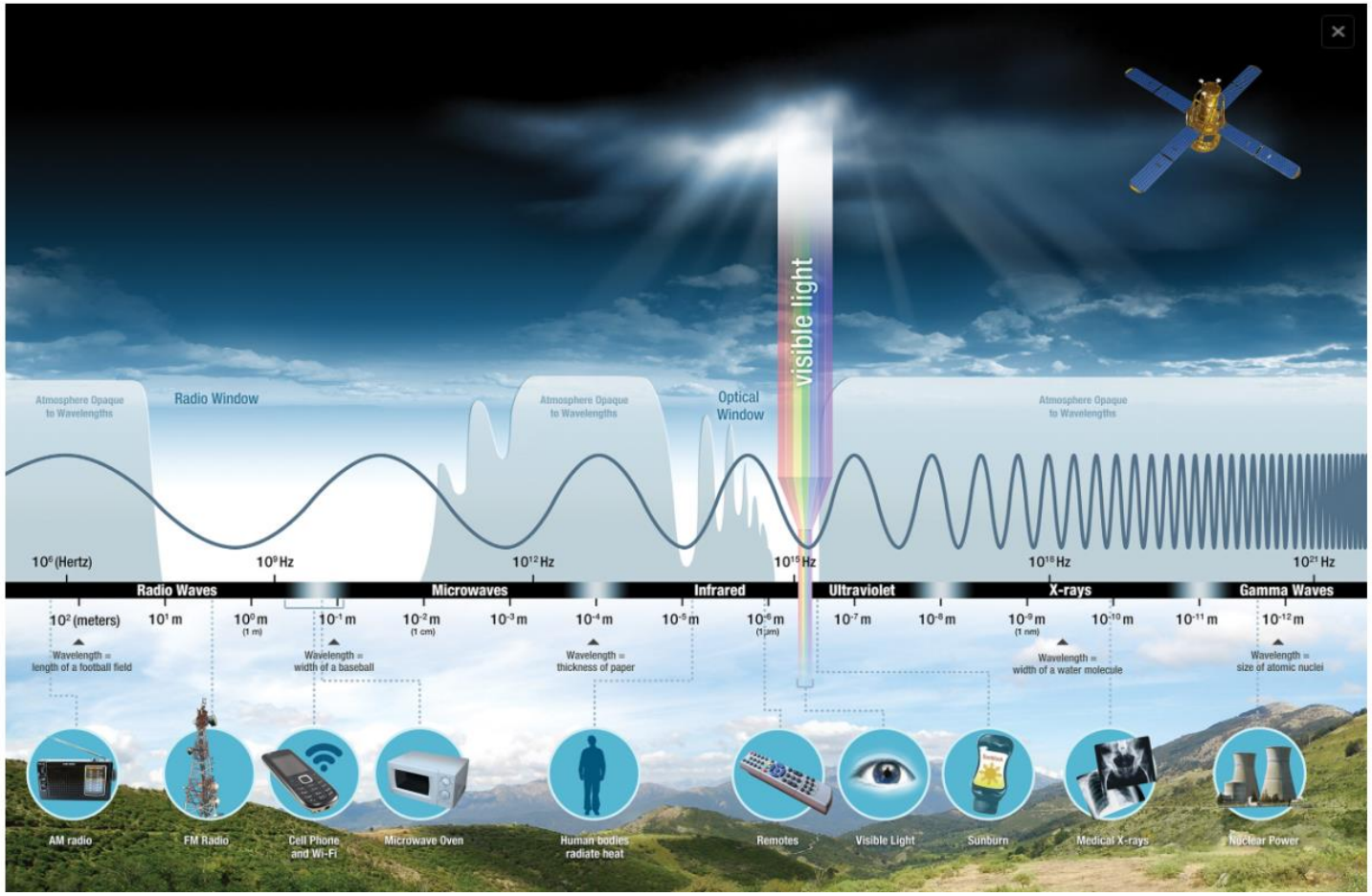

$$\lambda = \frac{c}{f_0}$$

f_0: frequenza
λ: lunghezza d'onda
c: velocità della luce (3×10^8 m/s)

Synthetic Aperture Radar (SAR)

Microwave frequencies for radar applications (IEEE* standard)

Band	Frequency	Wavelength
HF	3 - 30 MHz	100 - 10 m
VHF	30 - 300 MHz	10 - 1 m
P	300 - 1000 MHz	1 - 0.3 m
L	1 - 2 GHz	30 - 15 cm
S	2 - 4 GHz	15 - 7.5 cm
C	4 - 8 GHz	7.5 - 3.75 cm
X	8 - 12 GHz	3.75 - 2.5 cm
Ku	12 - 18 GHz	2.5 - 1.7 cm
K	18 - 27 GHz	1.7 - 1.1 cm
Ka	27 - 40 GHz	1.1 - 0.75 cm

***** **I**nstitute of **E**lectrical and **E**lectronic **E**ngineers

Synthetic Aperture Radar (SAR)

Microwave frequencies for radar applications (IEEE* standard)

Band	Frequency	Wavelength
HF	3 - 30 MHz	100 - 10 m
VHF	30 - 300 MHz	10 - 1 m
P	300 - 1000 MHz	1 - 0.3 m
L	1 - 2 GHz	30 - 15 cm
S	2 - 4 GHz	15 - 7.5 cm
C	4 - 8 GHz	7.5 - 3.75 cm
X	8 - 12 GHz	3.75 - 2.5 cm
Ku	12 - 18 GHz	2.5 - 1.7 cm
K	18 - 27 GHz	1.7 - 1.1 cm
Ka	27 - 40 GHz	1.1 - 0.75 cm

Most employed by SAR systems

***** **I**nstitute of **E**lectrical and **E**lectronic **E**ngineers

Synthetic Aperture Radar (SAR)

SAR APPLICATIONS

Synthetic Aperture Radar (SAR)

Acquisition geometry

Coherent sensors

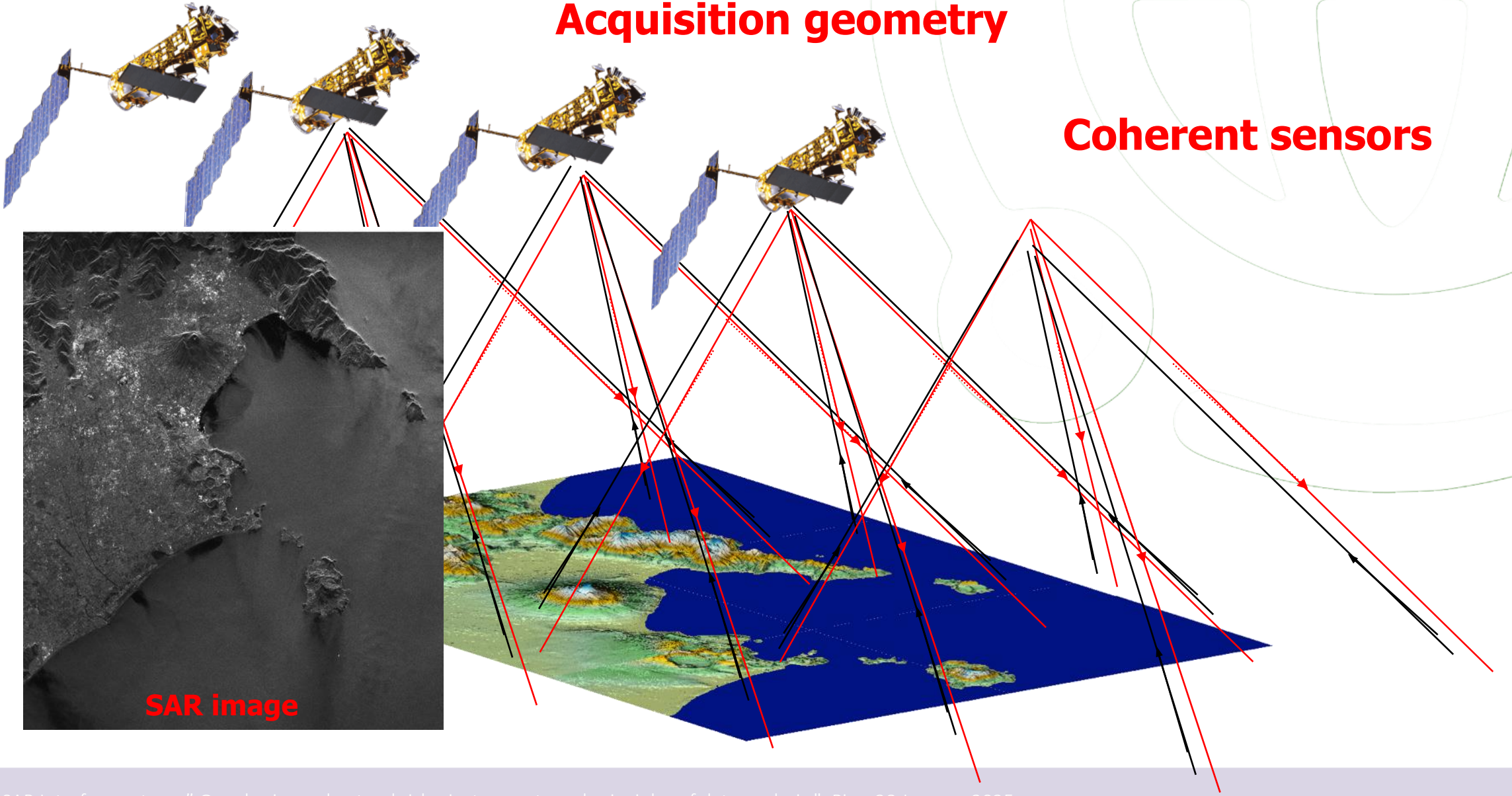

Synthetic Aperture Radar (SAR)

SAR configurations

Space

Aerial

Small aircrafts

Big aircrafts

Helicopters

UAV

Terrestrial

Cars

Rails

Synthetic Aperture Radar (SAR)

SAR configurations

Space

Aerial

Small aircrafts

Big aircrafts

Helicopters

UAV

Terrestrial

Cars

Rails

Operational flexibility

Planetary coverage

Synthetic Aperture Radar (SAR)

Some space-borne SAR missions

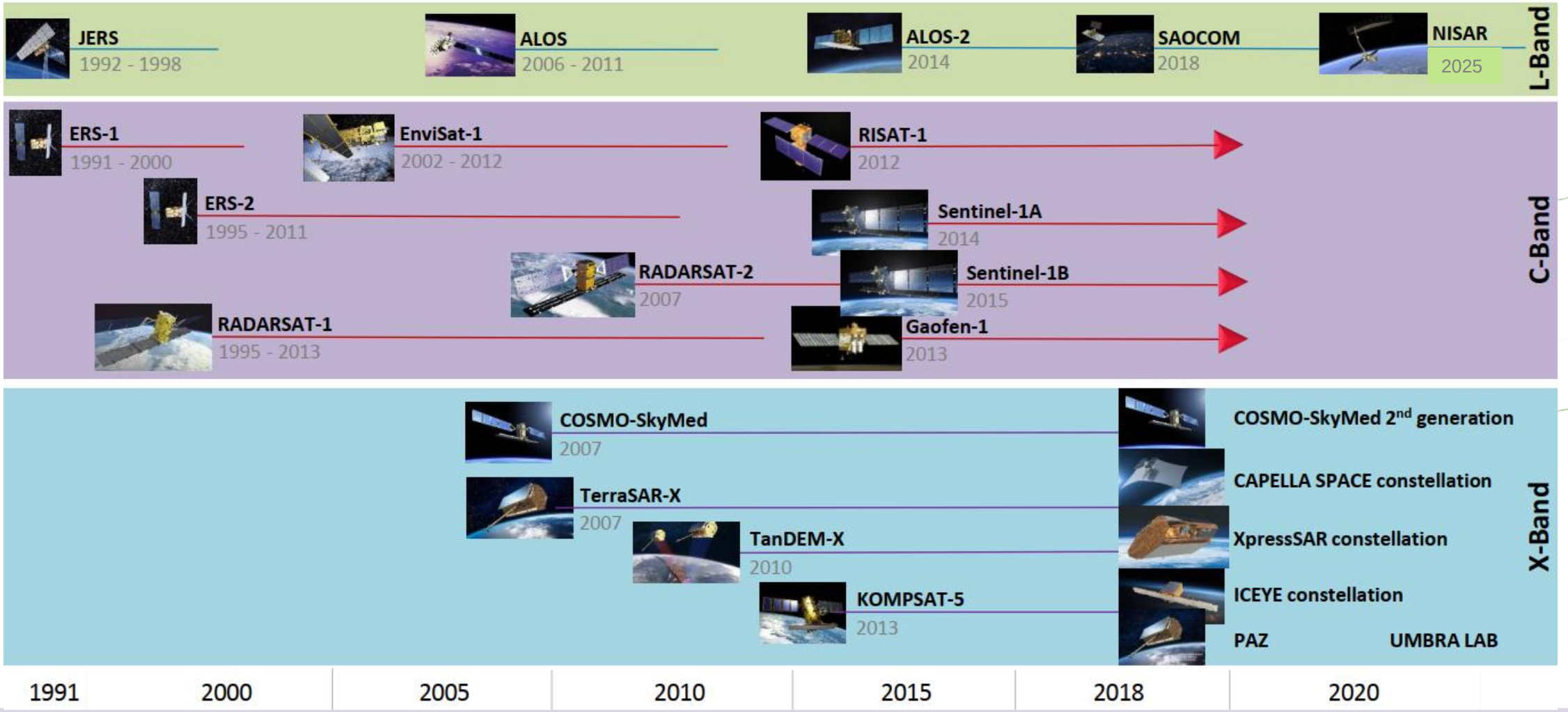

Synthetic Aperture Radar (SAR)

SAR configurations

Space

Aerial

Small aircrafts

Big aircrafts

Helicopters

UAV

Terrestrial

Cars

Rails

Operational flexibility

Planetary coverage

Synthetic Aperture Radar (SAR)

SAR configurations

Space

Aerial

Small aircrafts

Big aircrafts

Helicopters

UAV

Operational flexibility

Terrestrial

Cars

Rails

Planetary coverage

SUMMARY

Synthetic Aperture Radar (SAR)

Geometry

SAR Raw Data

Geometric Resolution

SAR focusing

SAR Interferometry (InSAR)

DInSAR

An Airborne InSAR experiment

Geometry

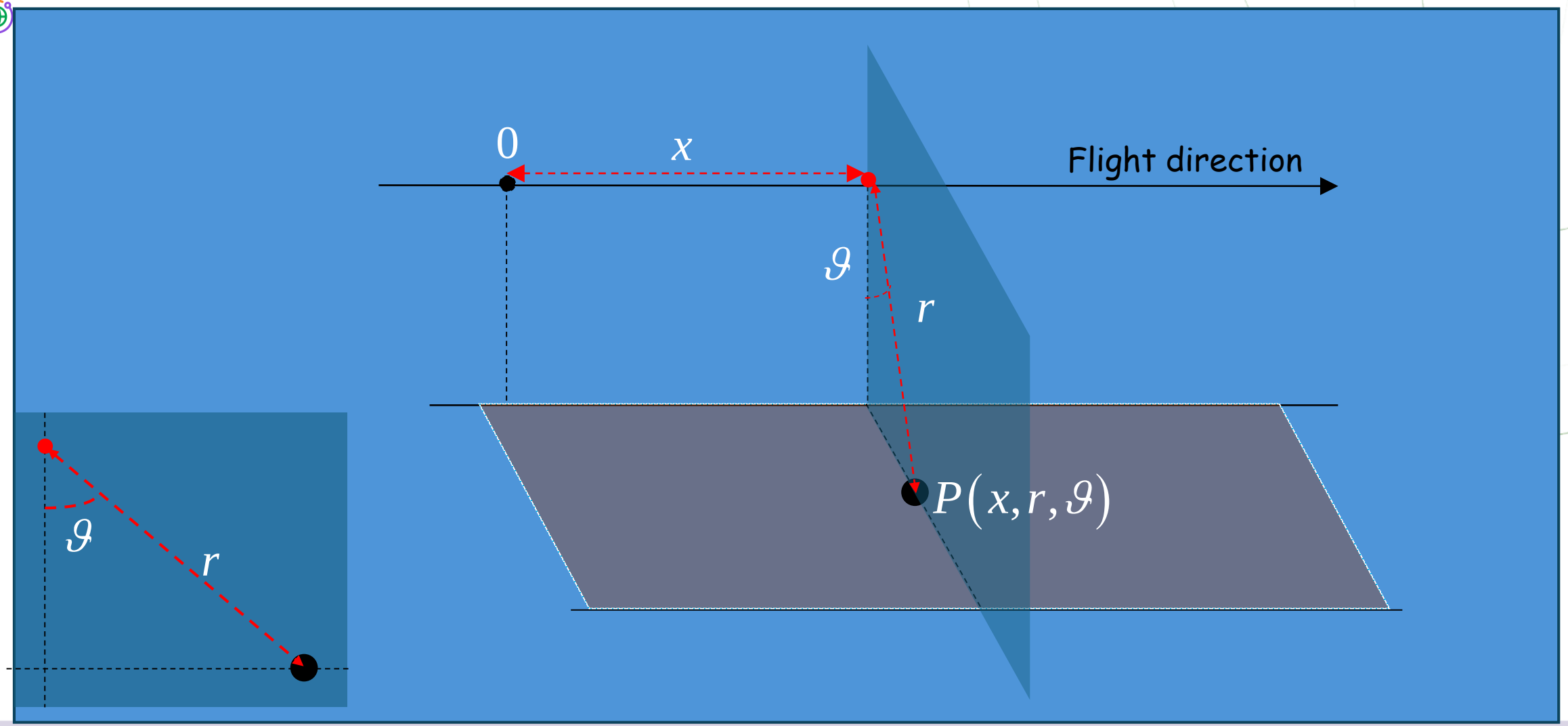

Geometry

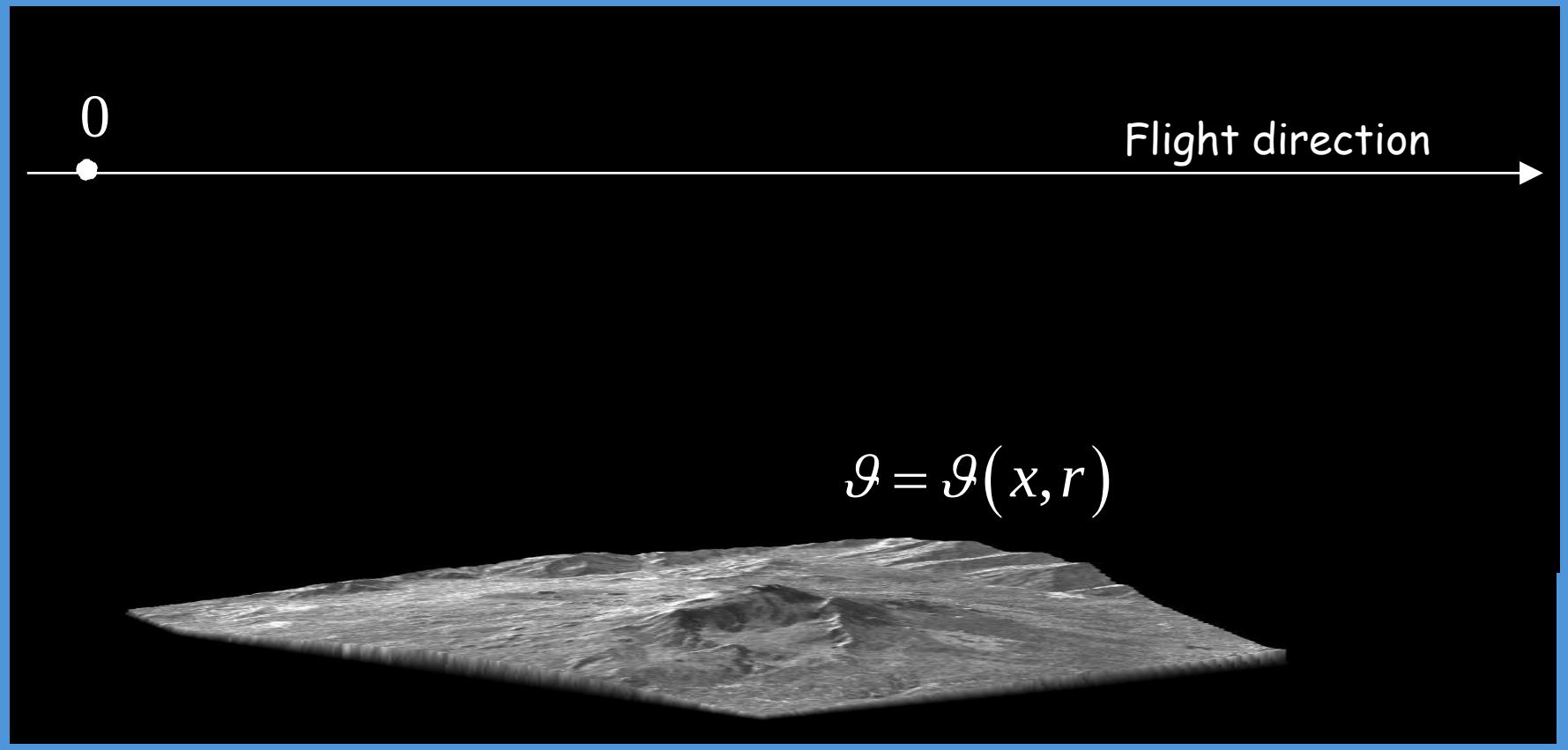

Geometry

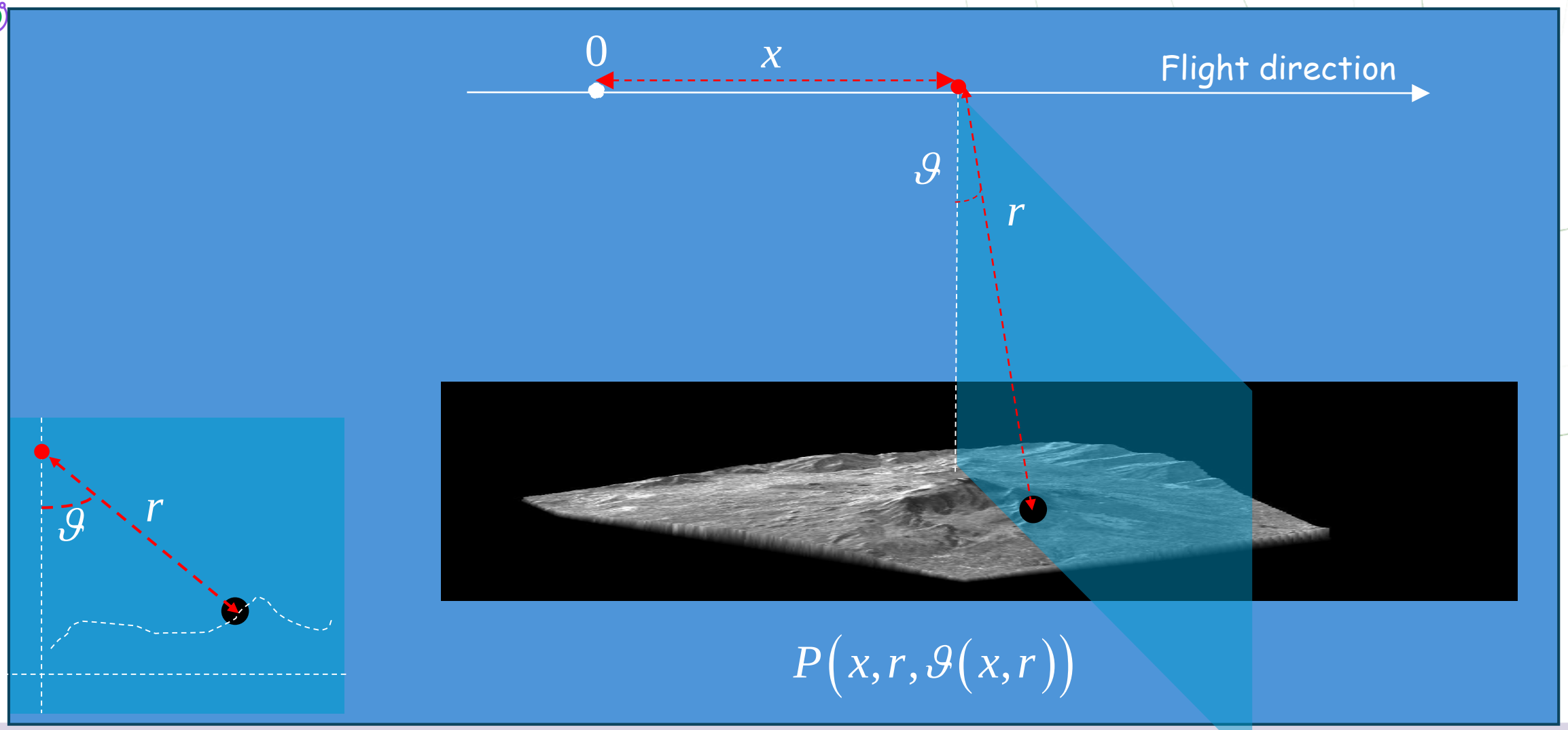
0
x
Flight direction
ϑ
r
ϑ
r
$P\left(x, r, \vartheta\left(x, r\right)\right)$

Geometry

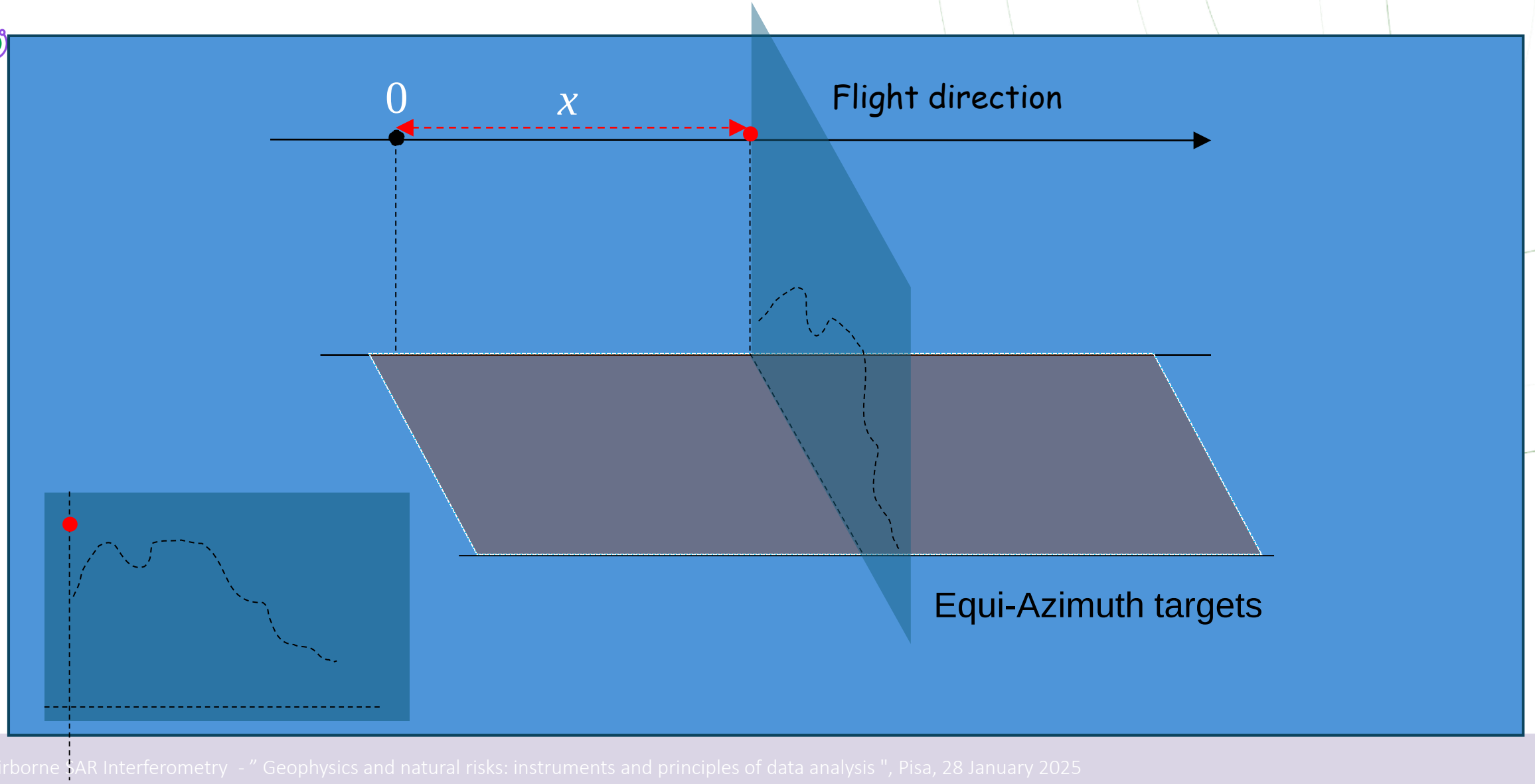

Geometry

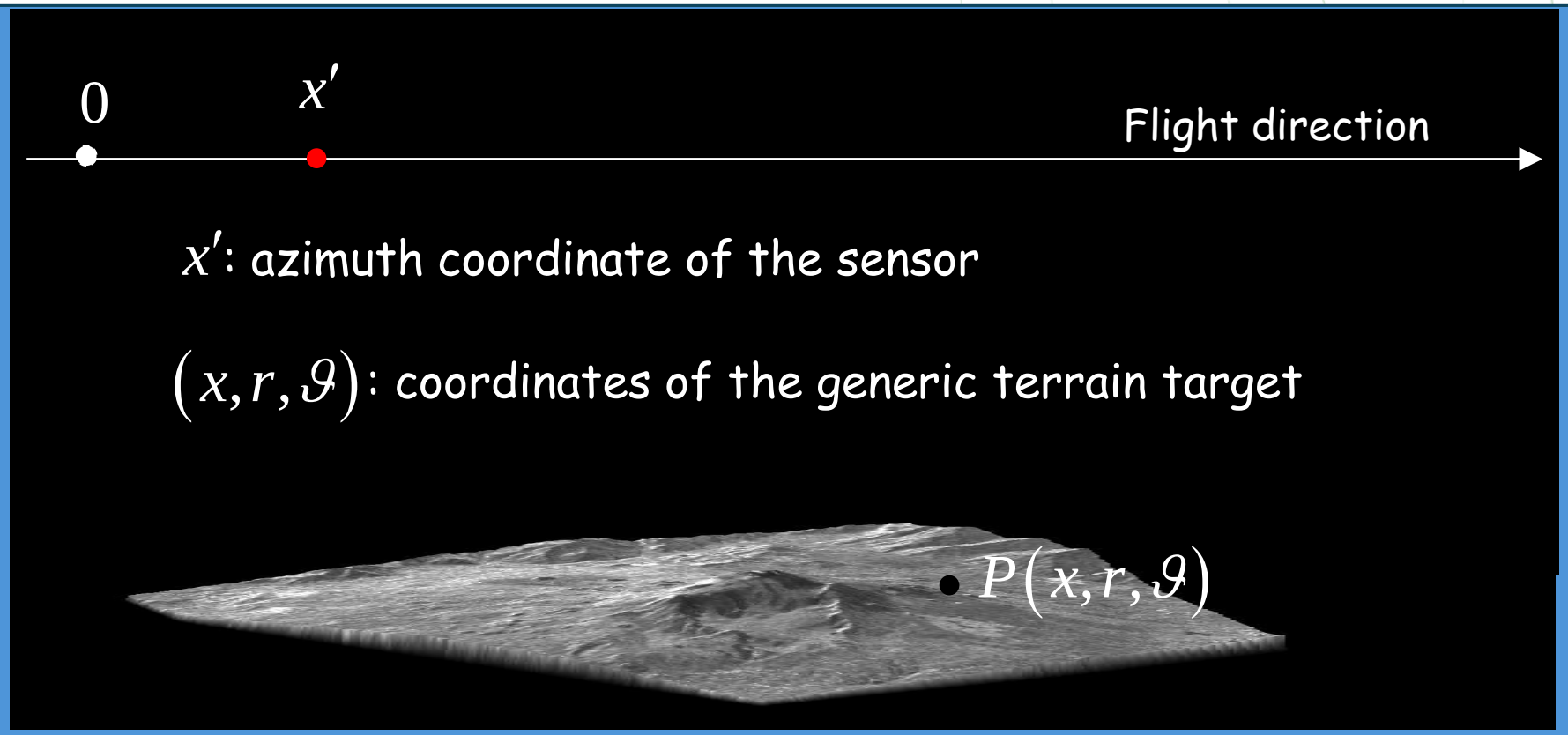

Cylindrical coordinates of the sensor : $(x', 0, \cdot)$

In the case of linear trajectory, the sensor position is defined by the sole azimuth coordinate

SUMMARY

Synthetic Aperture Radar (SAR)

Geometry

SAR Raw Data

Geometric Resolution

SAR focusing

SAR Interferometry (InSAR)

DInSAR

An Airborne InSAR experiment

SAR Raw Data

SAR raw data:

data collected onboard

SAR Raw Data

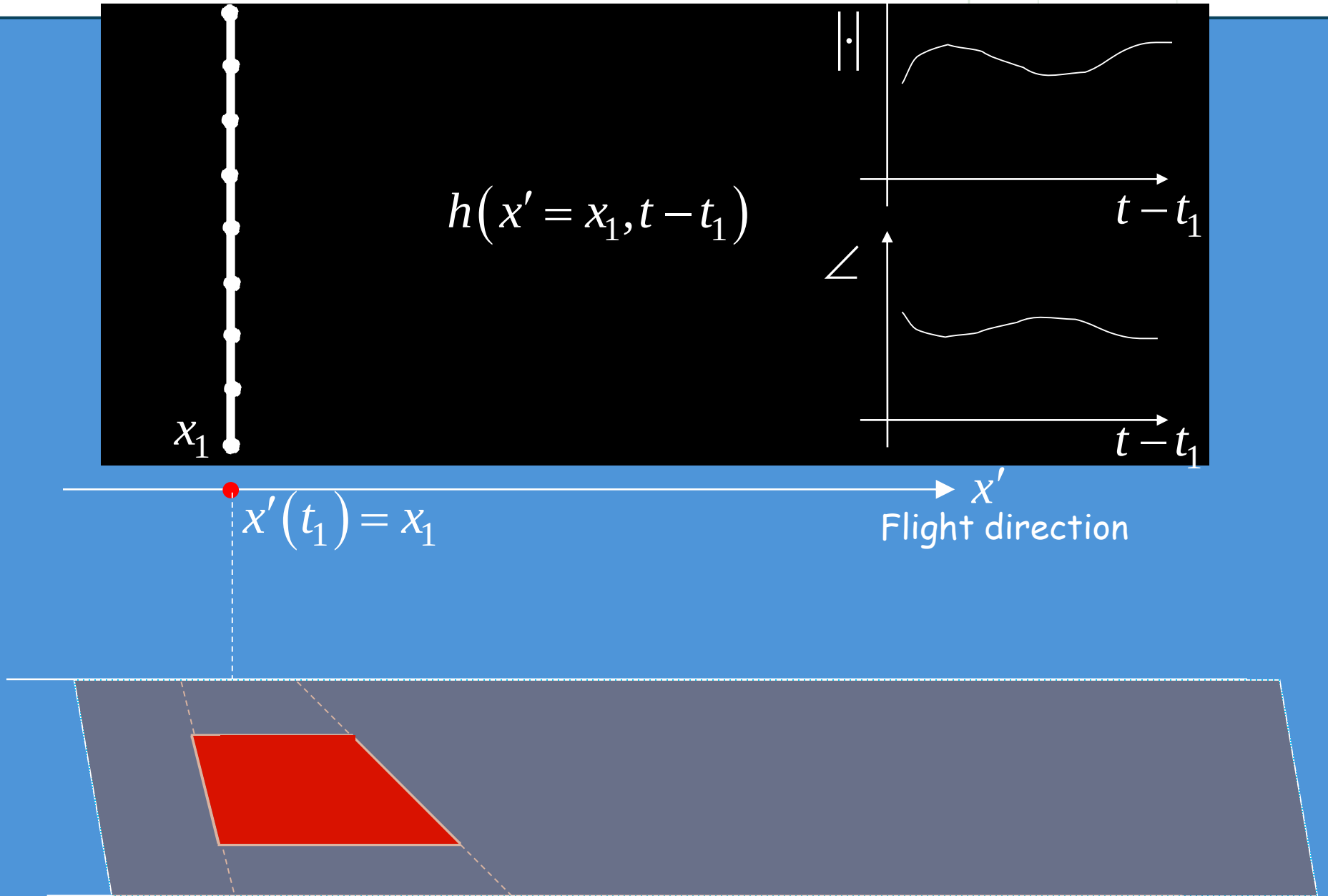

SAR Raw Data

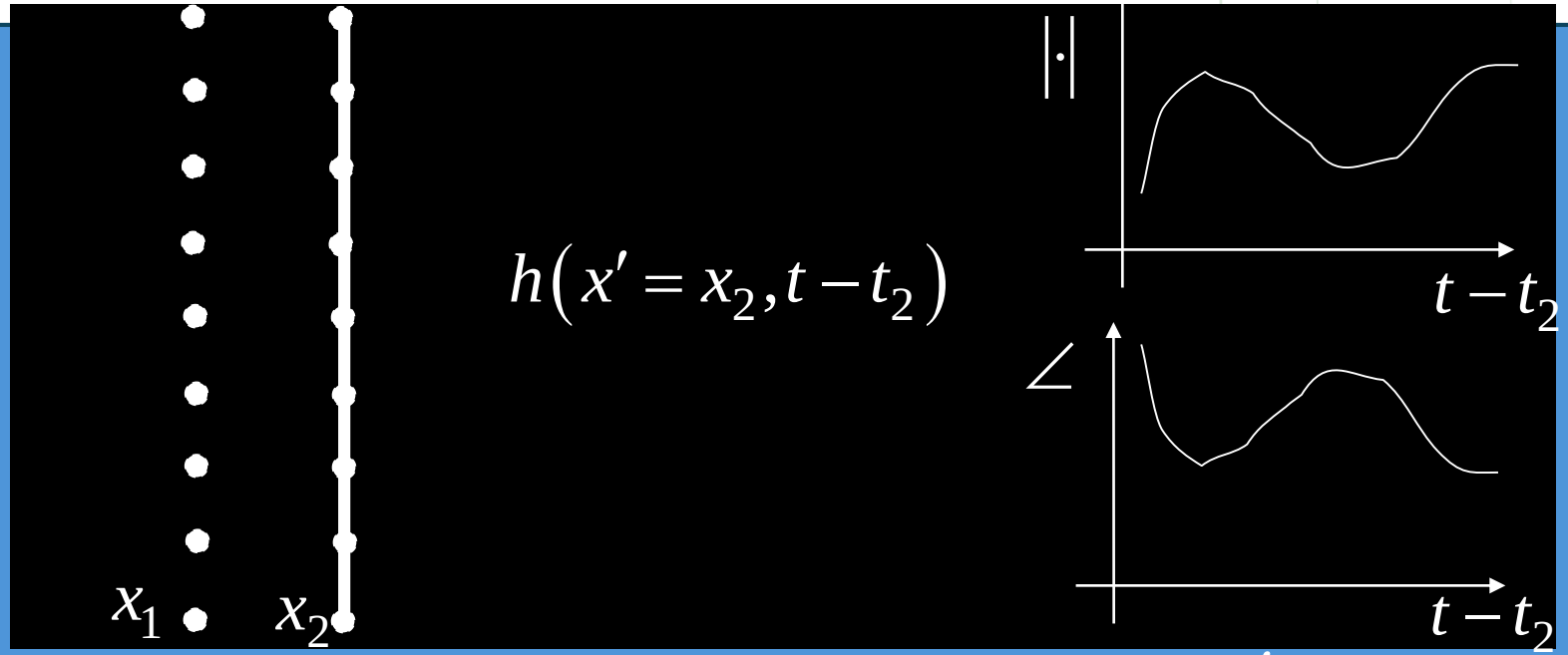

$x'(t_2) = x_2$

x'

Flight direction

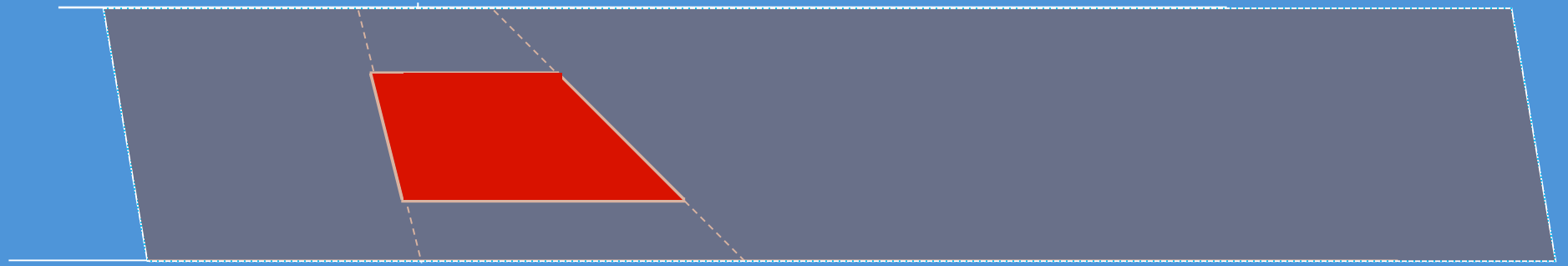

SAR Raw Data

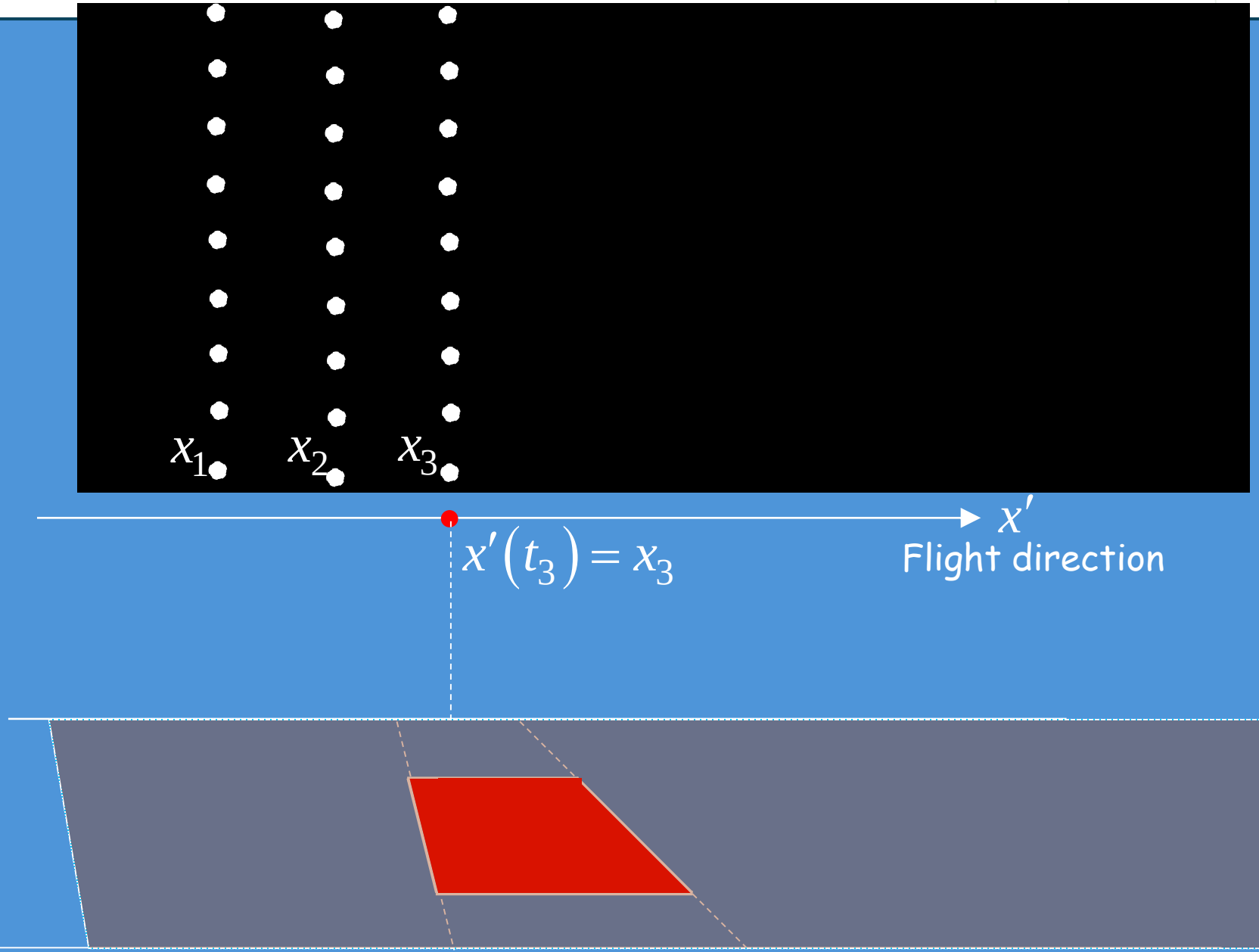

SAR Raw Data

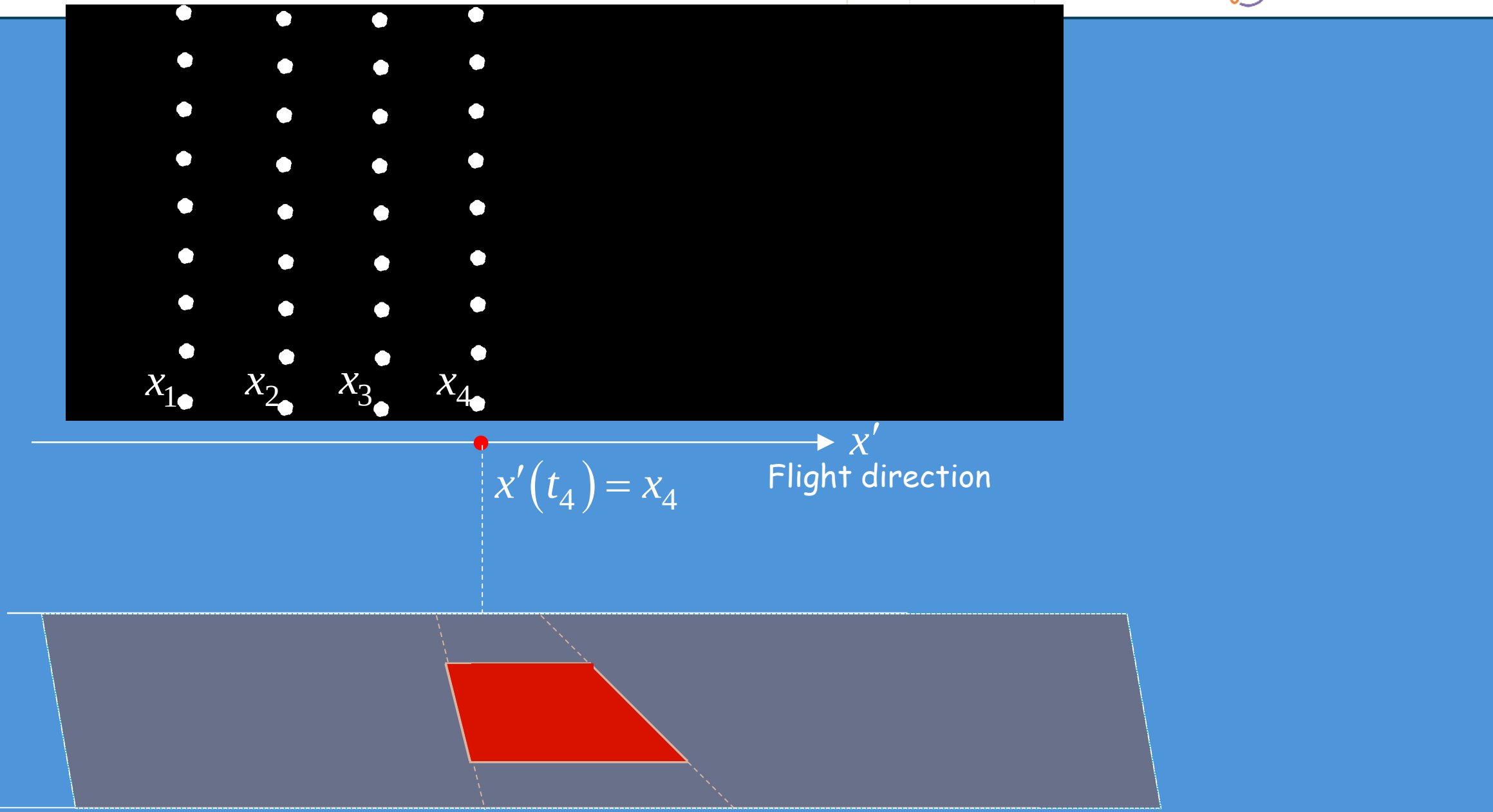

SAR Raw Data

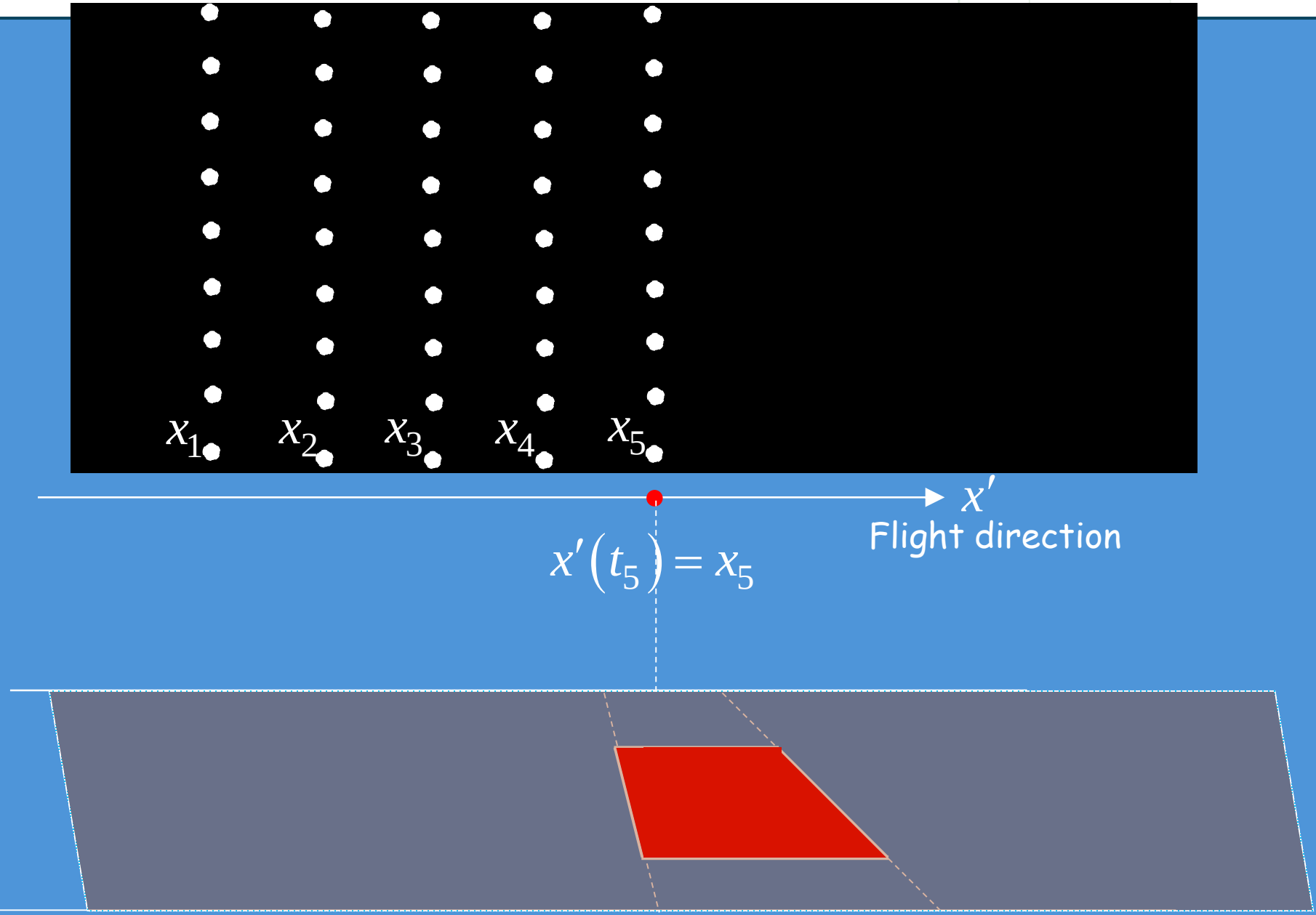

SAR Raw Data

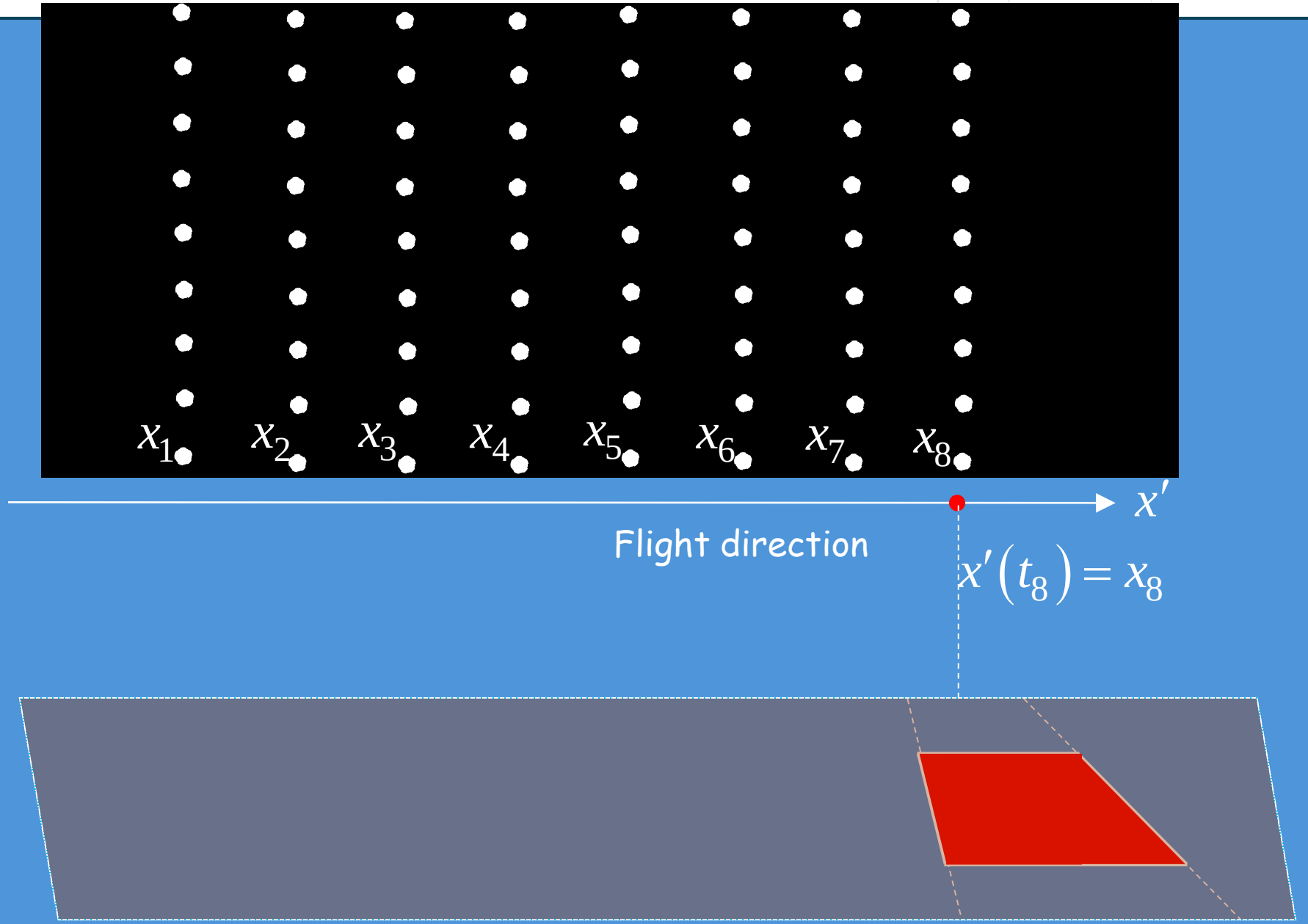

SAR Raw Data

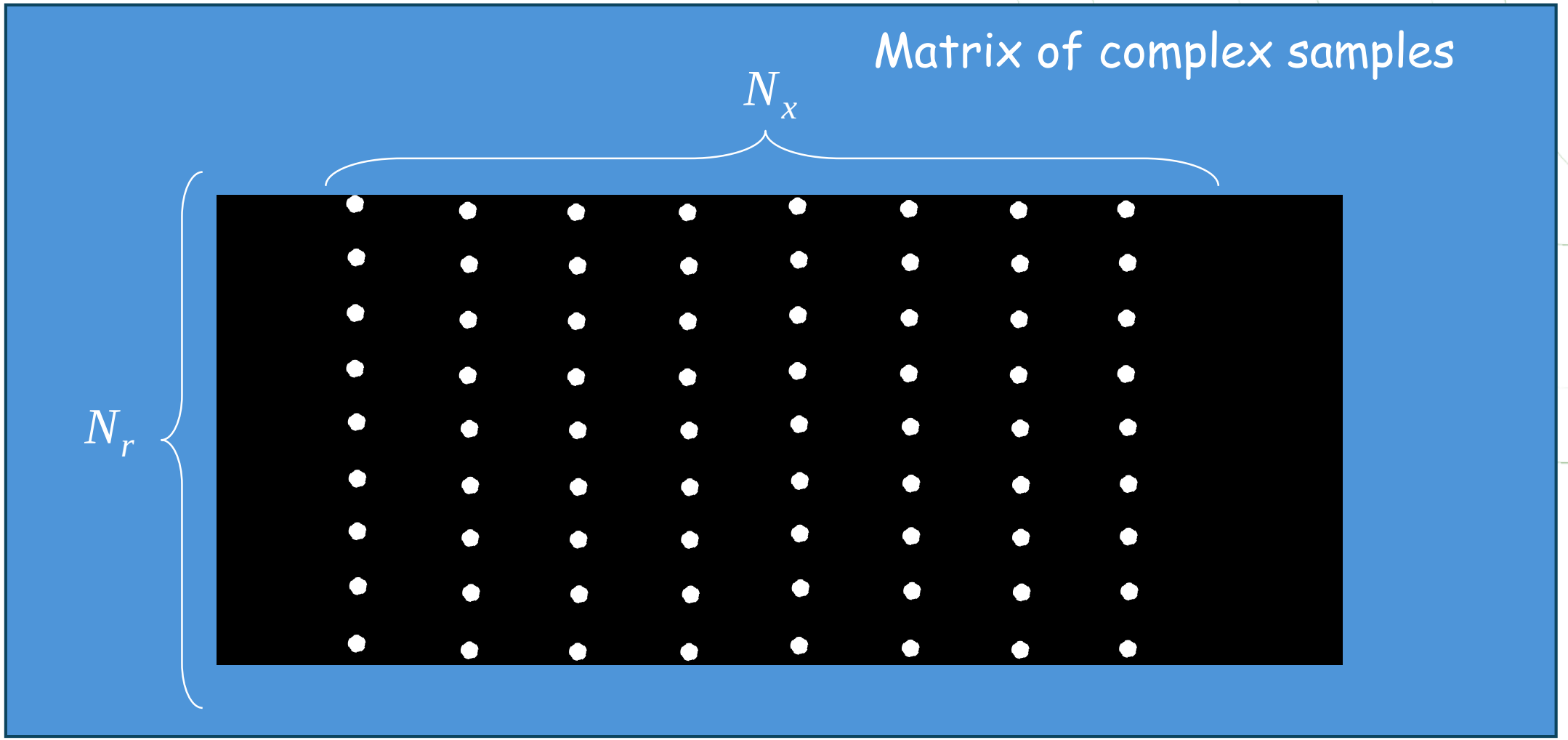

SAR Raw Data

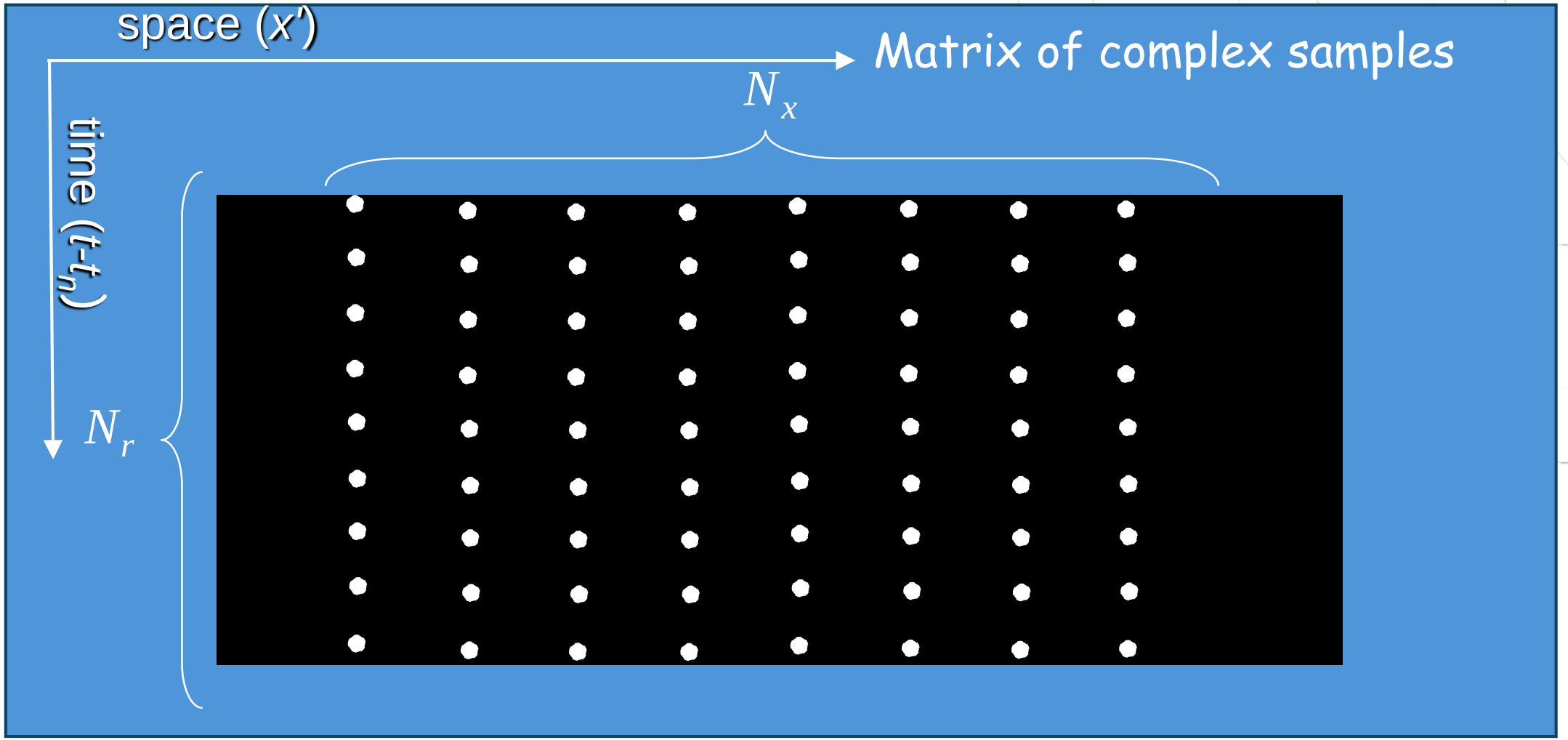

SAR Raw Data

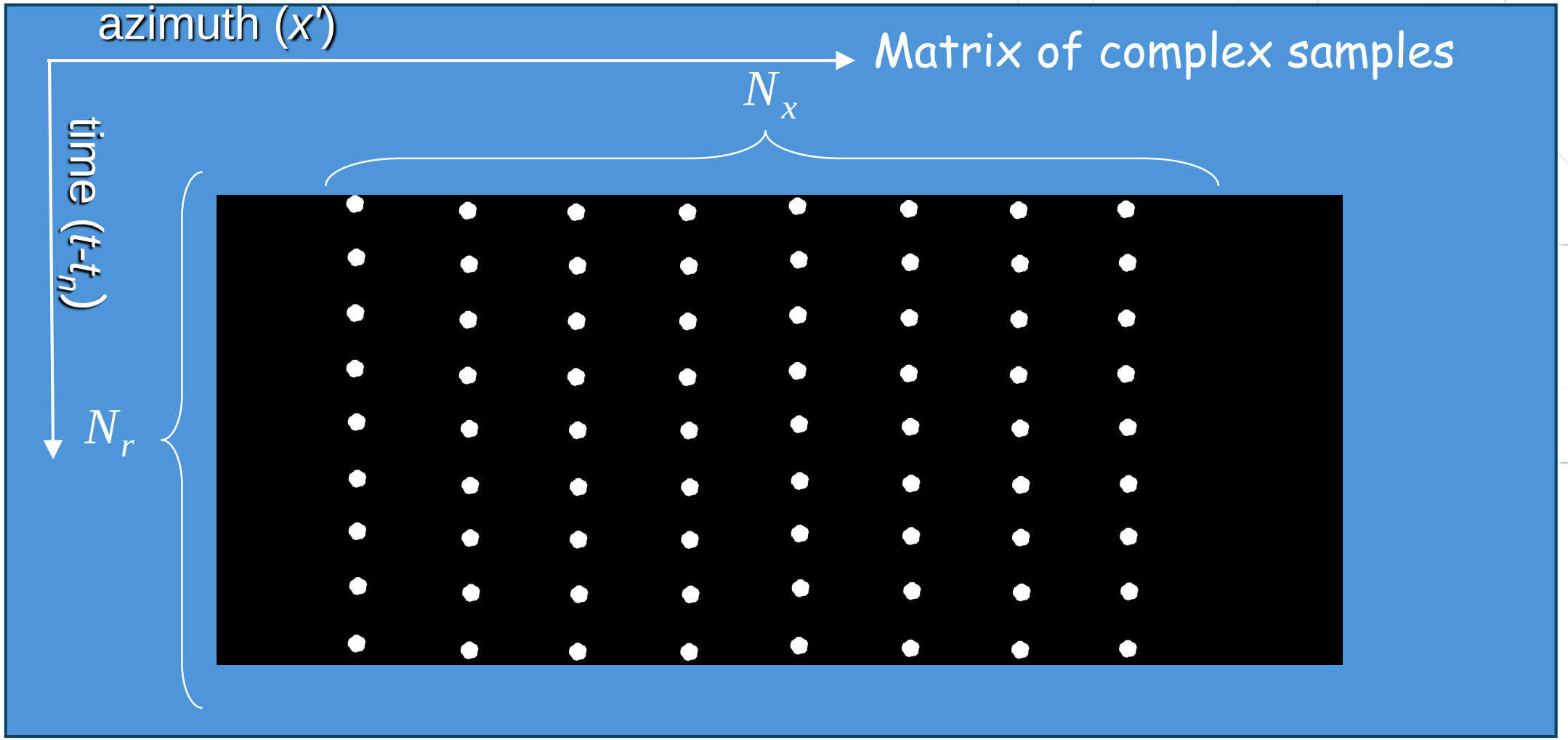

SAR Raw Data

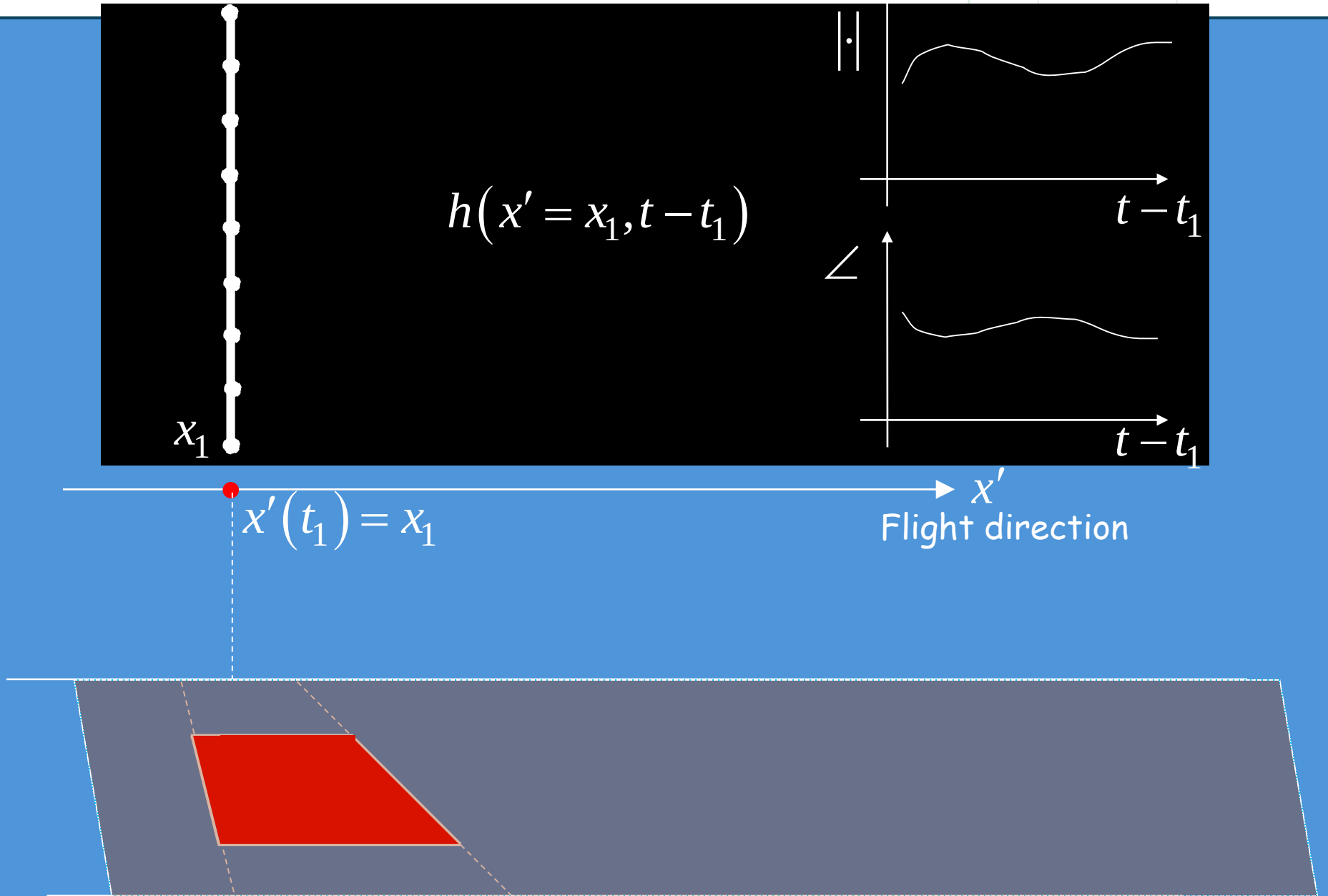

Sampling frequency

SAR Raw Data

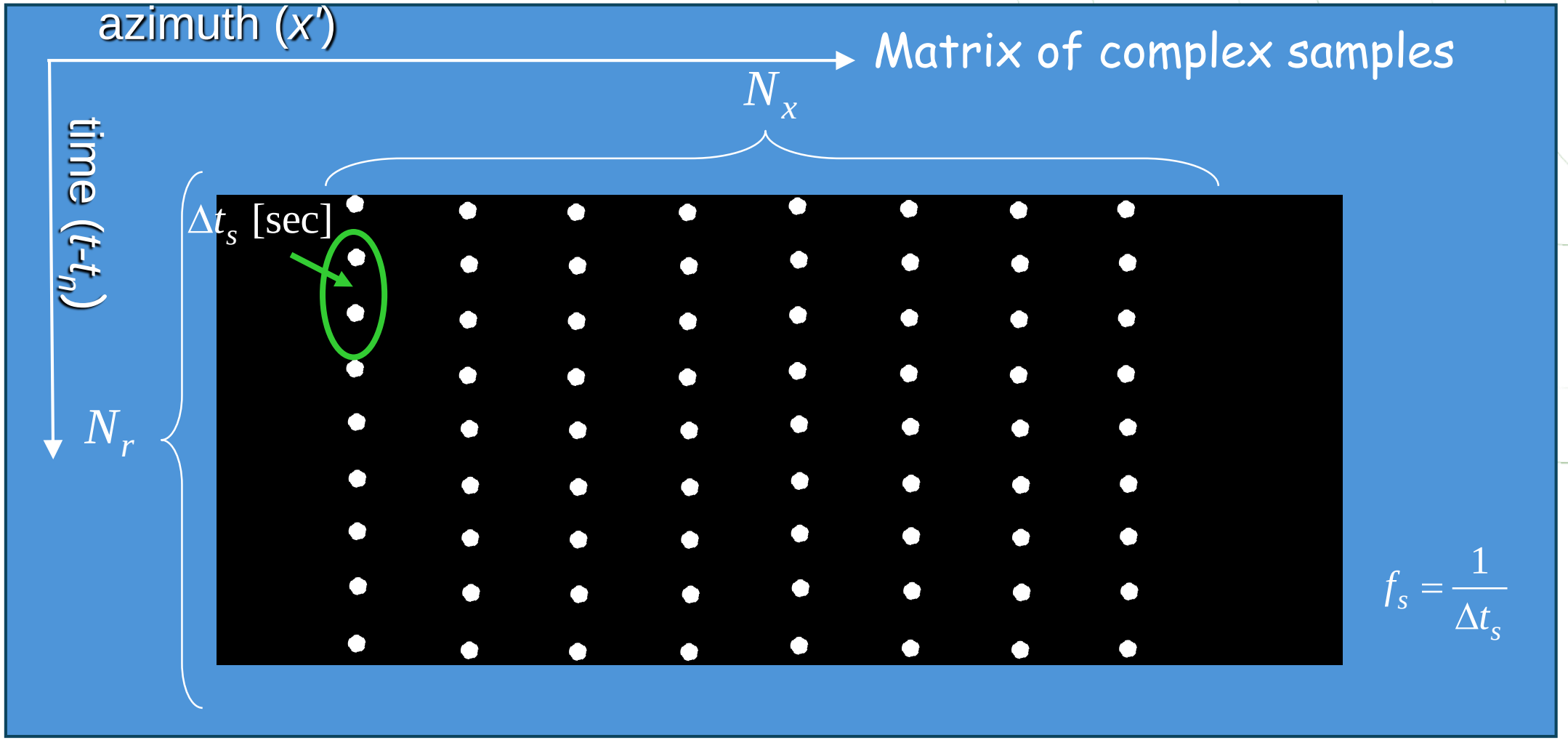
azimuth (x')
Matrix of complex samples
N_x
time (t-t_n)
Δt_s [sec]
N_r
$f_s = \frac{1}{\Delta t_s}$

Pulse Repetition Frequency

SAR Raw Data

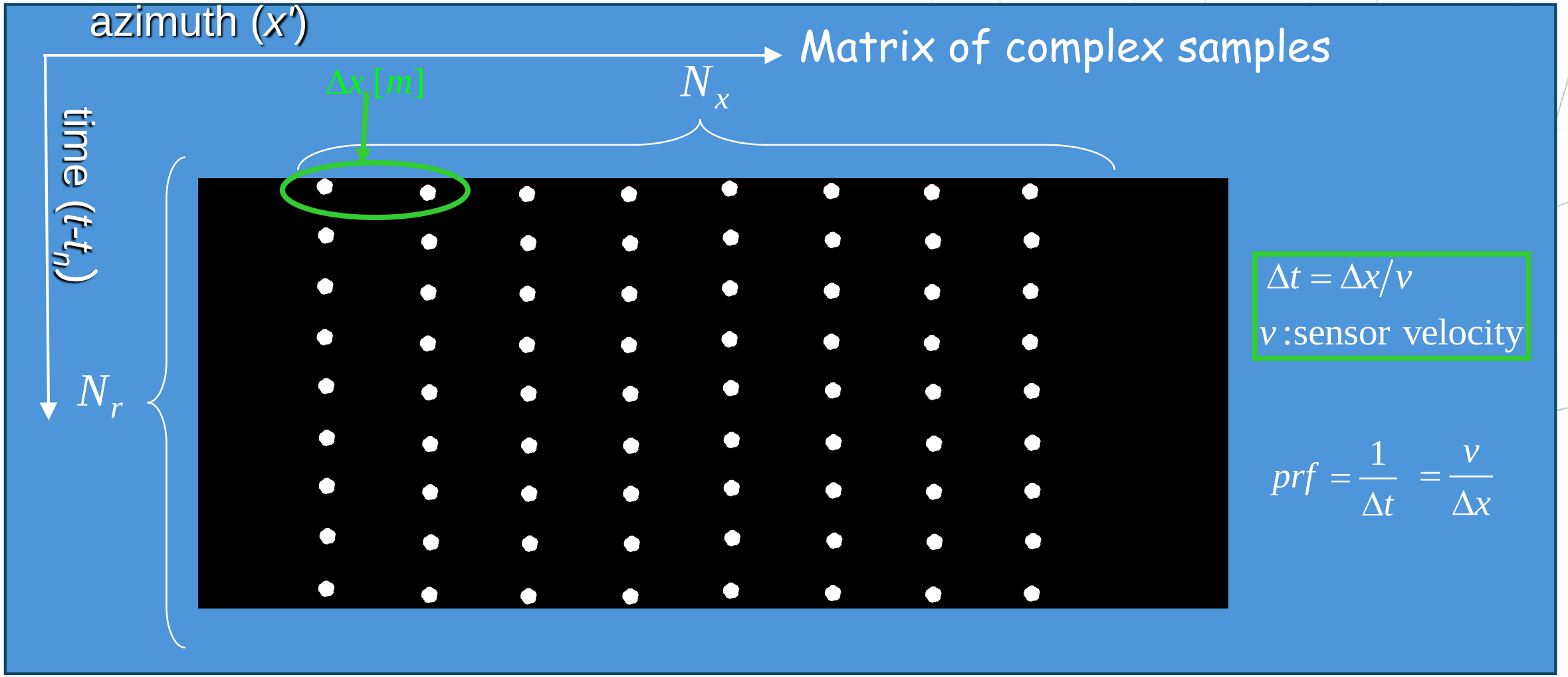
azimuth (x')
Matrix of complex samples
Δx [m]
N_x
time (t-t_n)
N_r
$\Delta t = \Delta x / v$
v :sensor velocity
$prf = \frac{1}{\Delta t} = \frac{v}{\Delta x}$

SAR Raw Data

Which is the information relevant to each pixel ?

SAR Raw Data

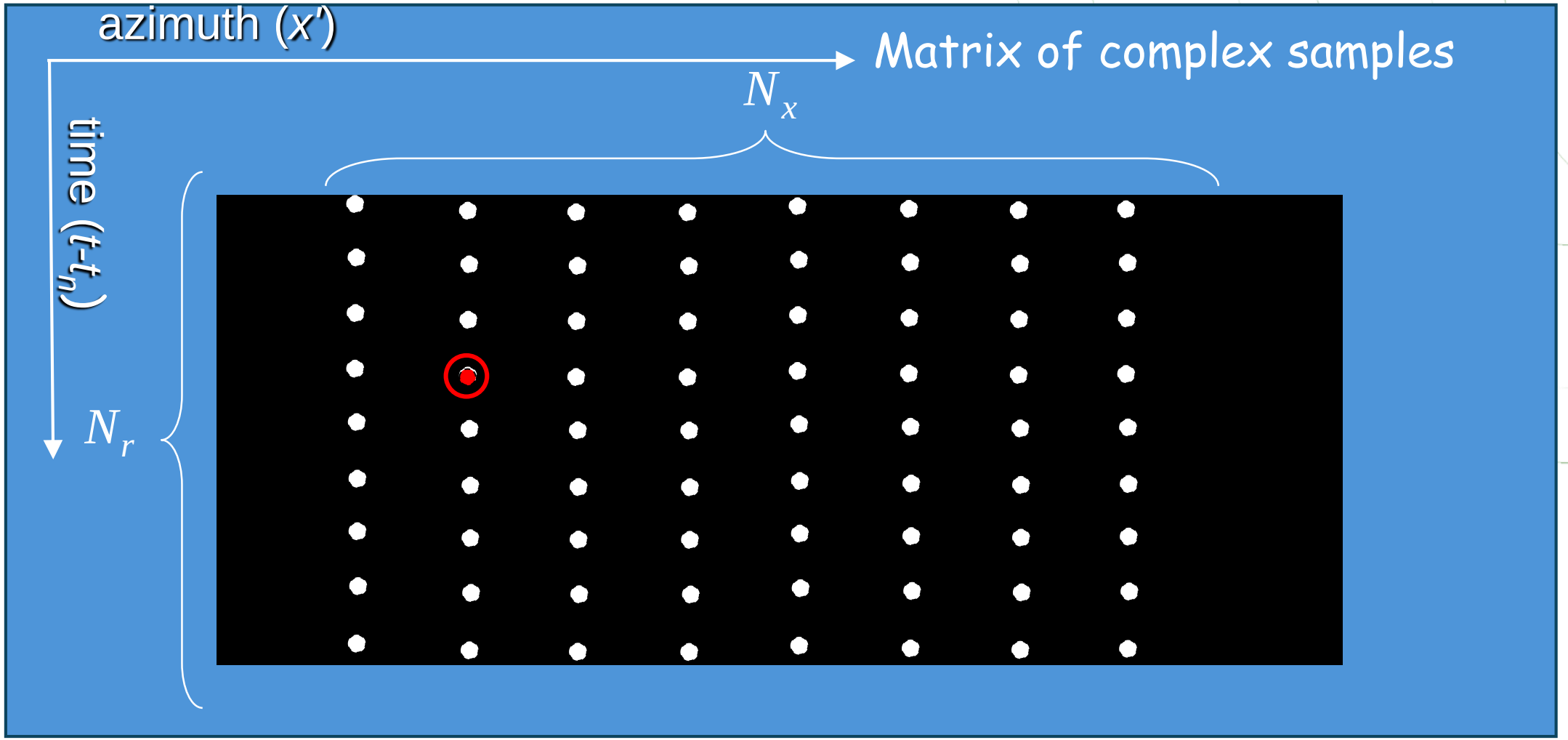

SAR Raw Data

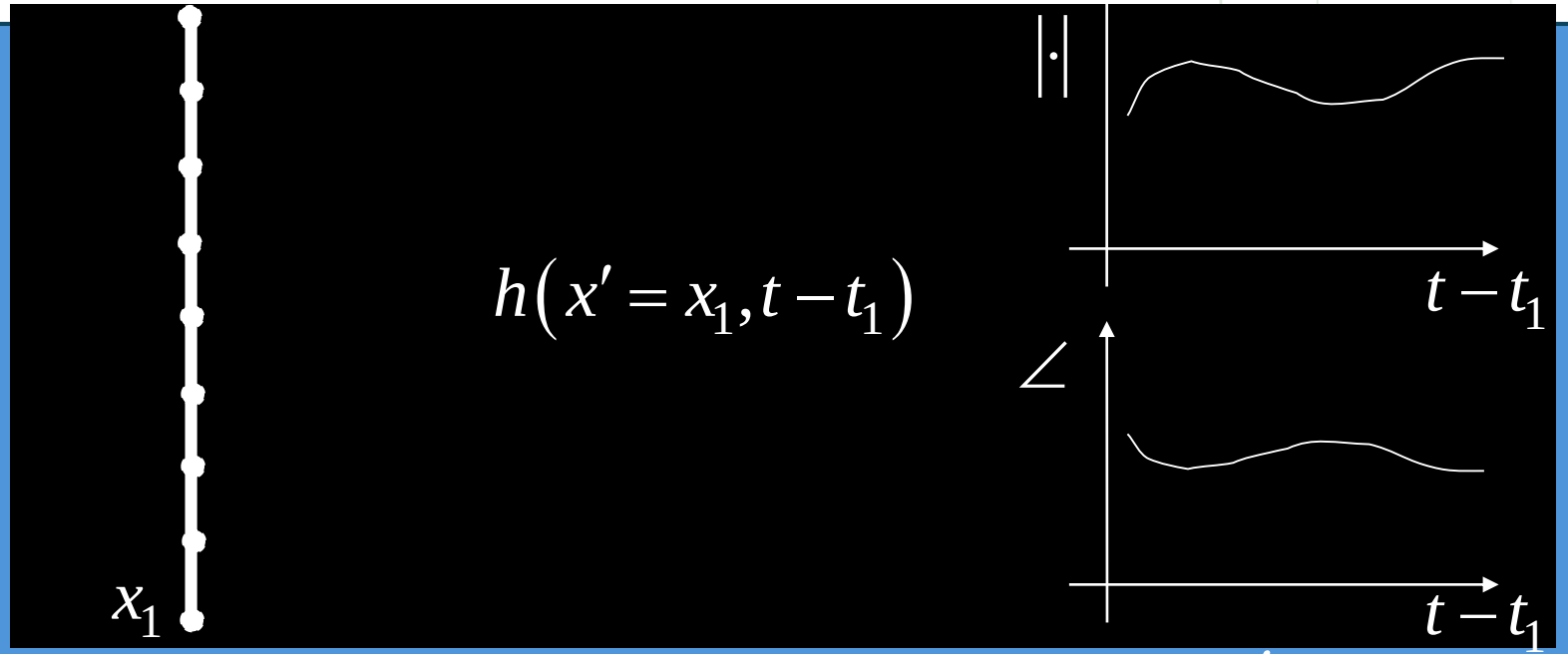

x'

$x'(t_1) = x_1$

Flight direction

SAR Raw Data

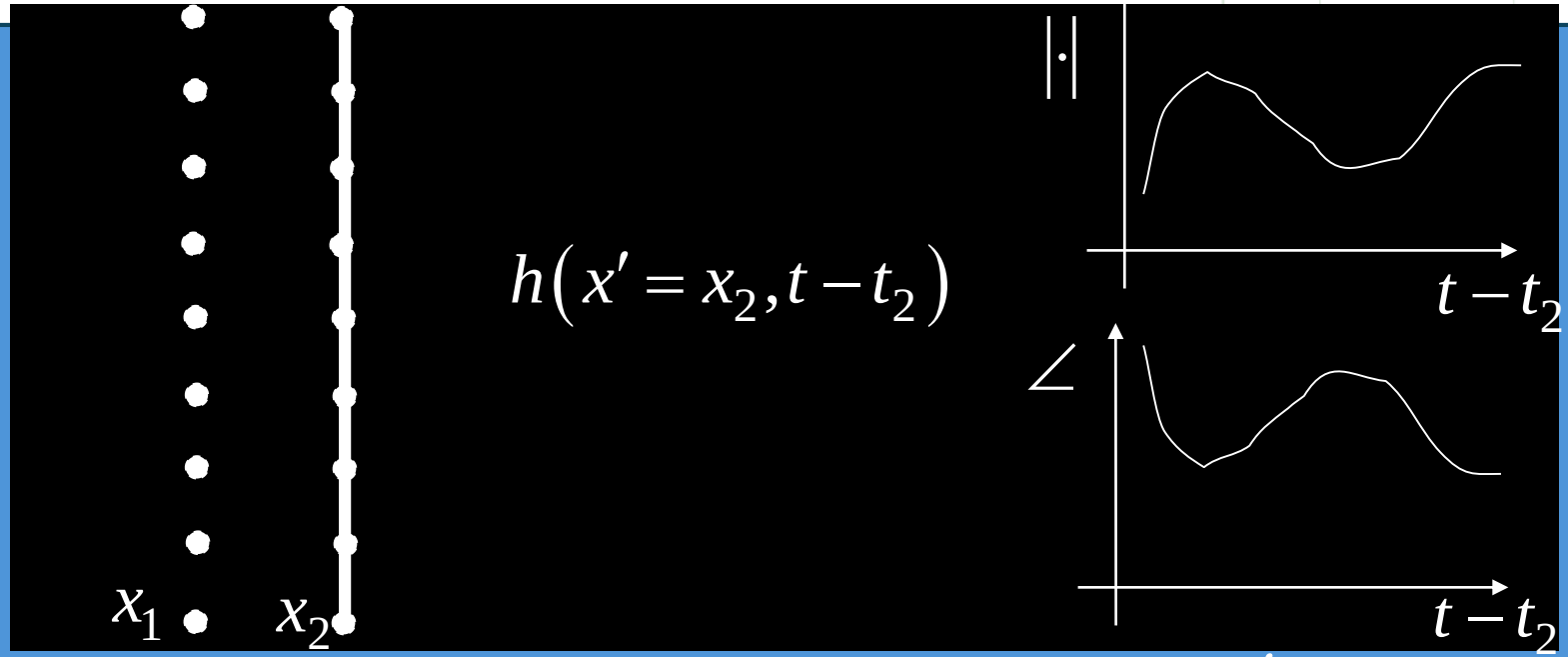

x'

$x'(t_2)=x_2$

Flight direction

SAR Raw Data

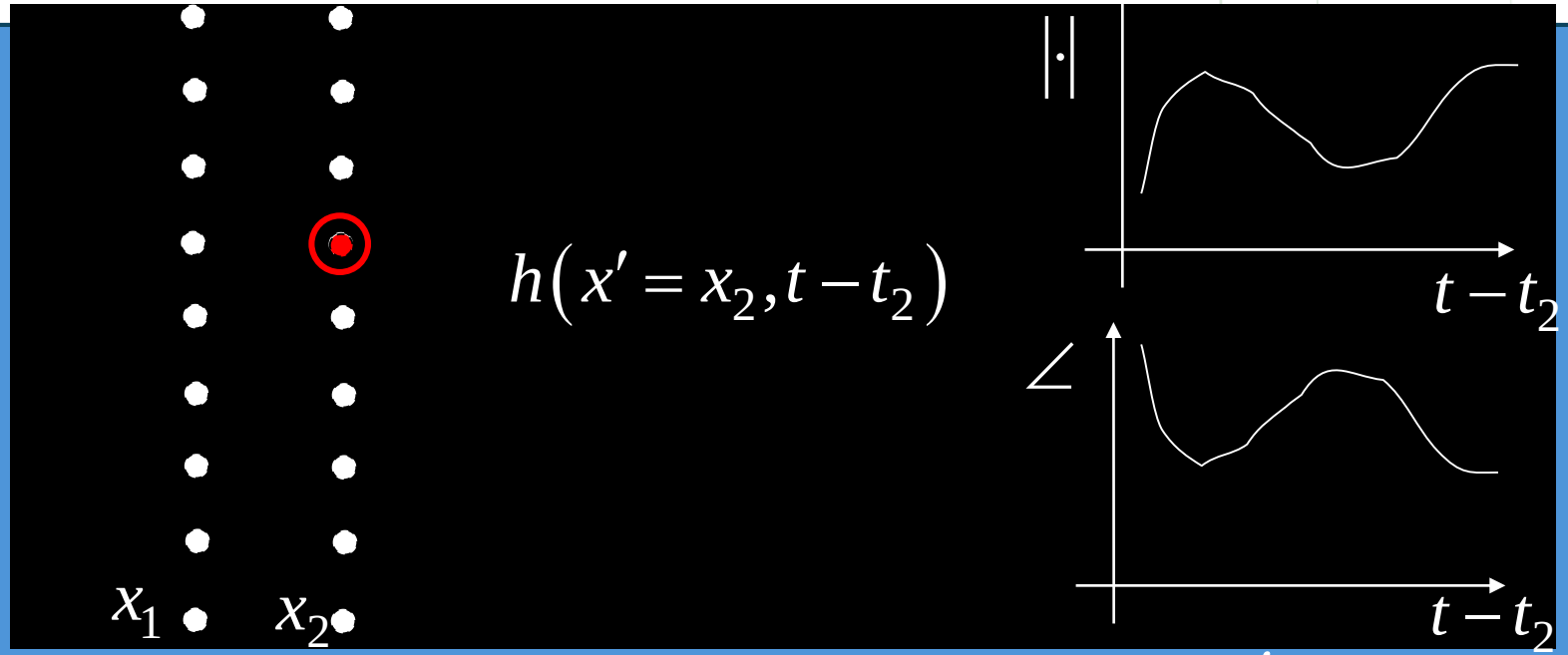

x'

$x'(t_2)=x_2$

Flight direction

SAR Raw Data

Time – Distance relationship

SAR Raw Data

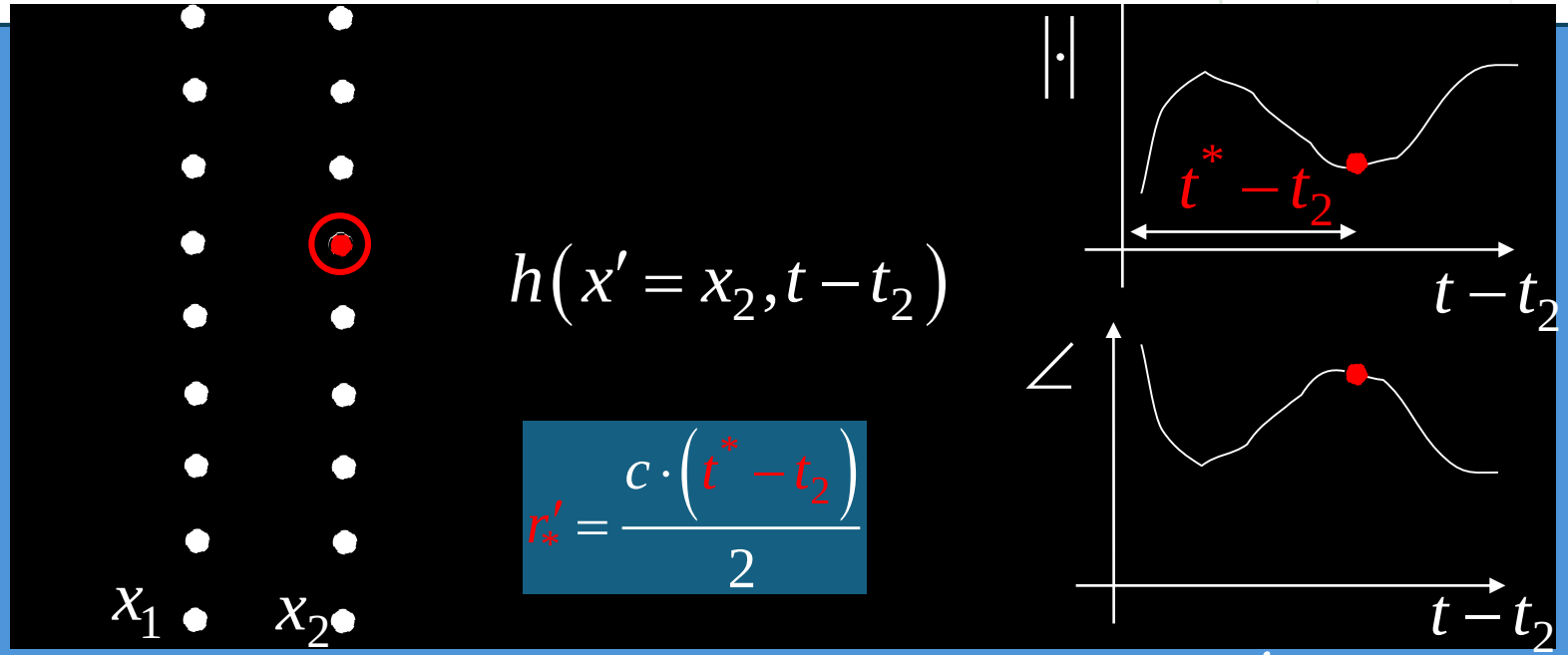
$h(x' = x_2, t - t_2)$
$r'_* = \frac{c \cdot (t^* - t_2)}{2}$
x_1
x_2
$|\cdot|$
$t^* - t_2$
$t - t_2$
$\angle$
$t - t_2$

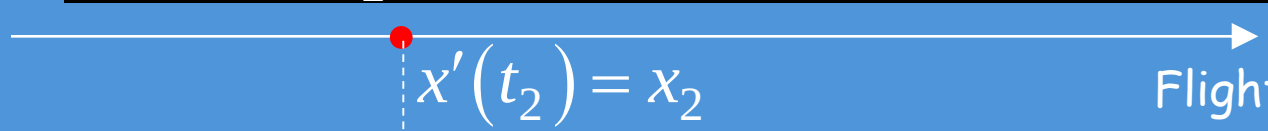
x'
$x'(t_2) = x_2$
Flight direction

SAR Raw Data

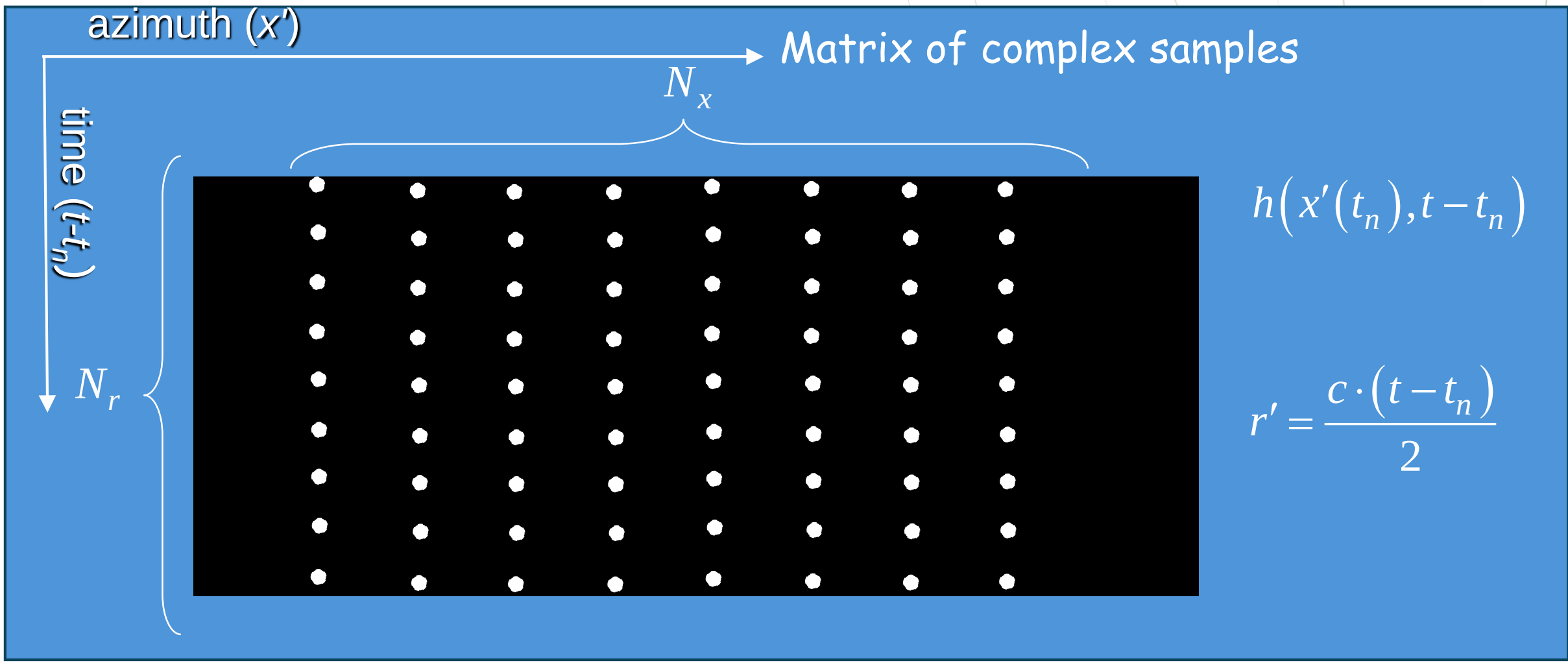
azimuth (x')
Matrix of complex samples
N_x
time (t-t_n)
N_r
$h\left(x'\left(t_n\right), t-t_n\right)$
$r' = \frac{c \cdot \left(t-t_n\right)}{2}$

SAR Raw Data

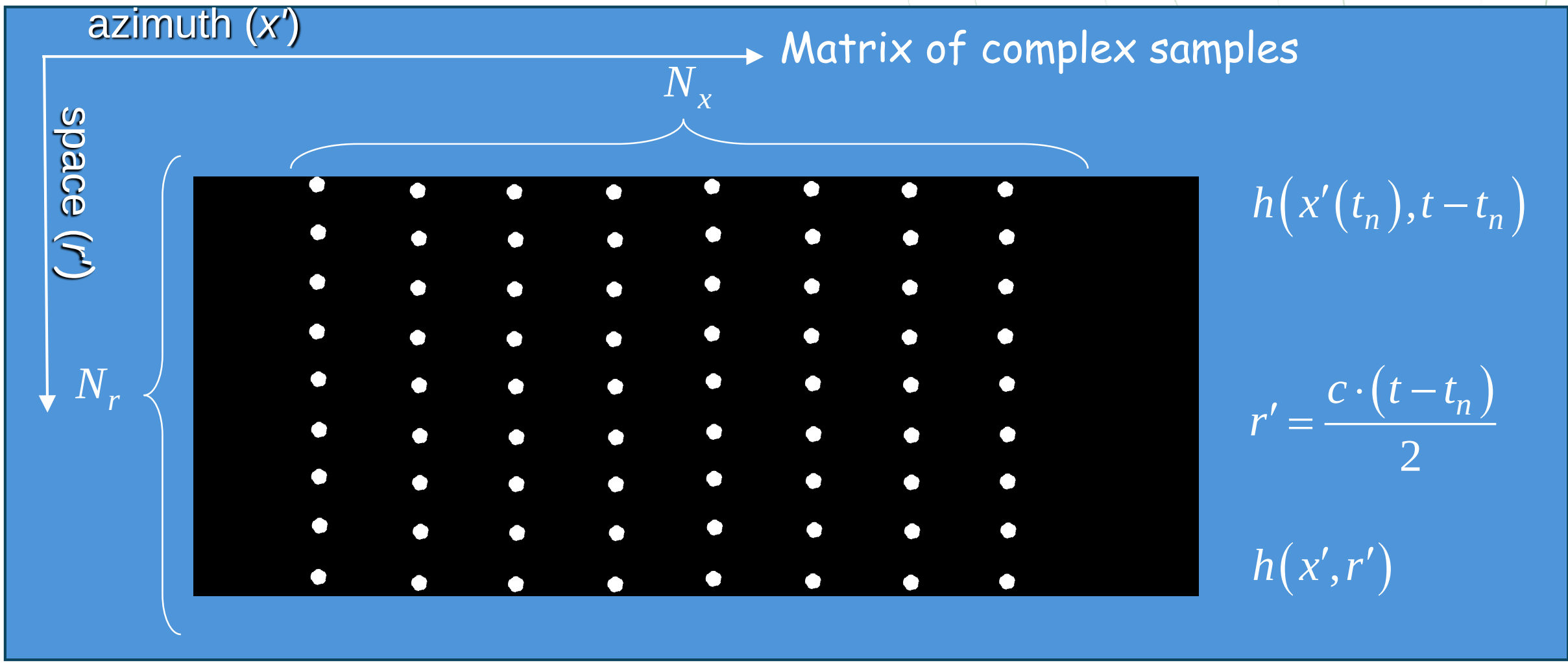
azimuth (x')
Matrix of complex samples
N_x
space (r')
N_r
$h\left(x'\left(t_n\right), t - t_n\right)$
$r' = \frac{c \cdot \left(t - t_n\right)}{2}$
$h\left(x', r'\right)$

SAR Raw Data

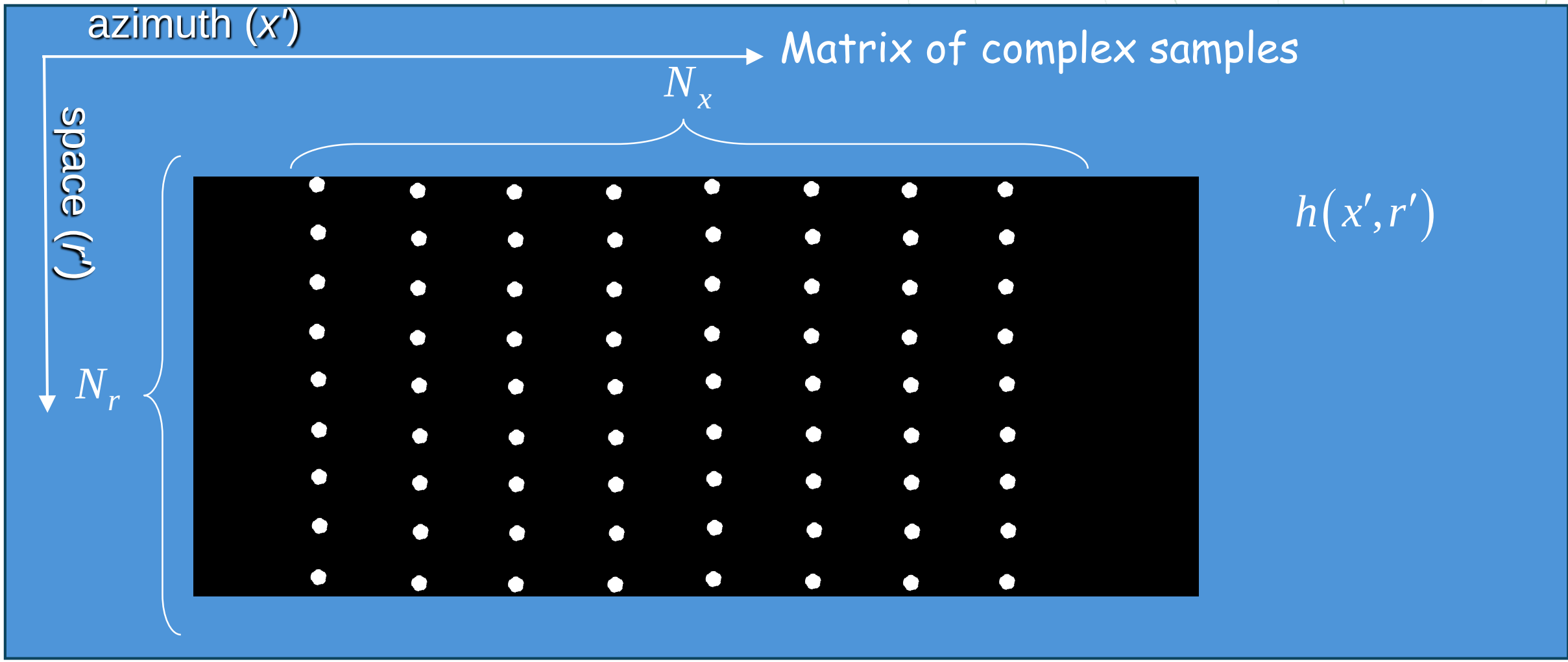

SAR Raw Data

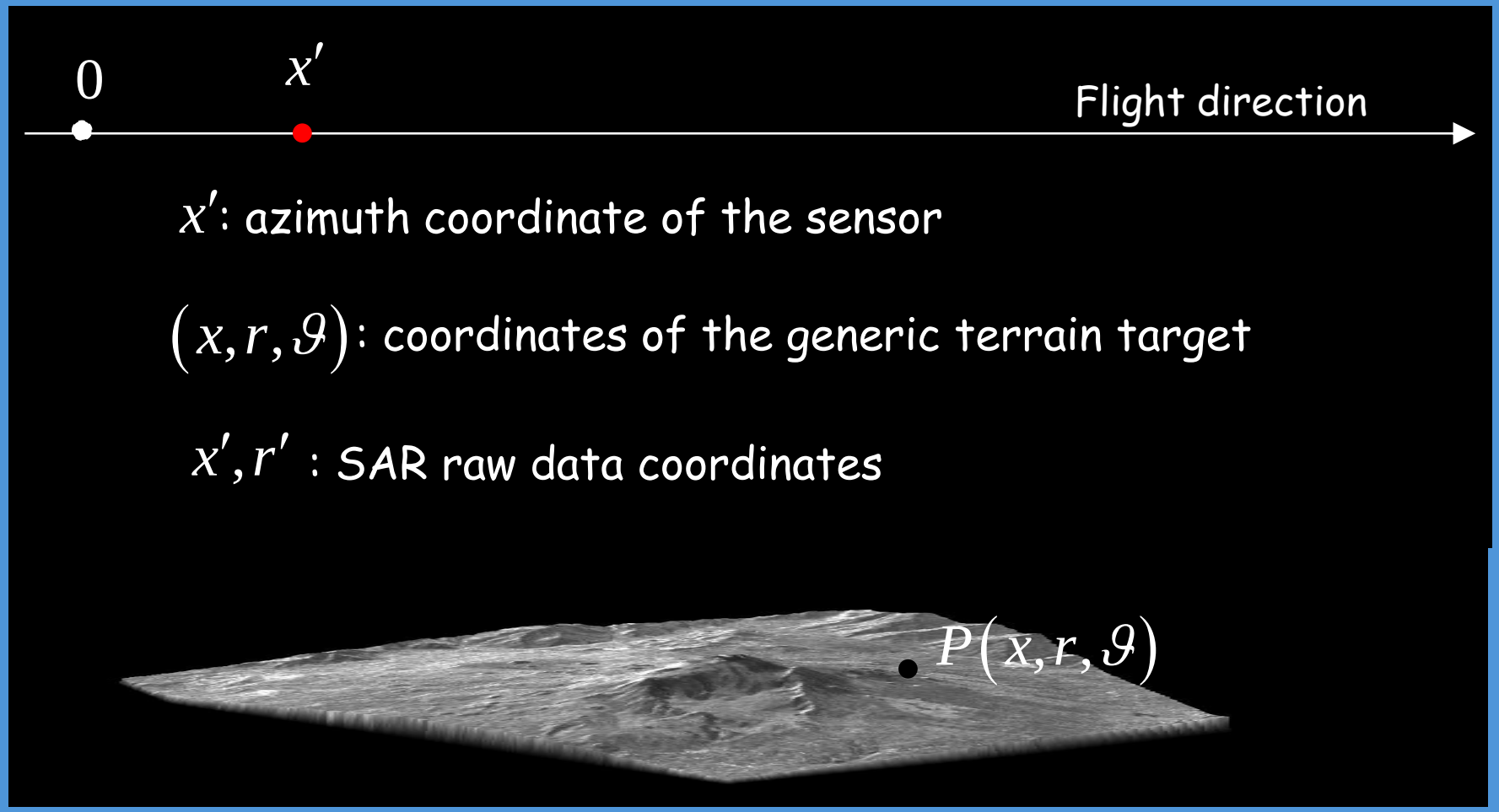
0
x'
Flight direction
x': azimuth coordinate of the sensor
(x, r, ϑ): coordinates of the generic terrain target
x', r' : SAR raw data coordinates
$P(x, r, \vartheta)$

SAR Raw Data

Are the SAR raw data coordinates (x',r')

related to the

(x,r) coordinates of the generic terrain target?

SAR Raw Data

To simplify the discussion, let's assume a scatterer P in the position (x, r, ϑ), within a completely absorbing scene

SAR Raw Data

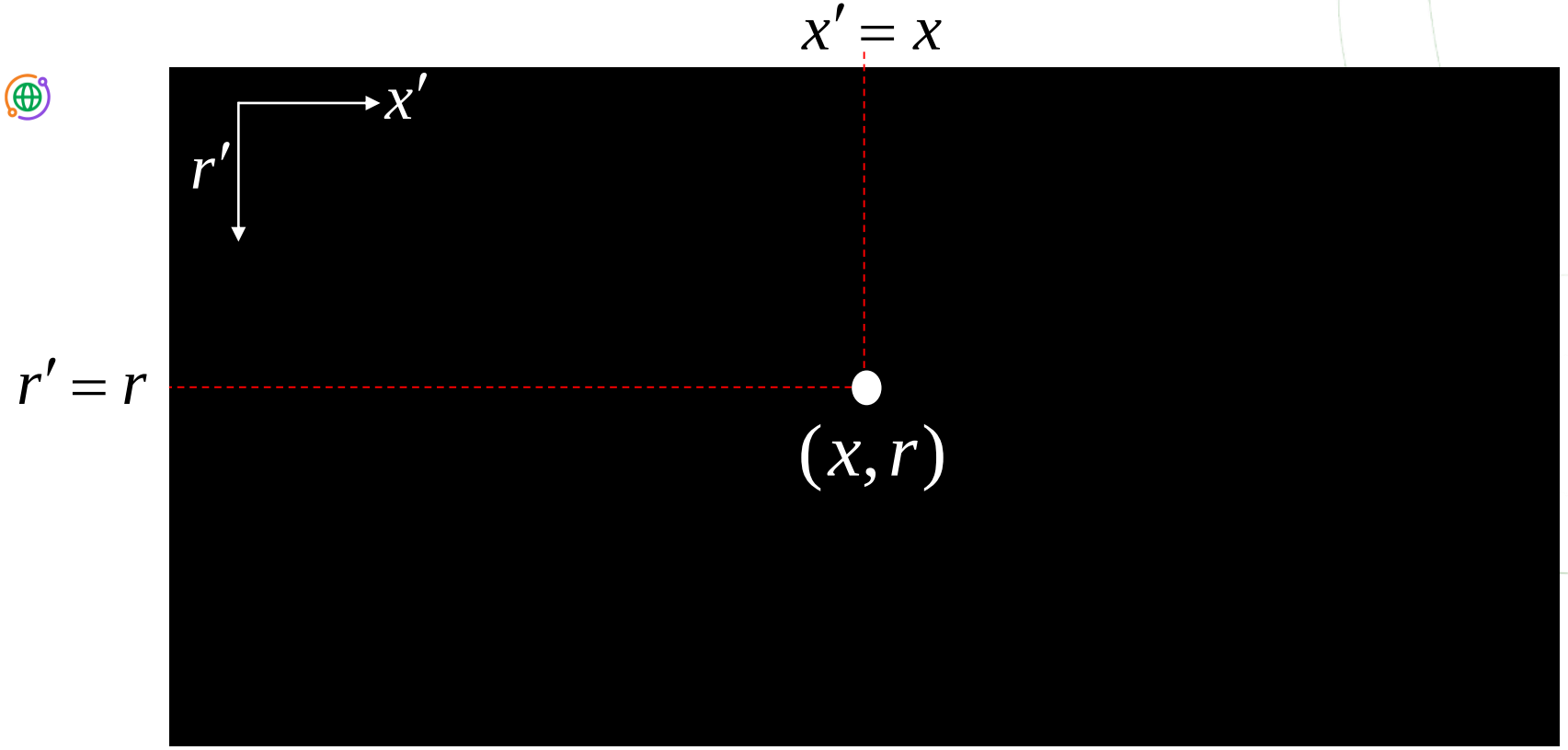

SAR Raw Data

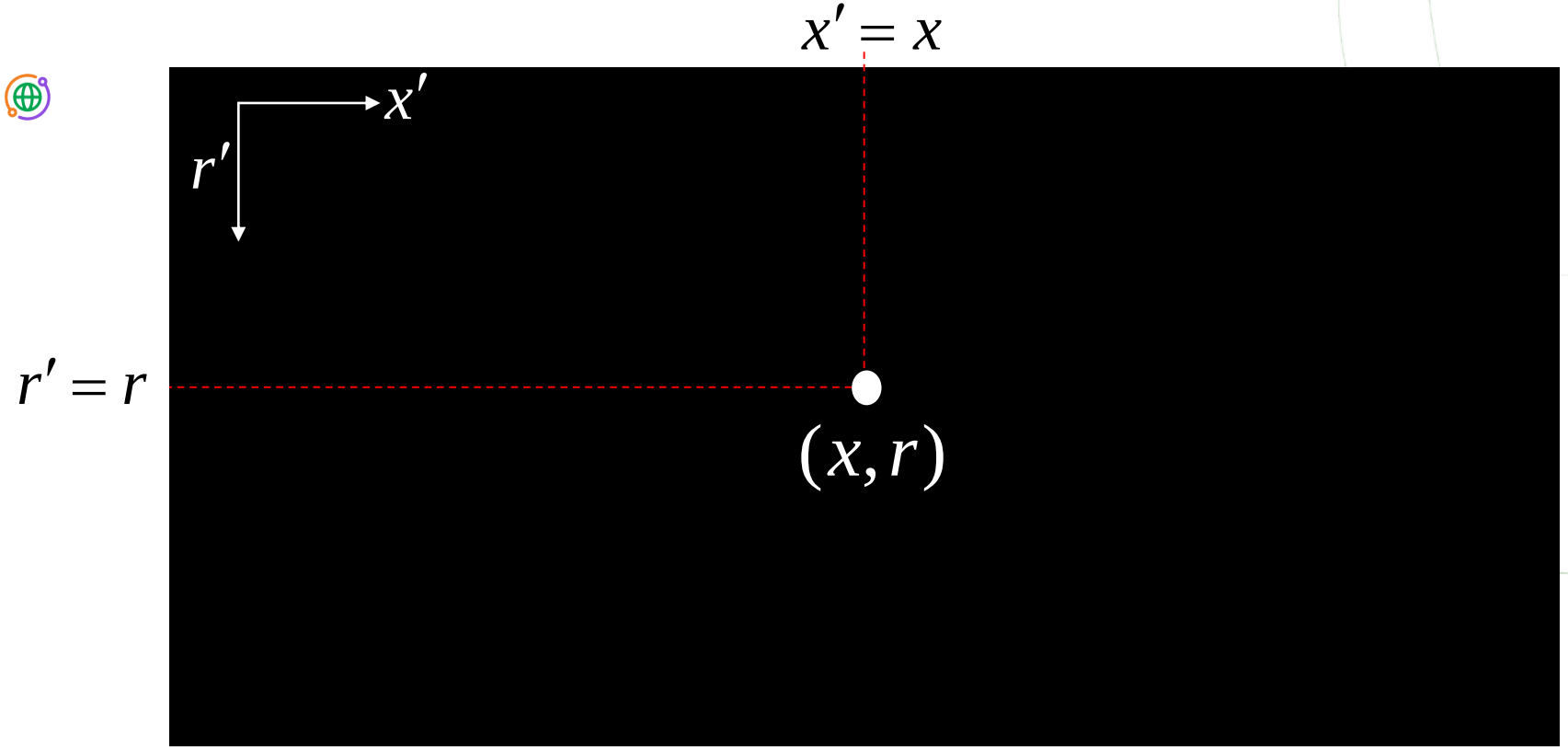

Which pixels are switched on in the image?

Only the one highlighted in the figure? Sure?

SAR Raw Data

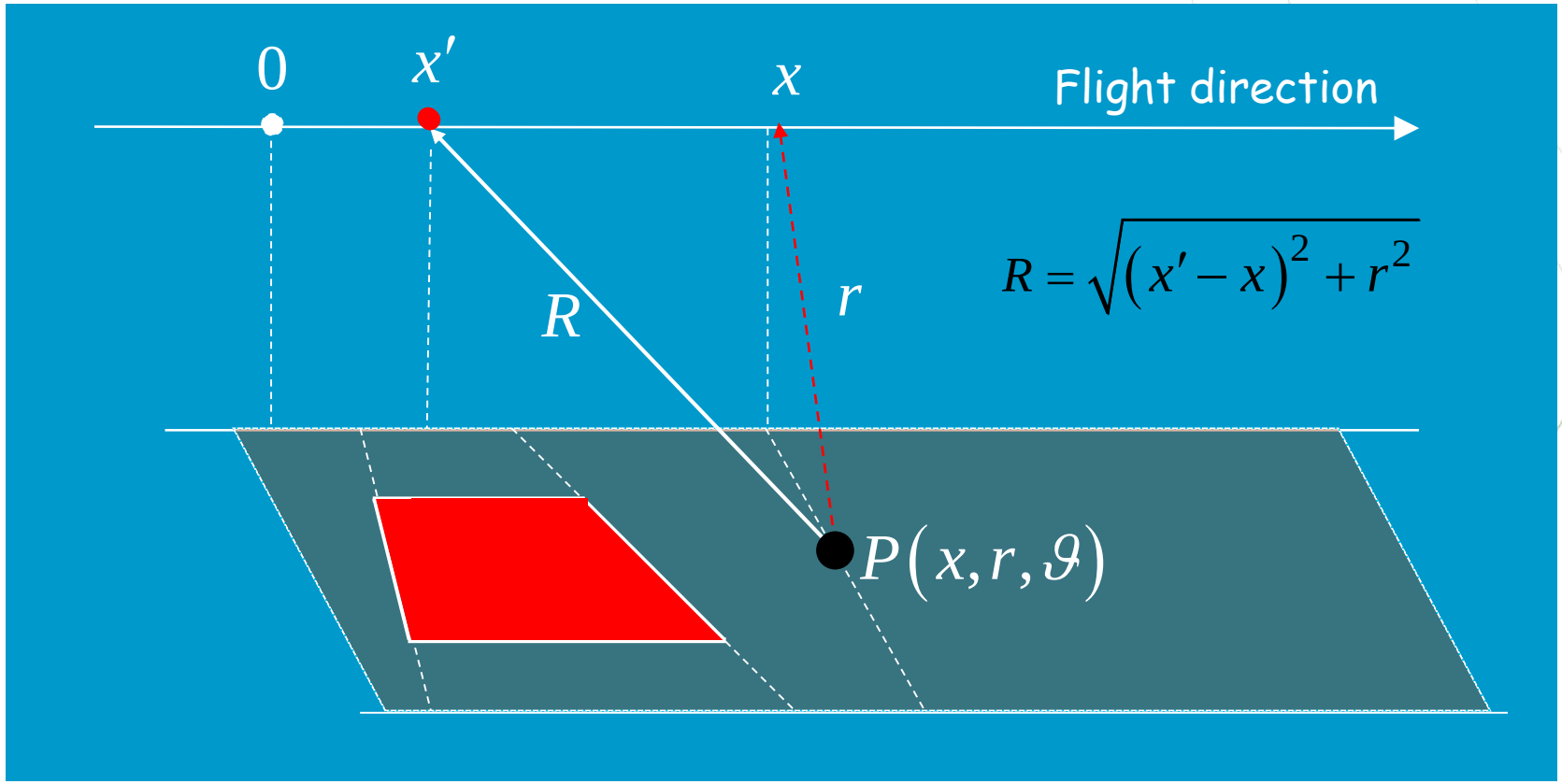

SAR Raw Data

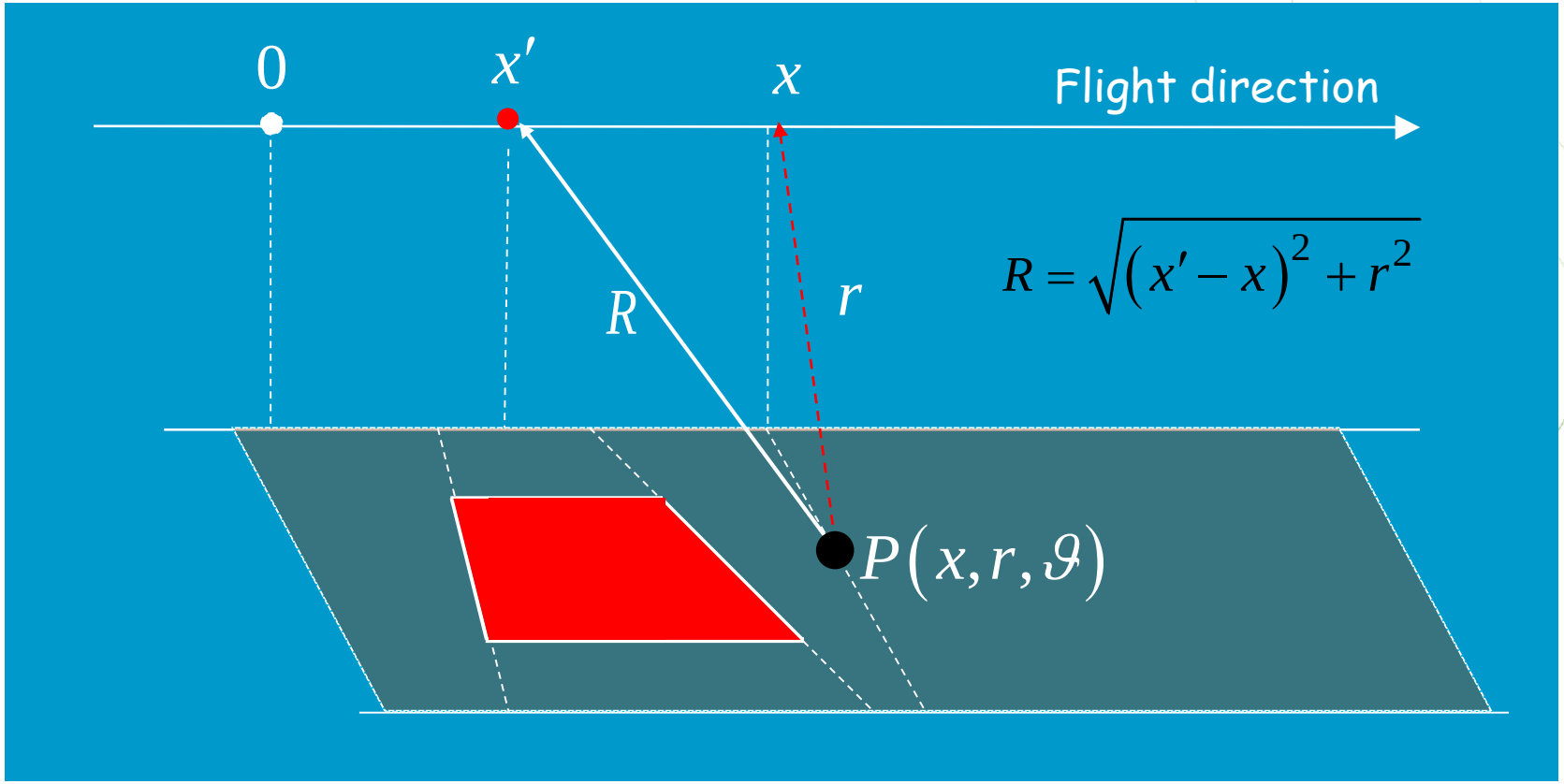

SAR Raw Data

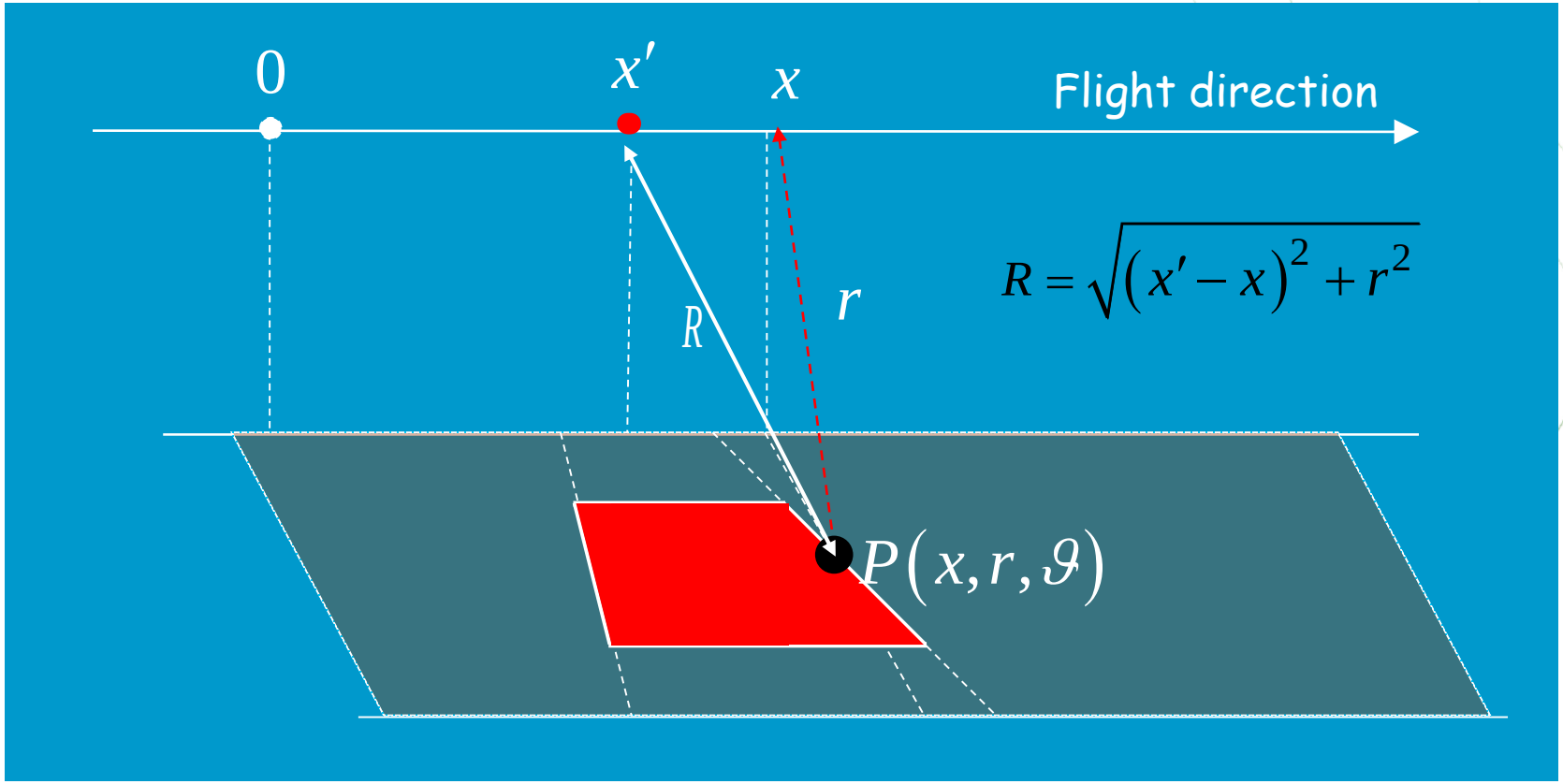

SAR Raw Data

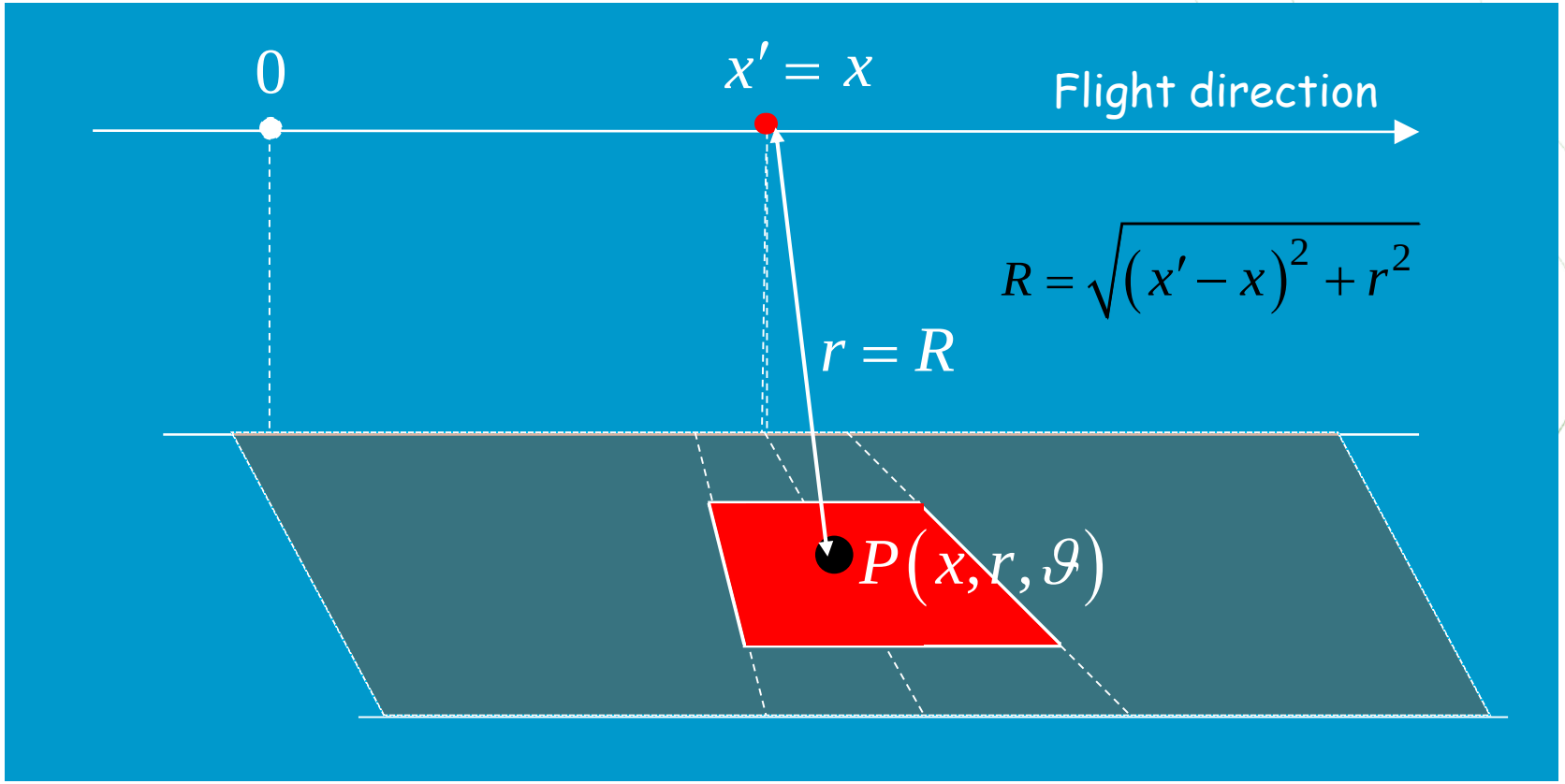

SAR Raw Data

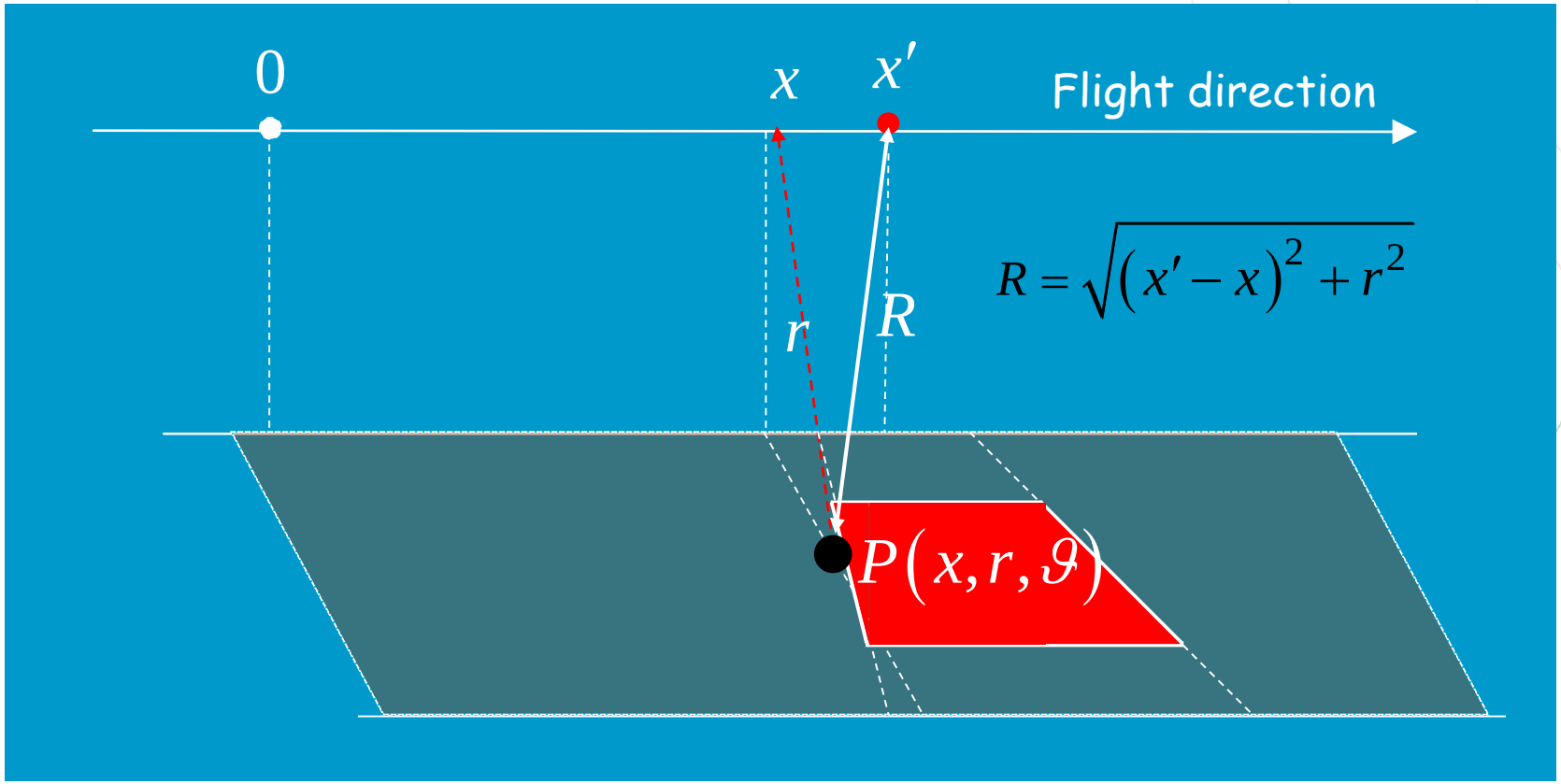

SAR Raw Data

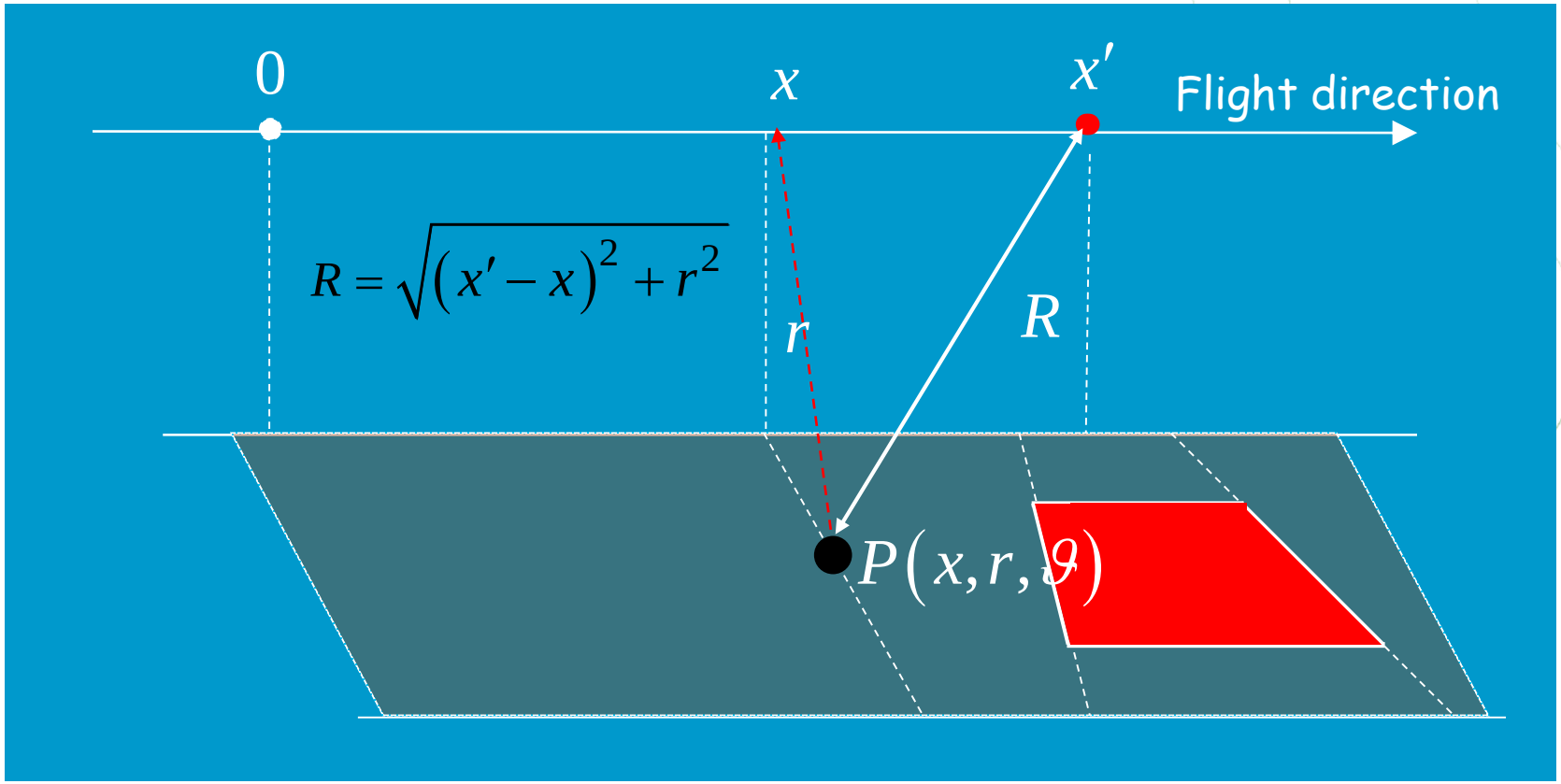

SAR Raw Data

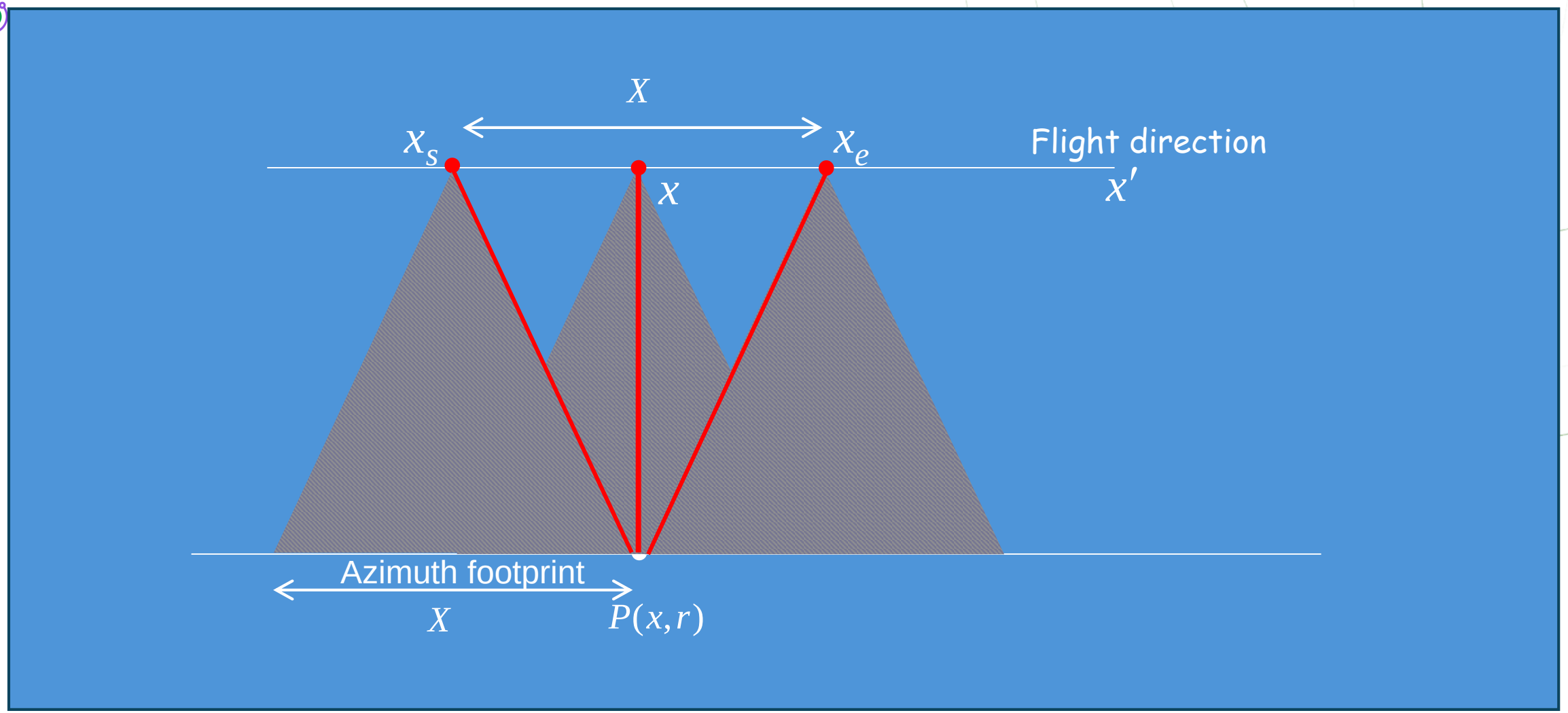

SAR Raw Data

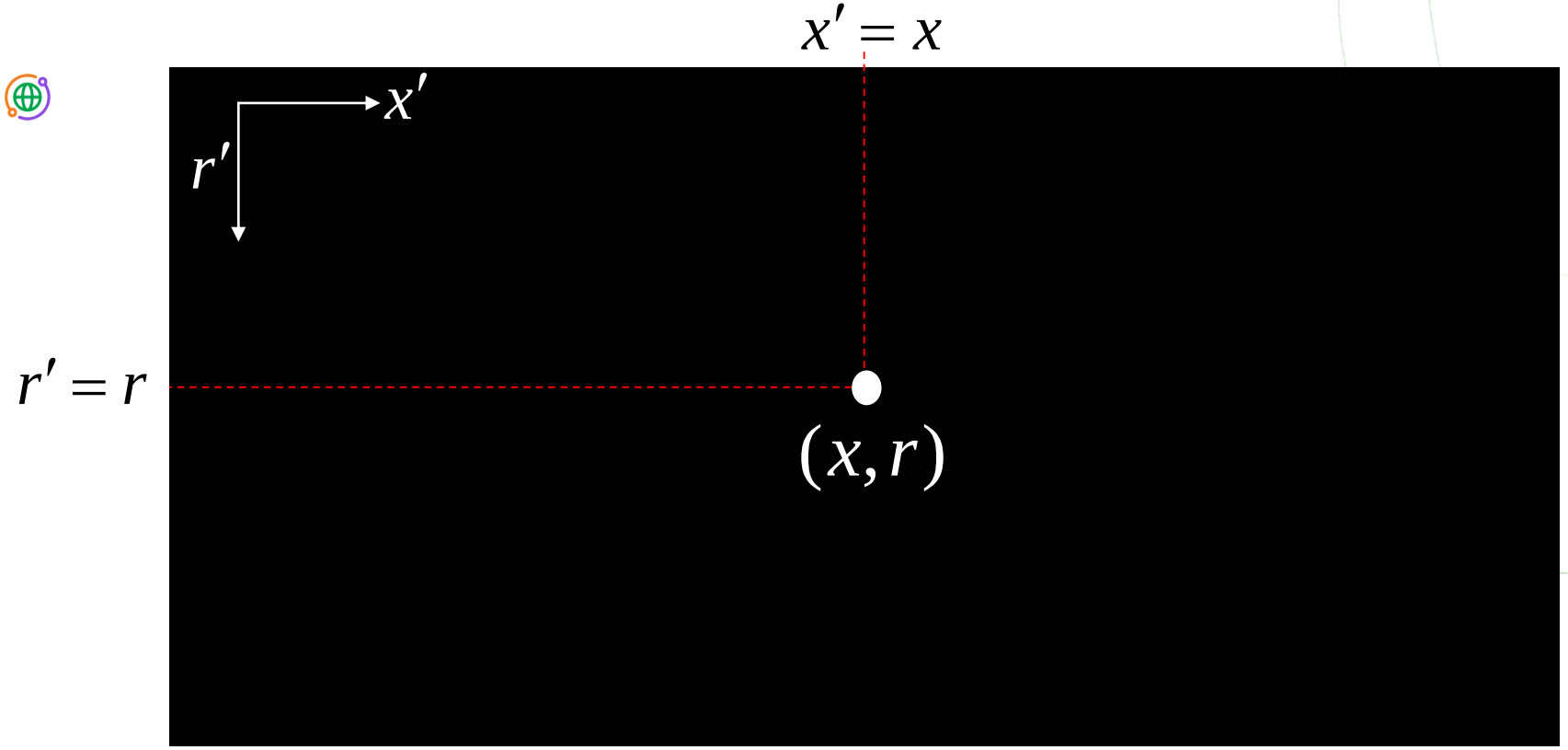

Which pixels are switched on in the image?

Only the one highlighted in the figure? Sure?

SAR Raw Data

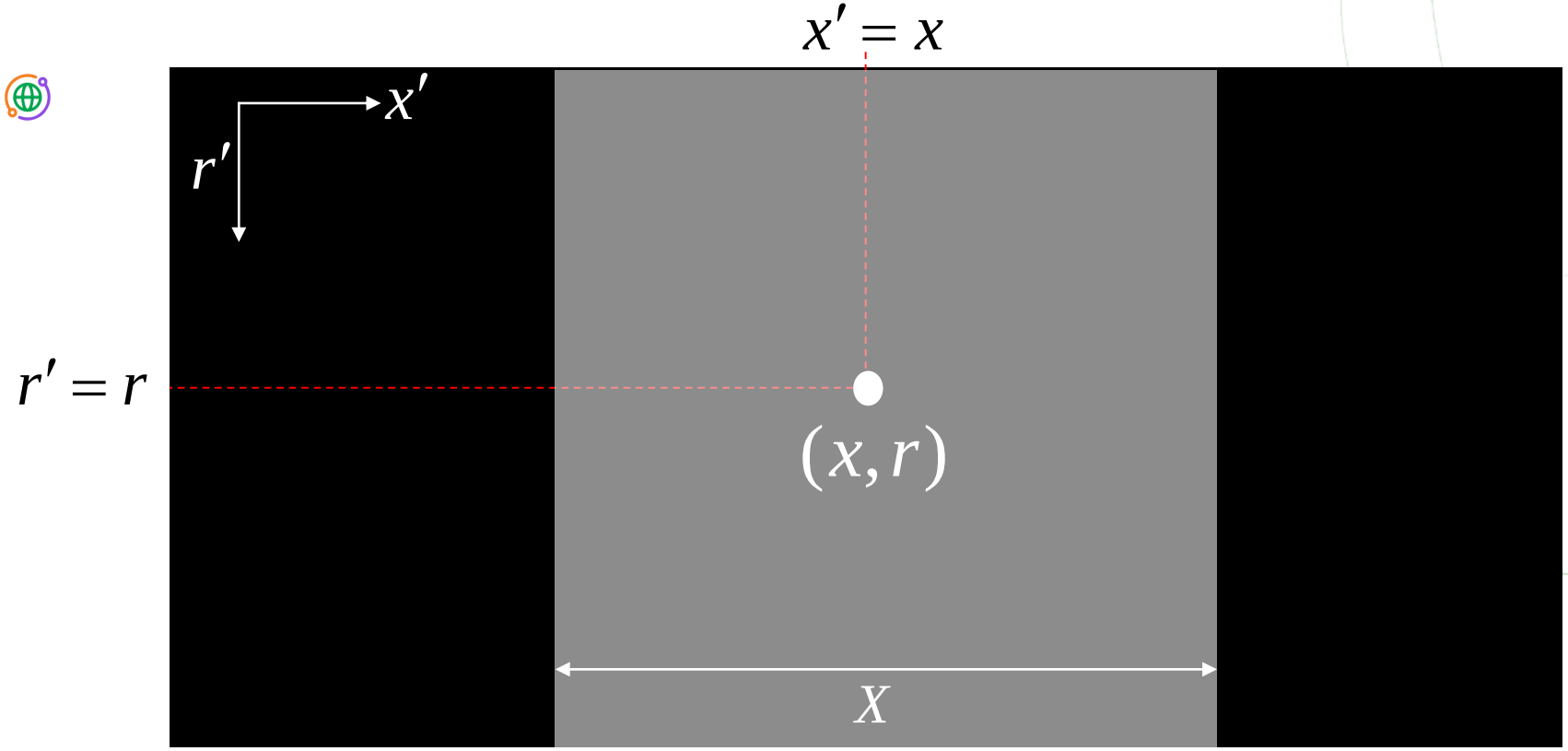

Which pixels are switched on in the image?

Only the one highlighted in the figure? Sure?

SAR Raw Data

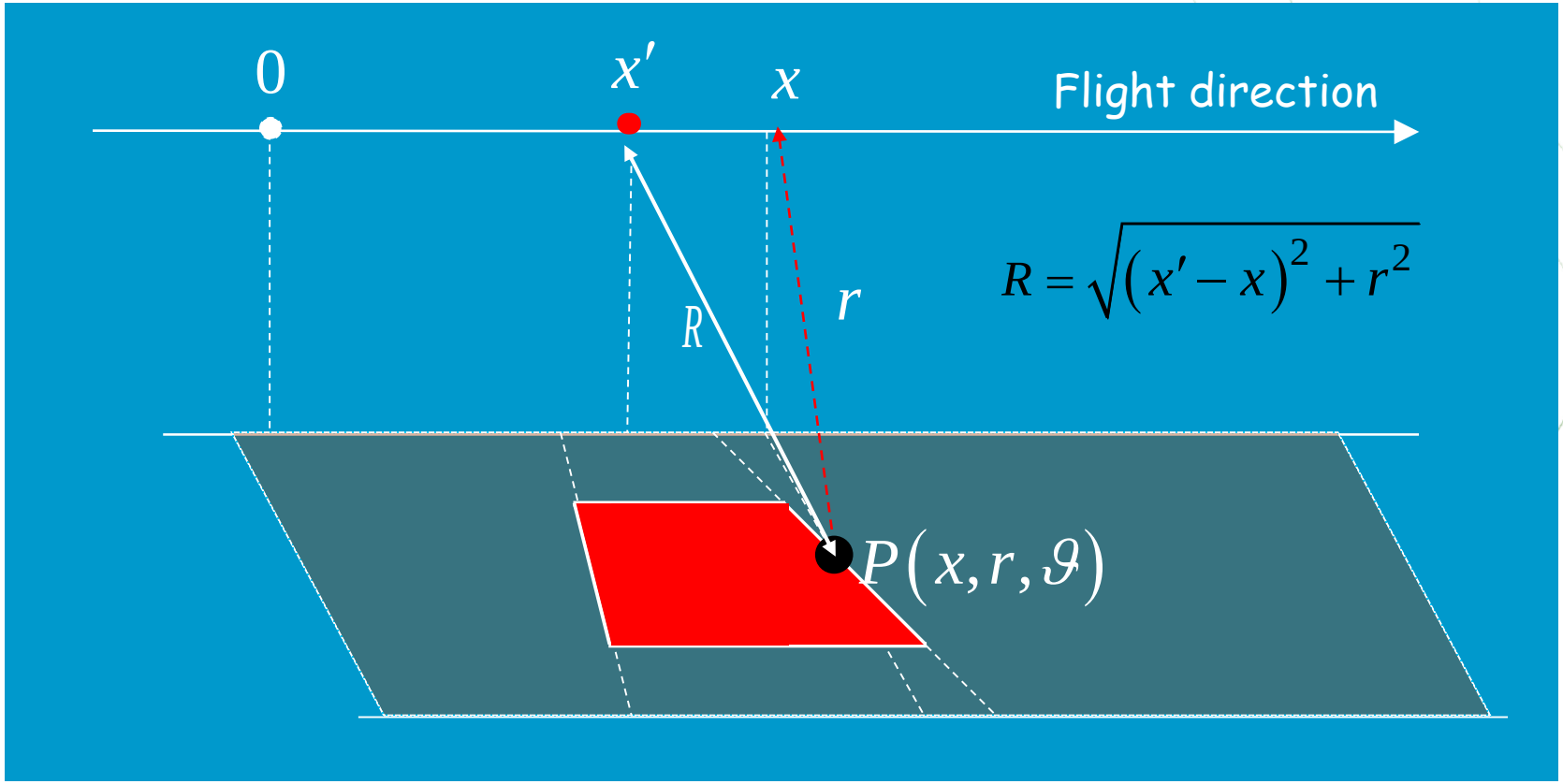

SAR Raw Data

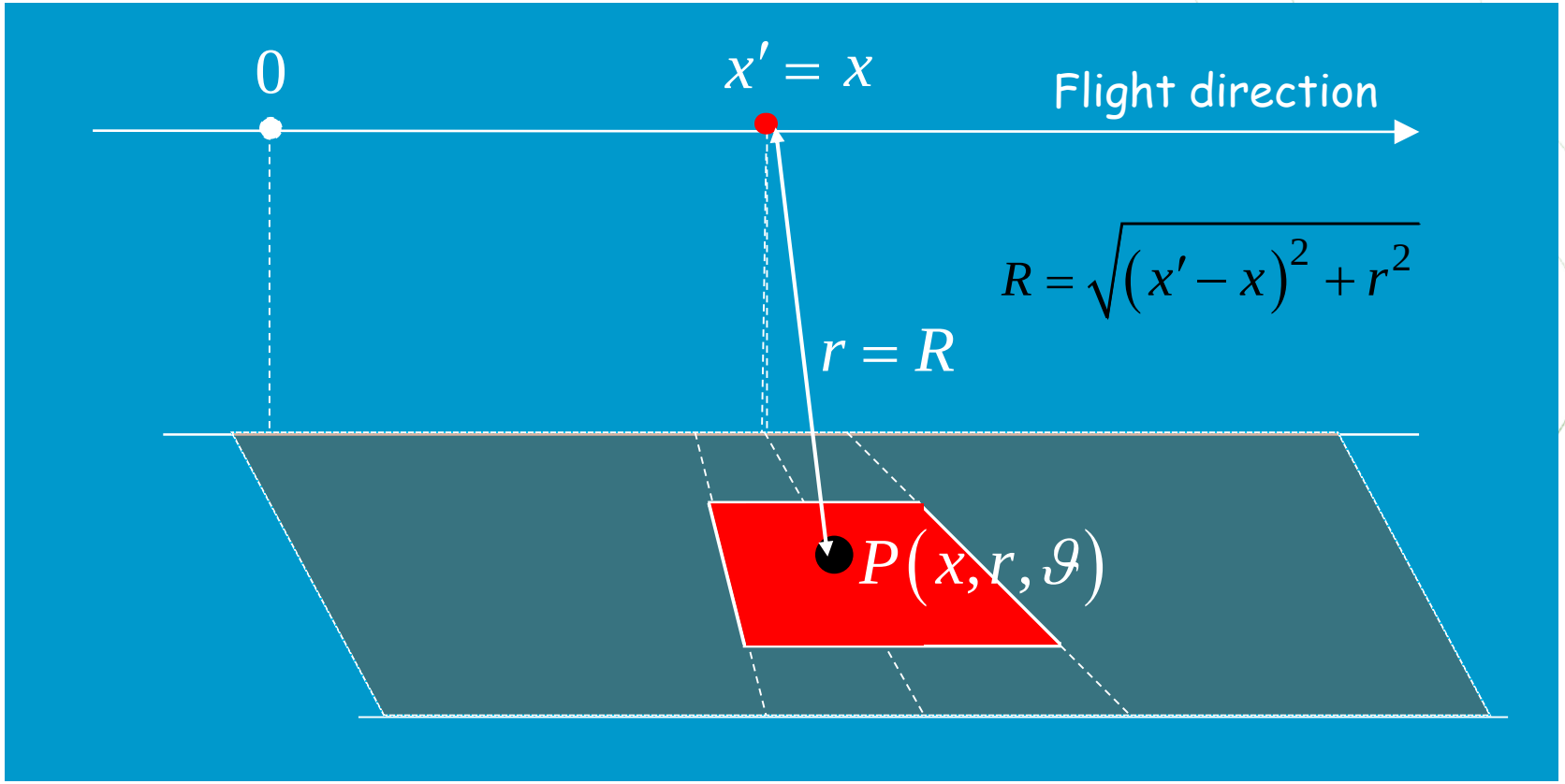

SAR Raw Data

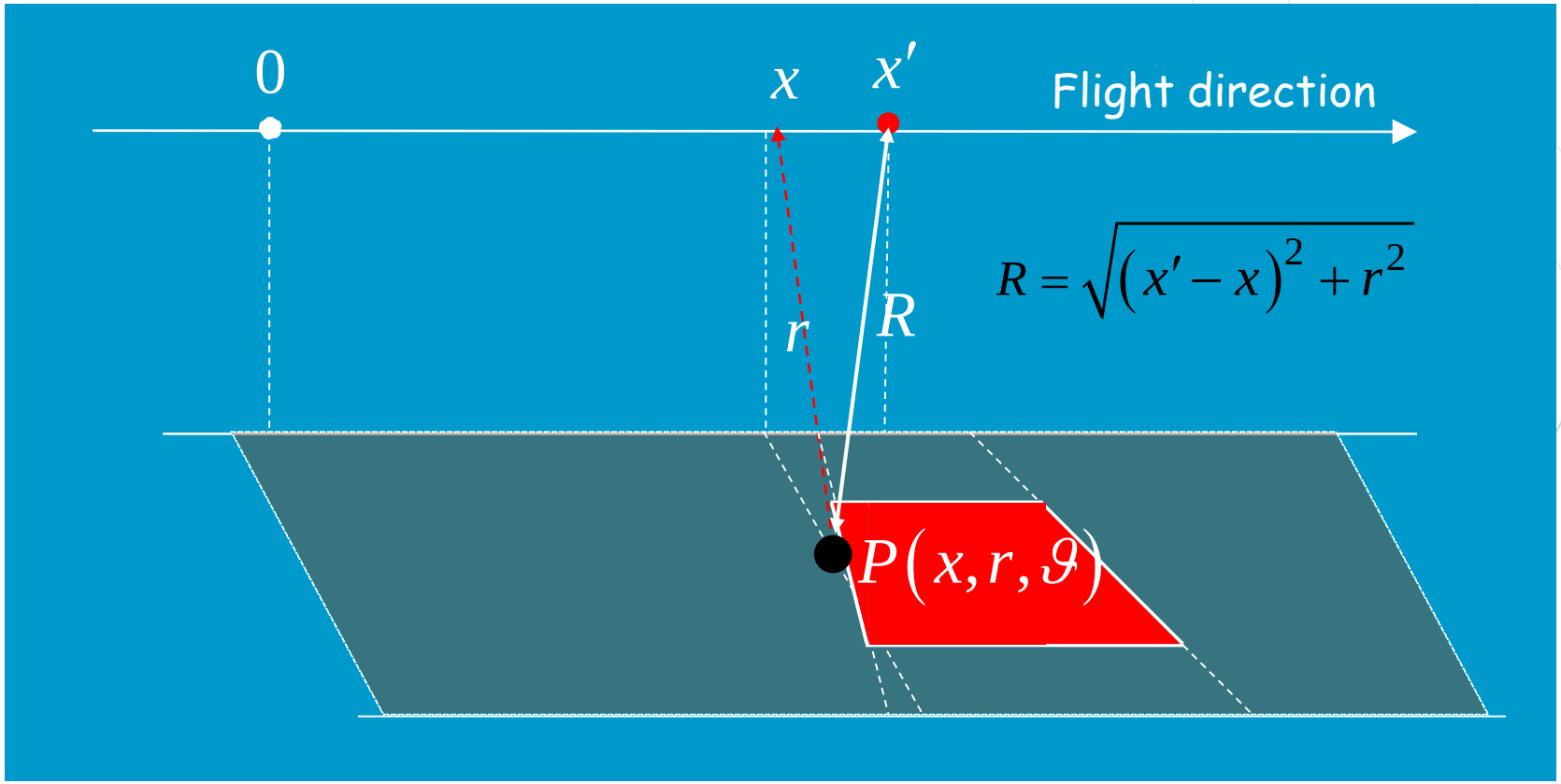

SAR Raw Data

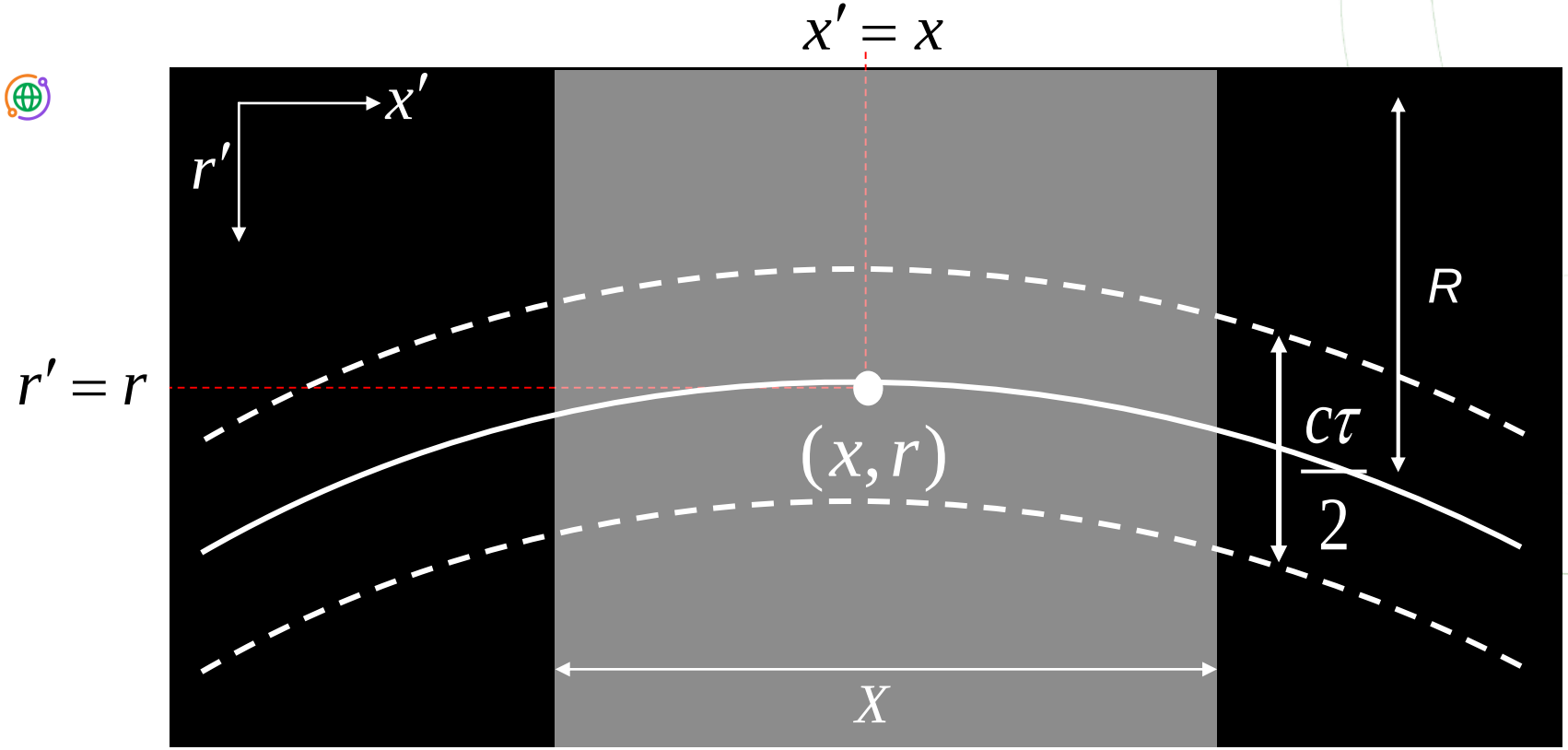

If we transmit a pulse with time duration τ, in the presence of a single target I will receive a pulse of the same duration τ.

From the time-to-space conversion rule

$$space = \frac{c}{2} time$$

we will achieve

$$space\ duration = \frac{c}{2}\tau$$

Which pixels are switched on in the image?

Only the one highlighted in the figure? Sure?

SAR Raw Data

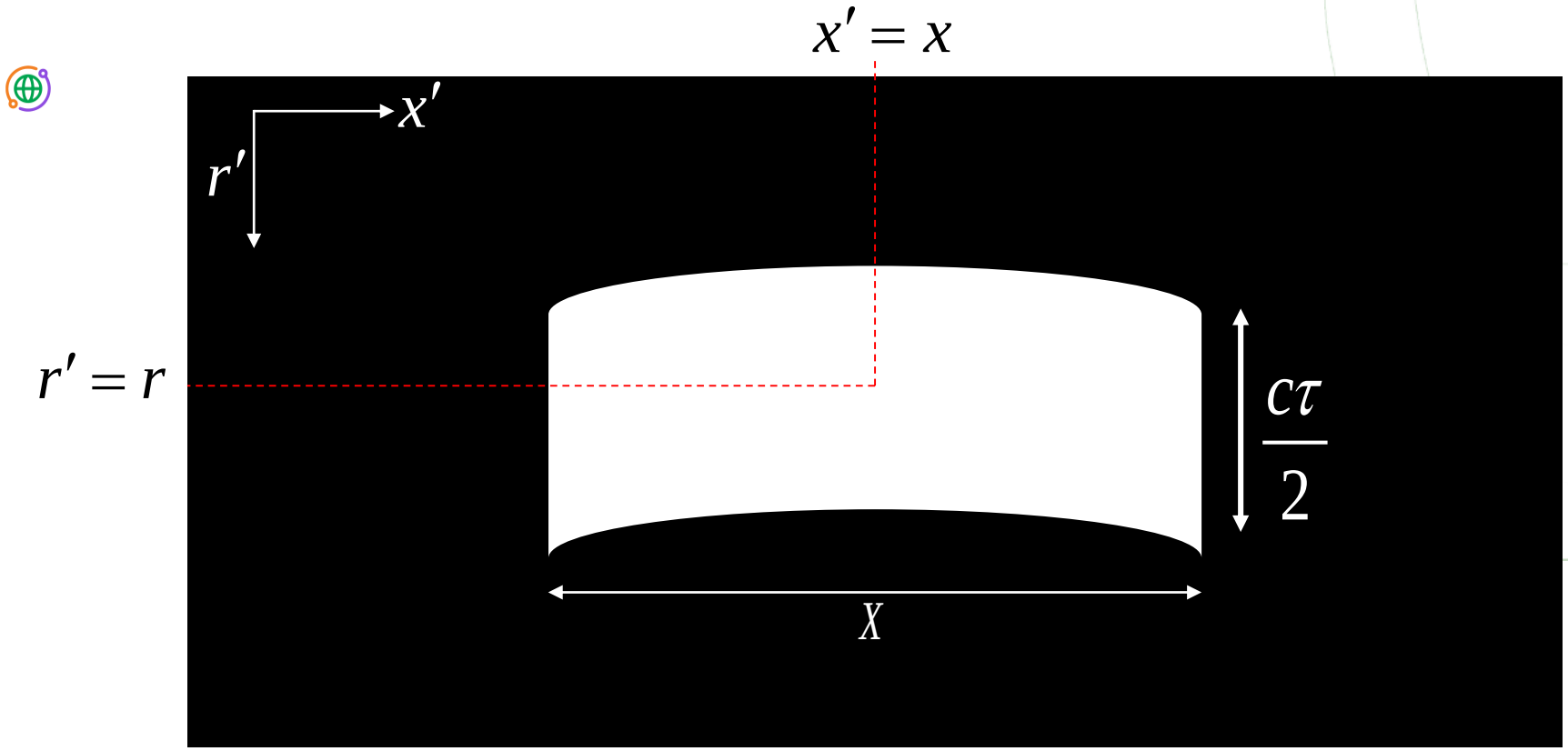

SAR Raw Data

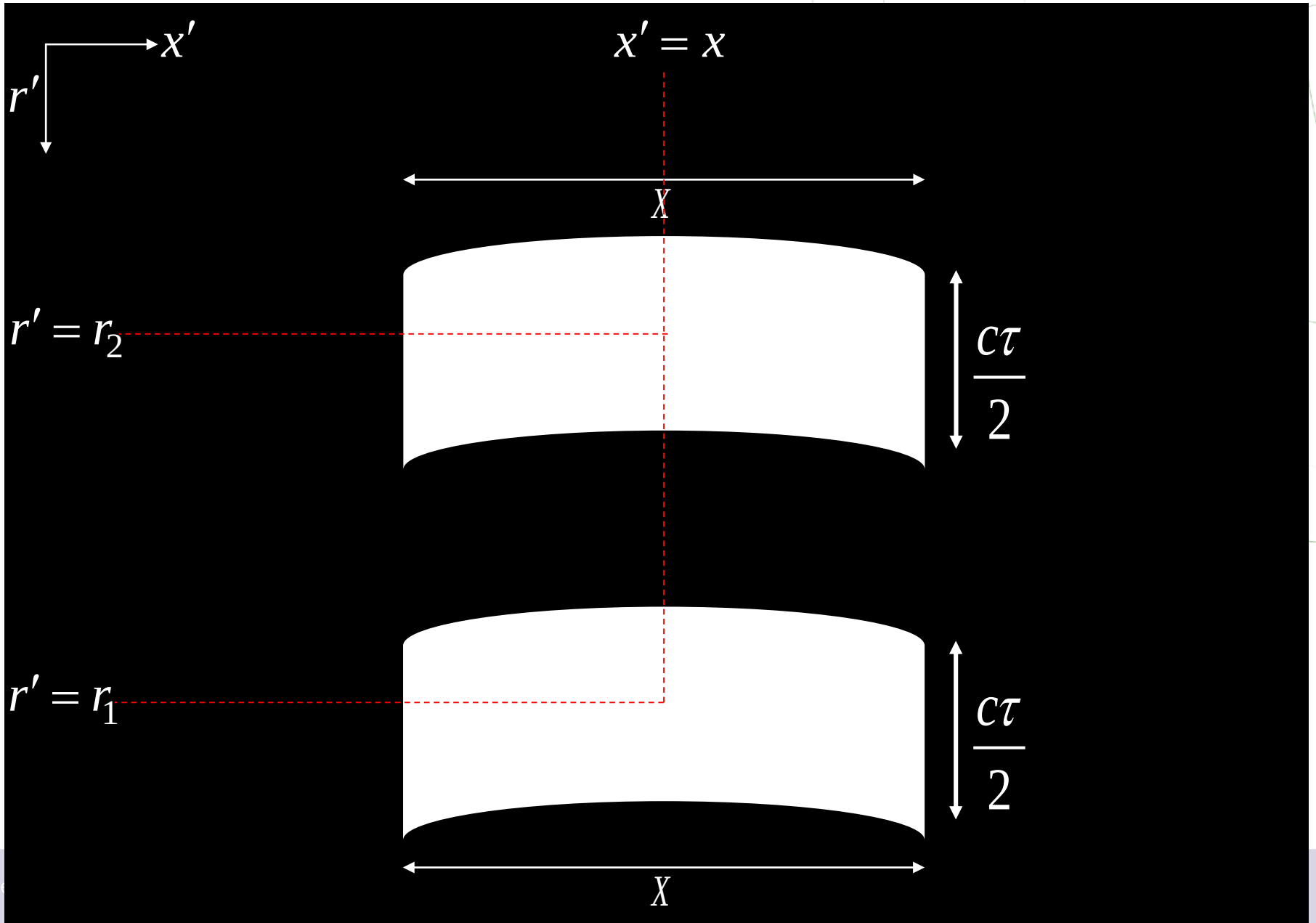

SAR Raw Data

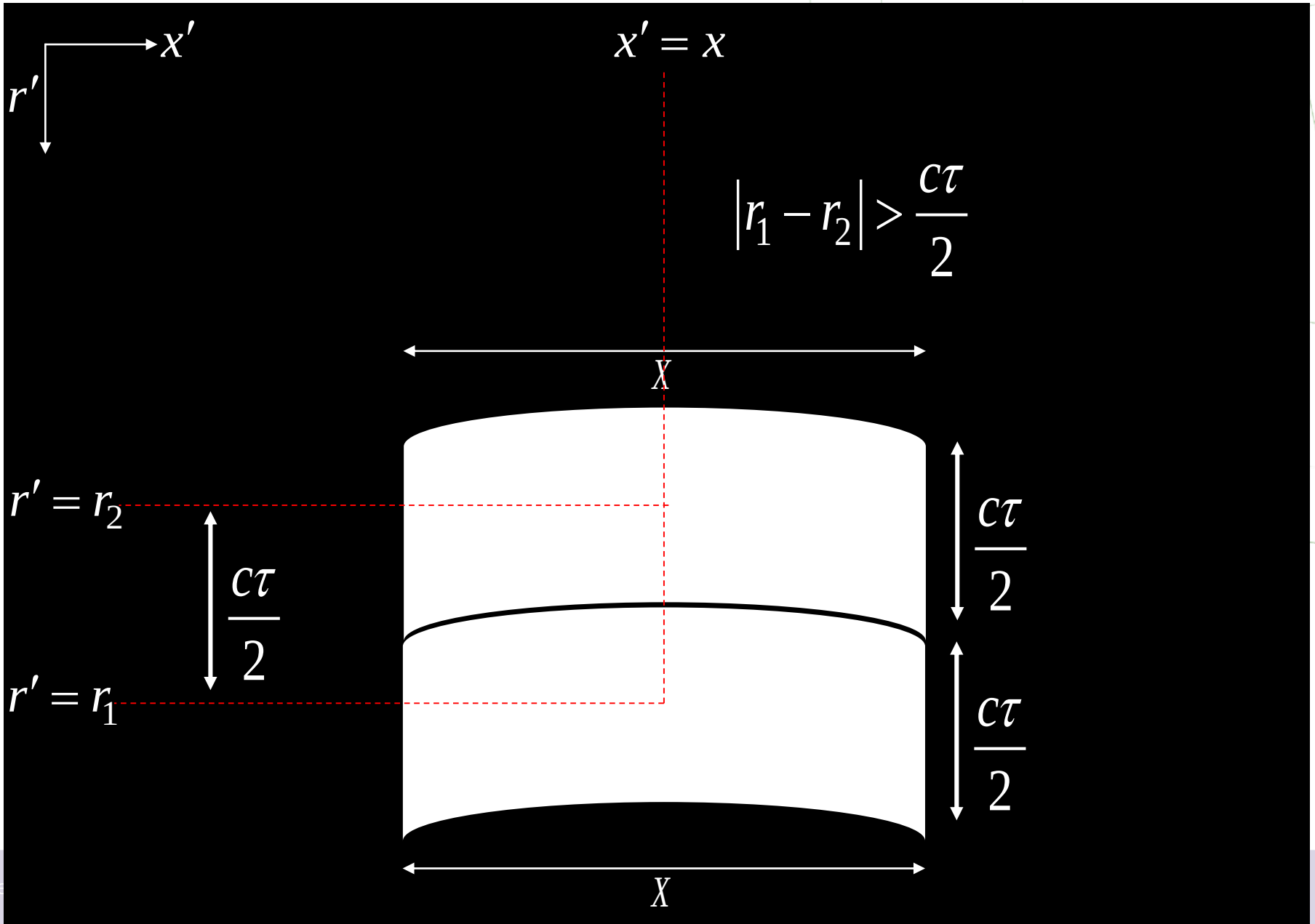
x'
r'
$x' = x$
$|r_1 - r_2| > \frac{c\tau}{2}$
X
$r' = r_2$
$\frac{c\tau}{2}$
$r' = r_1$
$\frac{c\tau}{2}$
$\frac{c\tau}{2}$
X

SAR Raw Data

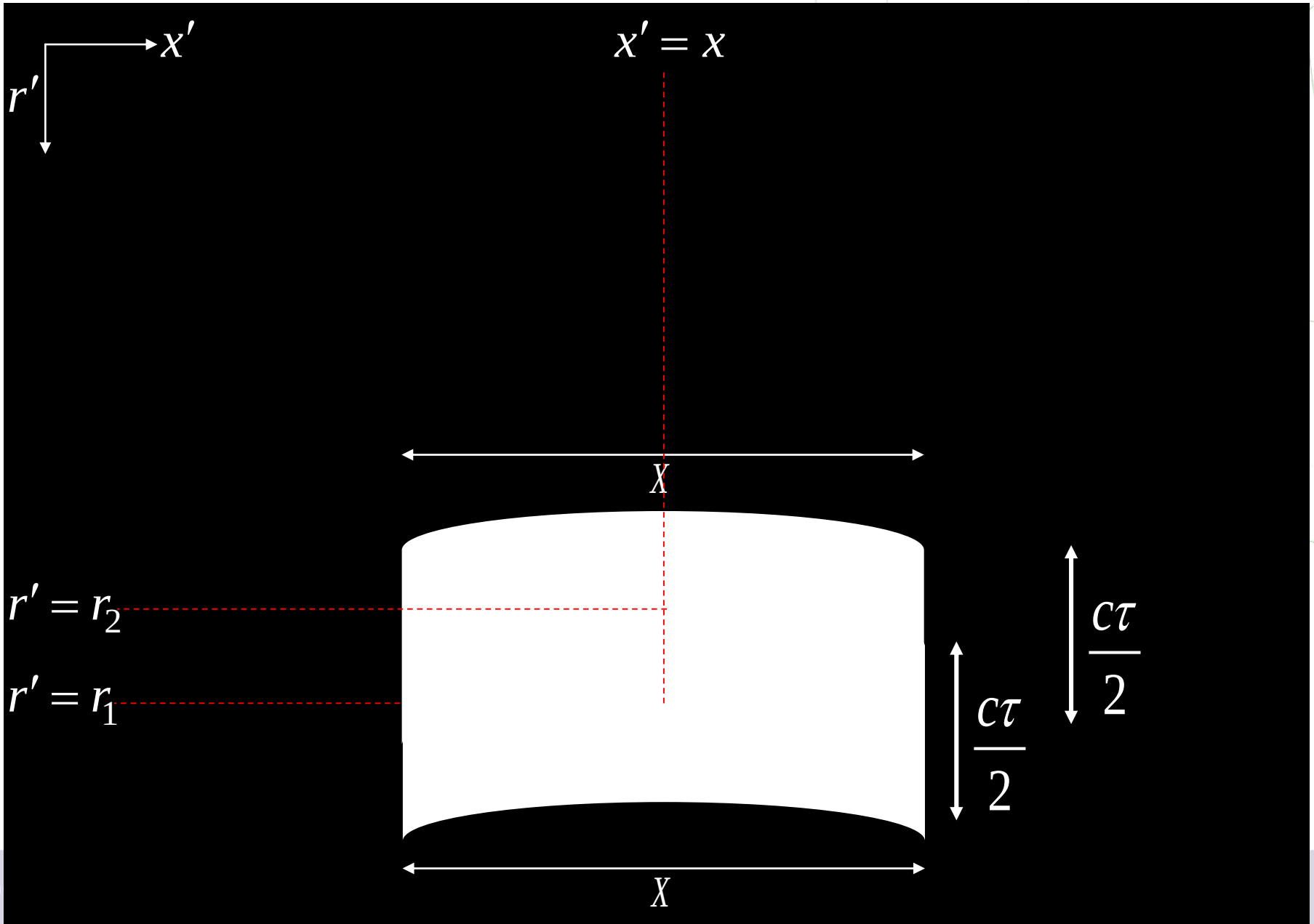

Geometric resolution (of the raw data)

Range resolution

$$\Delta r_{raw} = \frac{c\tau}{2}$$

Azimuth resolution

SAR Raw Data

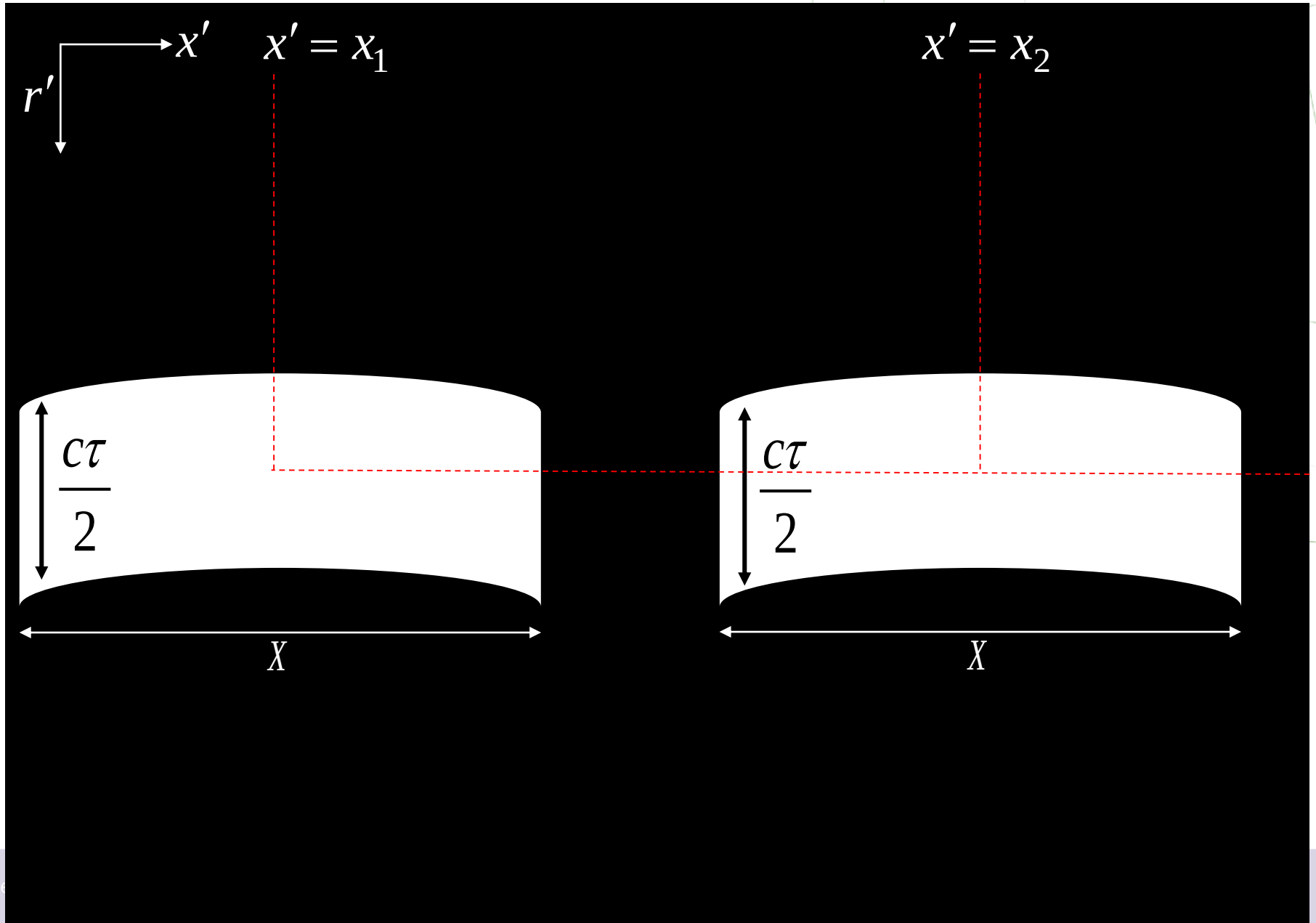

SAR Raw Data

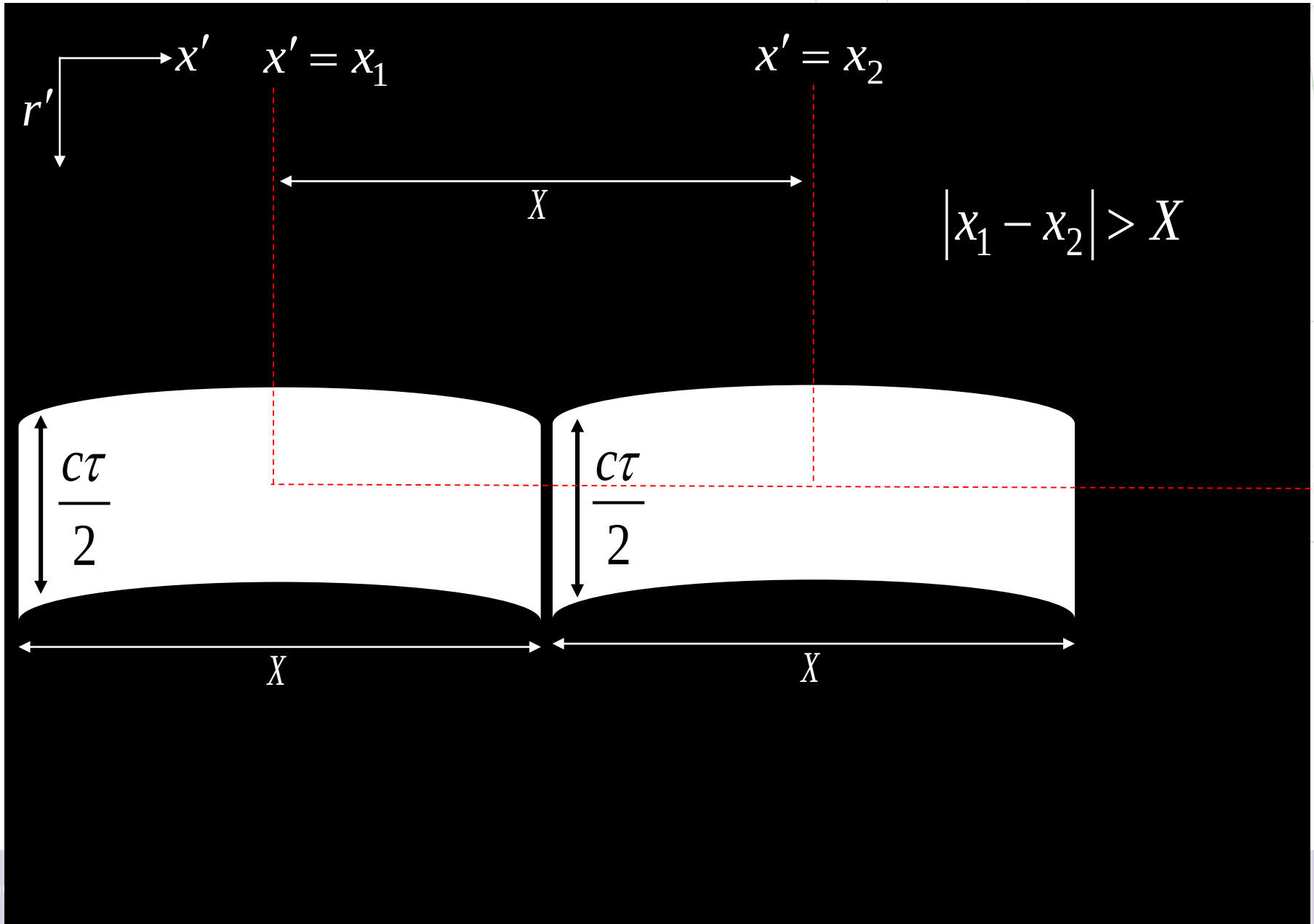

SAR Raw Data

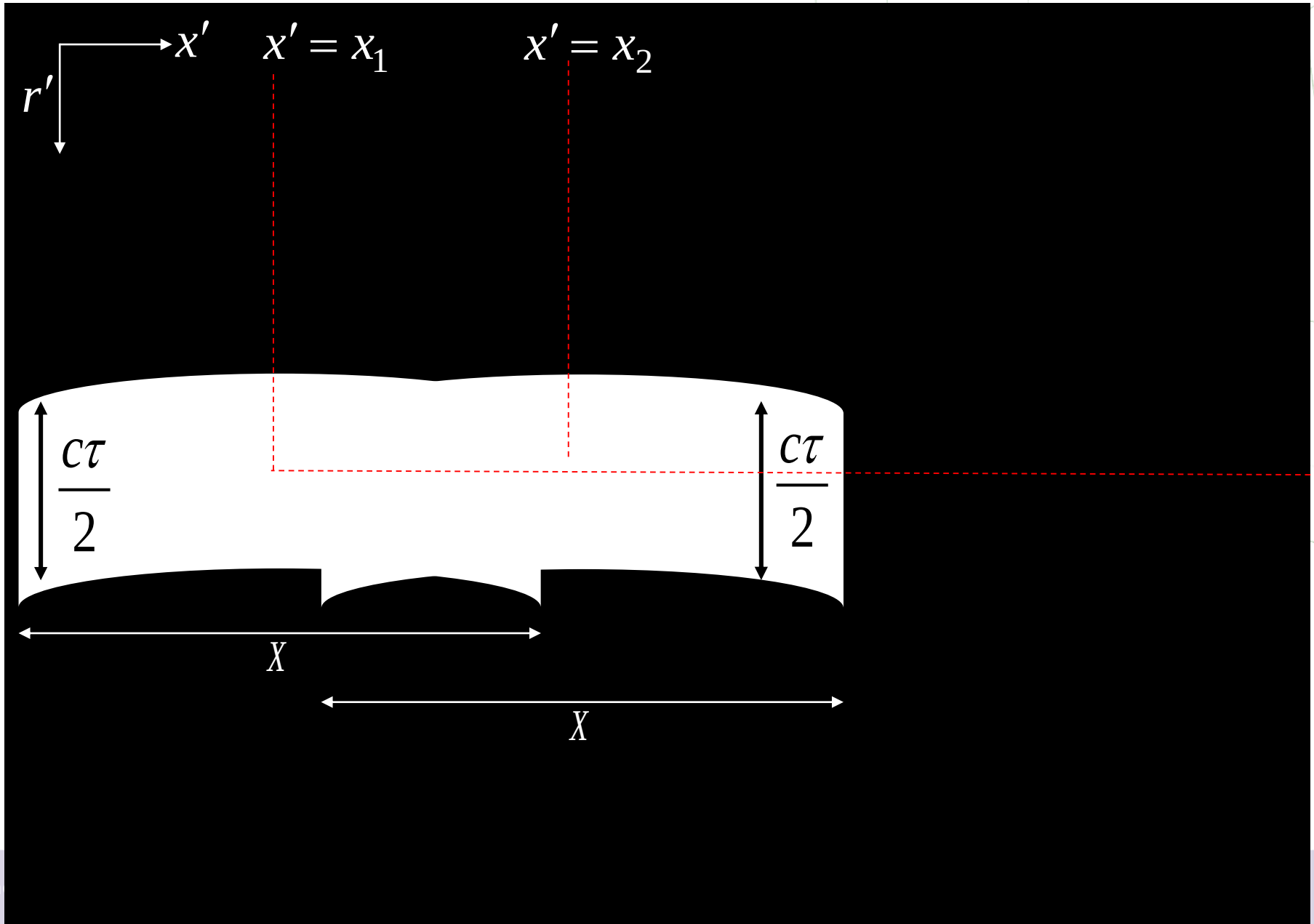

SAR Raw Data

Geometric resolution (of the raw data)

Range resolution $\Delta r_{raw} = \frac{c\tau}{2}$

Azimuth resolution $\Delta x_{raw} = X$

Geometric resolution (of the raw data)

Cosmo-SkyMed Parameters

Range resolution $\Delta r_{raw} = \frac{c\tau}{2} = 6\ \mathrm{Km}$

Azimuth resolution $\Delta x_{raw} = X = 5\ \mathrm{Km}$

SUMMARY

Synthetic Aperture Radar (SAR)

Geometry

SAR Raw Data

Geometric Resolution

SAR focusing

SAR Interferometry (InSAR)

DInSAR

An Airborne InSAR experiment

SAR Focusing

$$\Delta x_{raw} = X$$

$$\Delta r_{raw} = \frac{c\tau}{2}$$

Raw data

SAR Focusing

$$\Delta x_{raw} = X$$

$$\Delta r_{raw} = \frac{c\tau}{2}$$

Raw data

SAR FOCUSING

Focused data

Antenna length

$$\Delta x = \frac{L_x}{2}$$

Speed of the light

$$\Delta r = \frac{c}{2\Delta f}$$

Bandwidth of the TX signal

Geometric resolution (of the raw data)

Cosmo-SkyMed Parameters

Range resolution $\Delta r_{raw} = \frac{c\tau}{2} = 6\ \mathrm{Km}$

Azimuth resolution $\Delta x_{raw} = X = 5\ \mathrm{Km}$

Geometric resolution (of the focused data)

Cosmo-SkyMed Parameters

Range resolution $\Delta r = \frac{c}{2\Delta f} = 1.4\ \mathrm{m}$

Azimuth resolution $\Delta x = \frac{L_x}{2} = 3\ \mathrm{m}$

Synthetic Aperture Concept

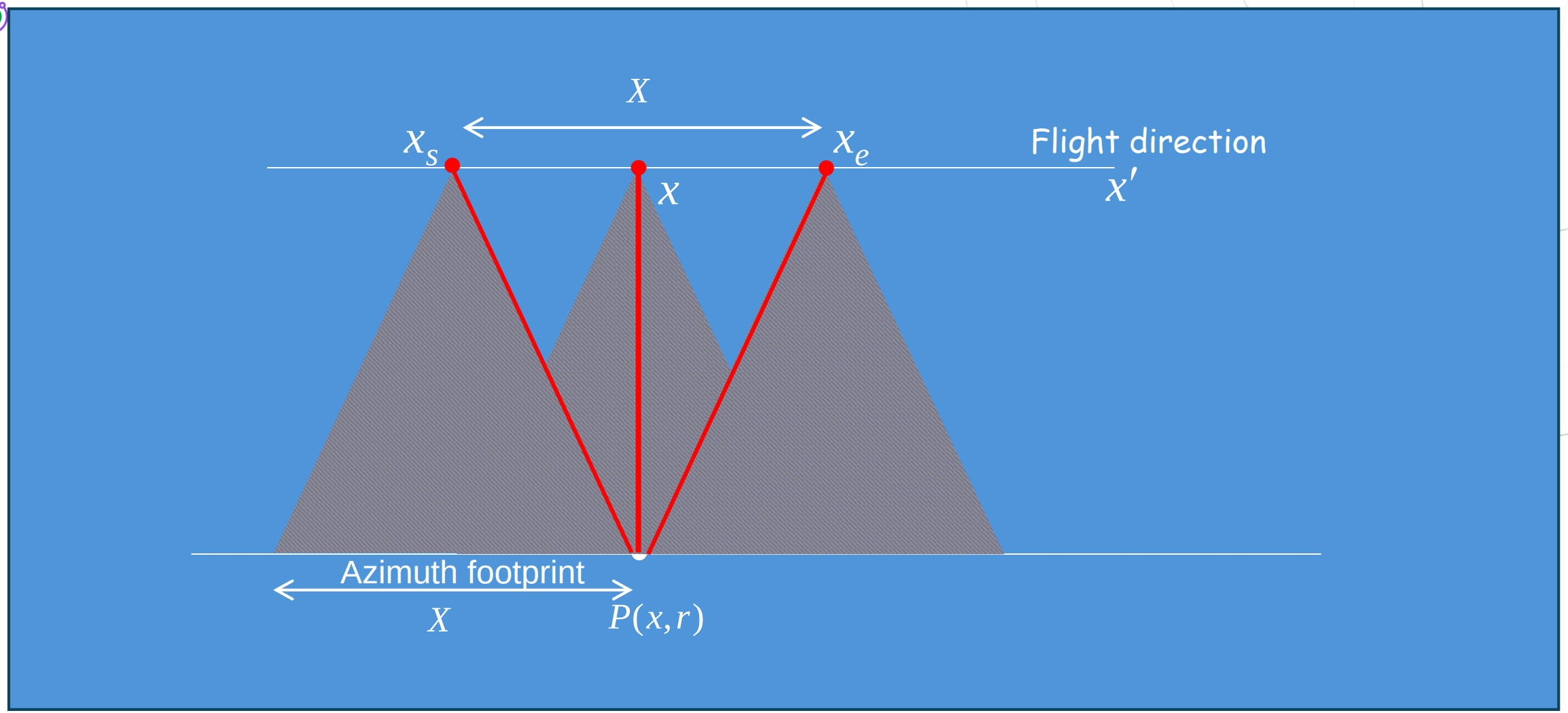

SAR Focusing

Geometric resolution (of the raw data)

Raw data

$$\Delta x_{raw} = X$$

$$\Delta r_{raw} = \frac{c\tau}{2}$$

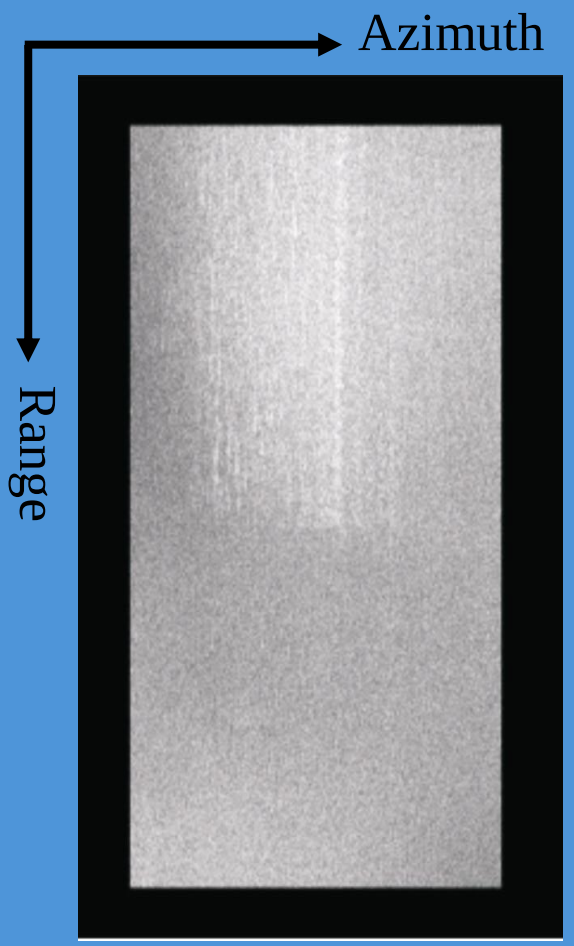

SAR Focusing

SAR FOCUSING

Raw data

SAR FOCUSING

Focused data

$$\Delta x_{raw} = X$$

$$\Delta r_{raw} = \frac{c\tau}{2}$$

$$\Delta x = \frac{L_x}{2}$$

$$\Delta r = \frac{c}{2\Delta f}$$

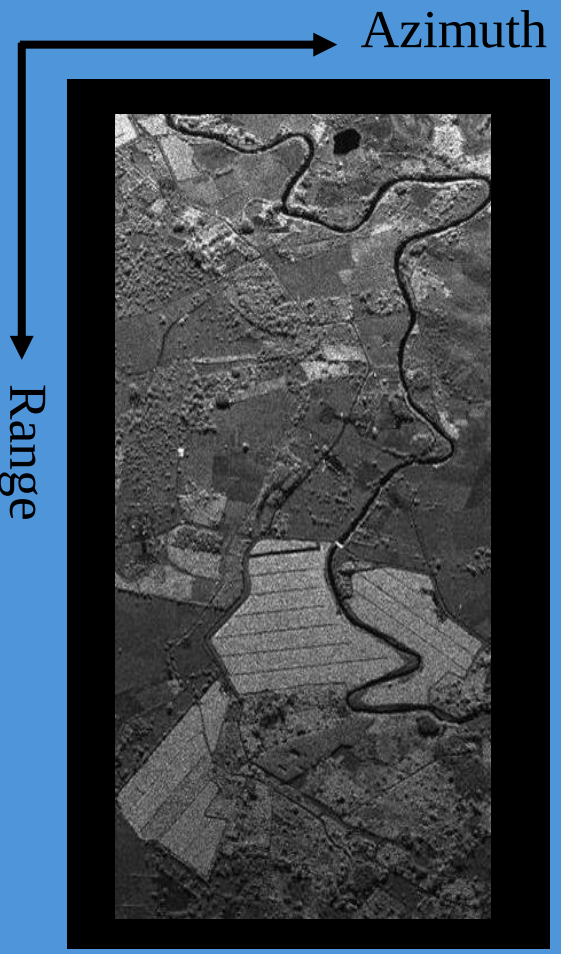

SAR Focusing

Are the SAR raw data coordinates (x',r')

related to the

(x,r) coordinates of the generic terrain target?

SAR Focusing

SAR FOCUSING

Raw data

SAR FOCUSING

Focused data

$$\Delta x = \frac{L_x}{2}$$

$$\Delta r = \frac{c}{2\Delta f}$$

$$\gamma(x,r)\exp\left[-j\frac{4\pi}{\lambda}r\right]$$

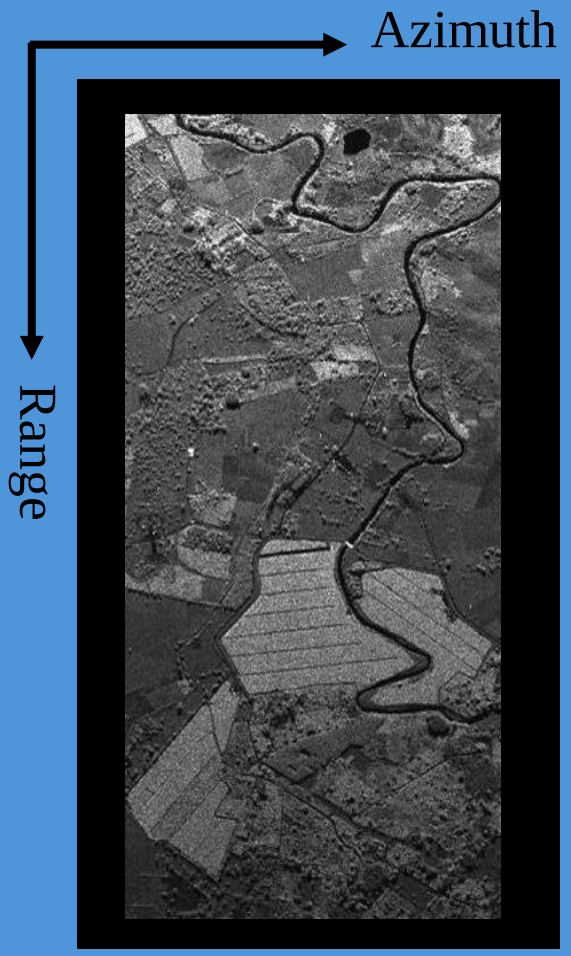

SAR Focusing

SAR FOCUSING

Raw data

SAR FOCUSING

Focused data

$$\Delta x = \frac{L_x}{2}$$

$$\Delta r = \frac{c}{2\Delta f}$$

$$\gamma(x,r)\exp\left[-j\frac{4\pi}{\lambda}r\right]$$

Reflectivity function, which accounts for the backscattering properties of the illuminated objects

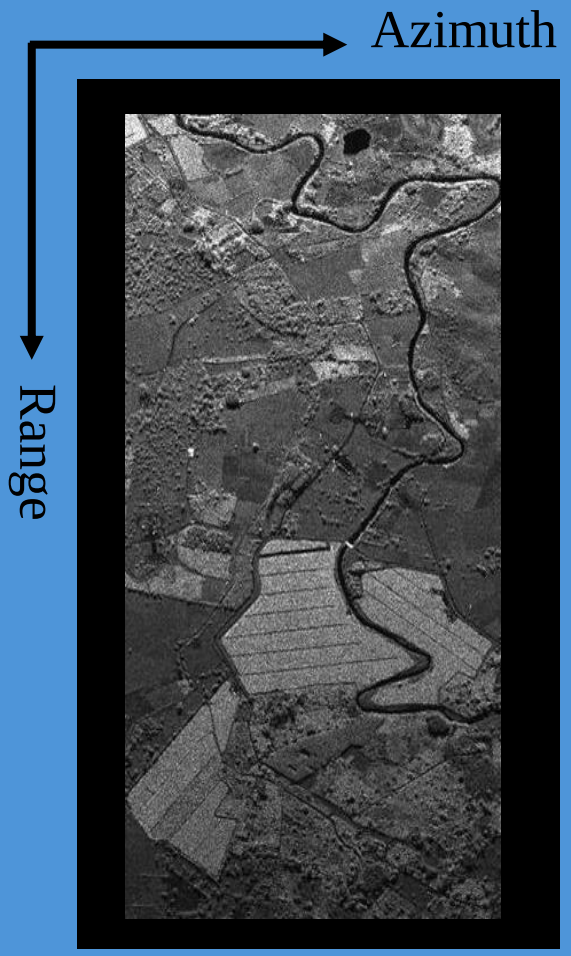

SAR Focusing

SAR FOCUSING

Raw data

SAR FOCUSING

Focused data

$$\Delta x = \frac{L_x}{2}$$

$$\Delta r = \frac{c}{2\Delta f}$$

$$\gamma(x,r)\exp\left[-j\frac{4\pi}{\lambda}r\right]$$

Wavelength

Reflectivity function, which accounts for the backscattering properties of the illuminated objects

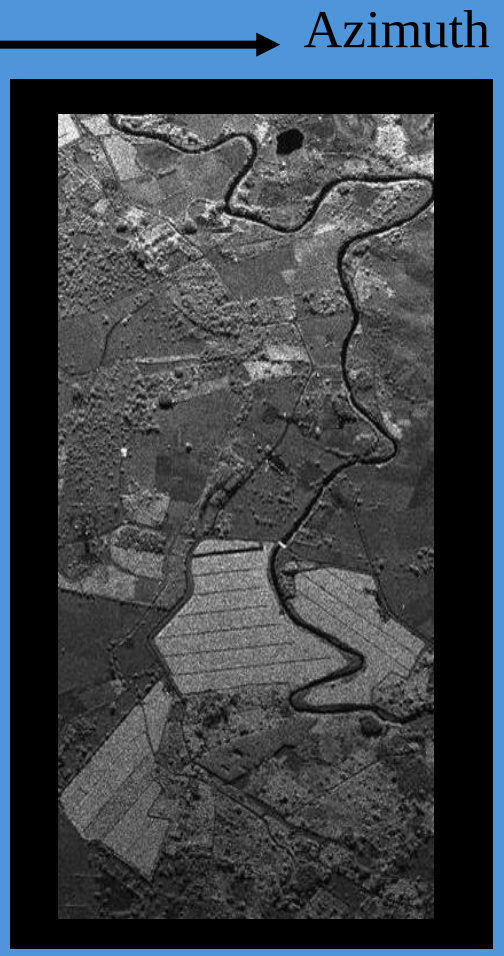

SAR Focusing

SAR FOCUSING

Raw data

SAR FOCUSING

Focused data

$$\Delta x = \frac{L_x}{2}$$

$$\Delta r = \frac{c}{2\Delta f}$$

$$\gamma(x,r)\exp\left[-j\frac{4\pi}{\lambda}r\right]$$

Reflectivity function, which accounts for the backscattering properties of the illuminated objects

Wavelength

Phase term, which accounts for the sensor-to-target distance … SAR systems are coherent radars

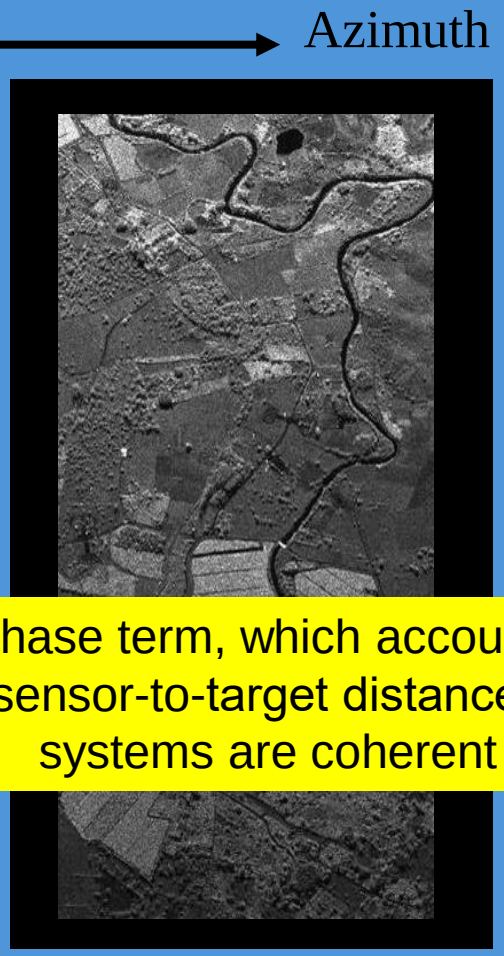

SAR Focusing

G.Franceschetti and R.Lanari; Synthetic Aperture Radar Processing, CRC PRESS, New York, 1999

SUMMARY

Synthetic Aperture Radar (SAR)

Geometry

SAR Raw Data

Geometric Resolution

SAR focusing

SAR Interferometry (InSAR)

DInSAR

An Airborne InSAR experiment

SAR Interferometry (InSAR)

Achieving the topography (z) requires knowledge of the angle θ

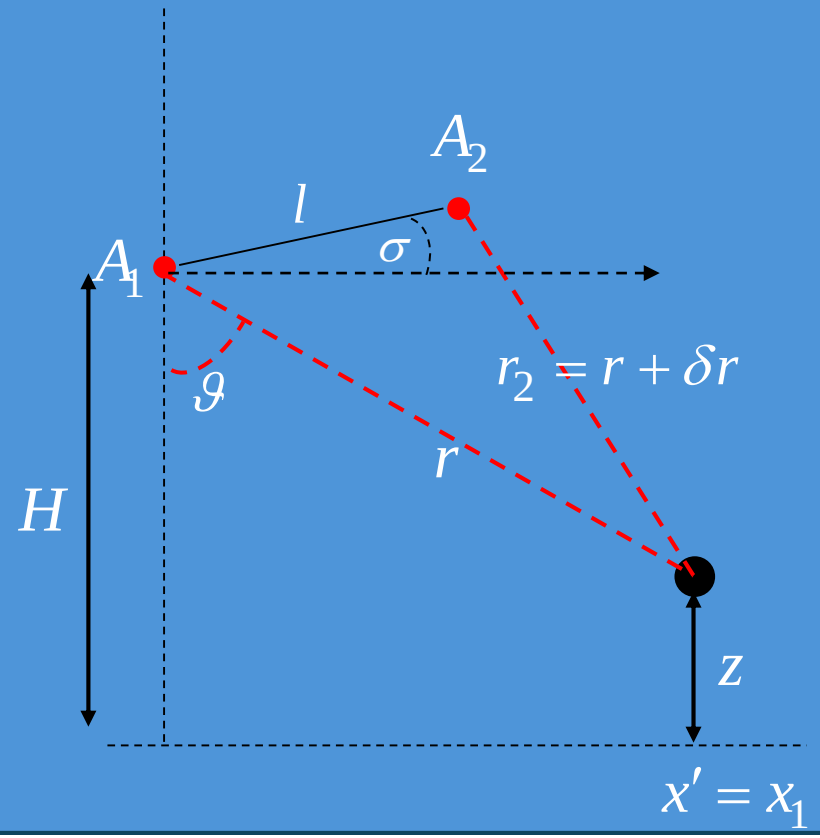

$$z = H - r\cos\vartheta \qquad \vartheta \rightarrow z$$

$$(r+\delta r)^2 = r^2 + l^2 - 2lr\sin(\vartheta - \sigma)$$

SAR Interferometry (InSAR)

Achieving the topography (z) requires knowledge of the angle θ

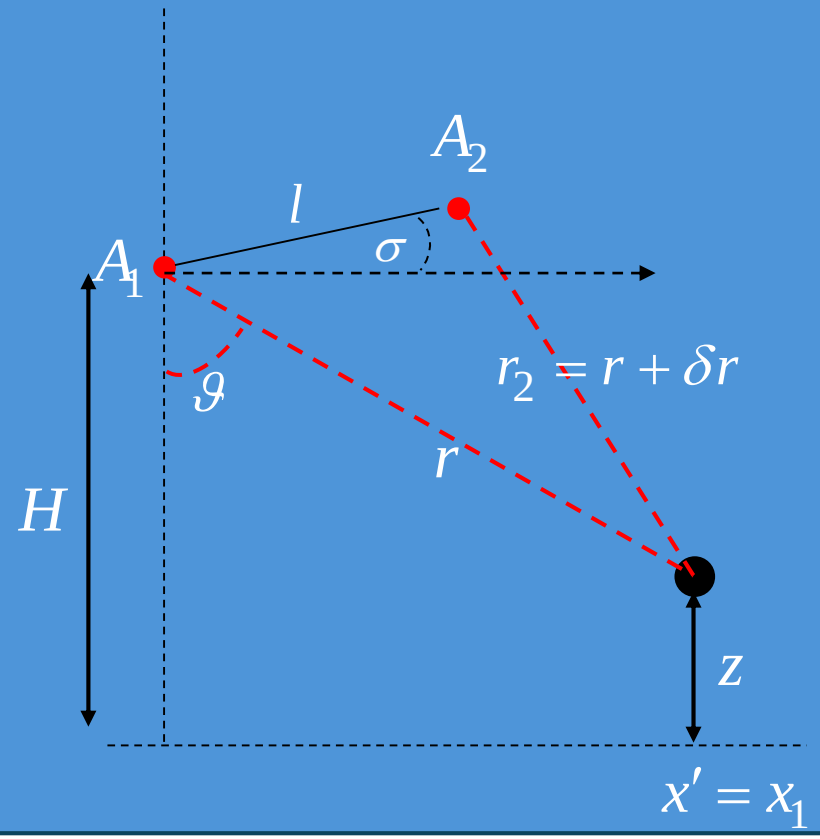

$$z = H - r\cos\vartheta \qquad \vartheta \rightarrow z$$

$$(r+\delta r)^2 = r^2 + l^2 - 2lr\sin(\vartheta - \sigma)$$

SAR Interferometry (InSAR)

Achieving the topography (z) requires knowledge of the angle θ

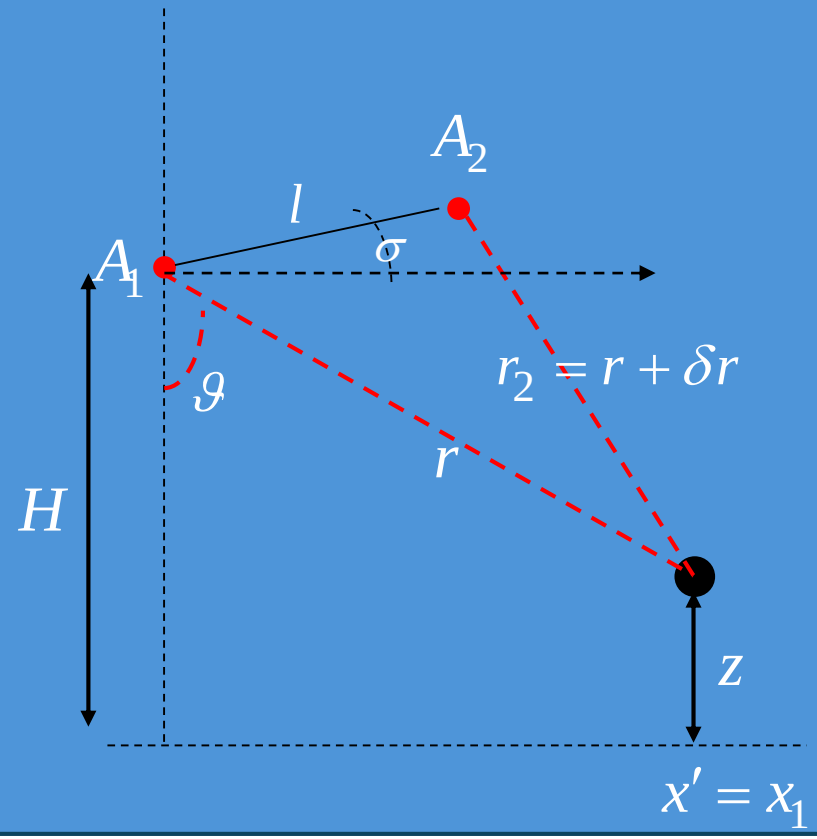

$$z = H - r\cos\vartheta \qquad \vartheta \rightarrow z$$

$$(r+\delta r)^2 = r^2 + l^2 - 2lr\sin(\vartheta - \sigma)$$

SAR Interferometry (InSAR)

Achieving the topography (z) requires knowledge of the angle θ

$$\delta r \approx l \sin(\vartheta - \sigma)$$

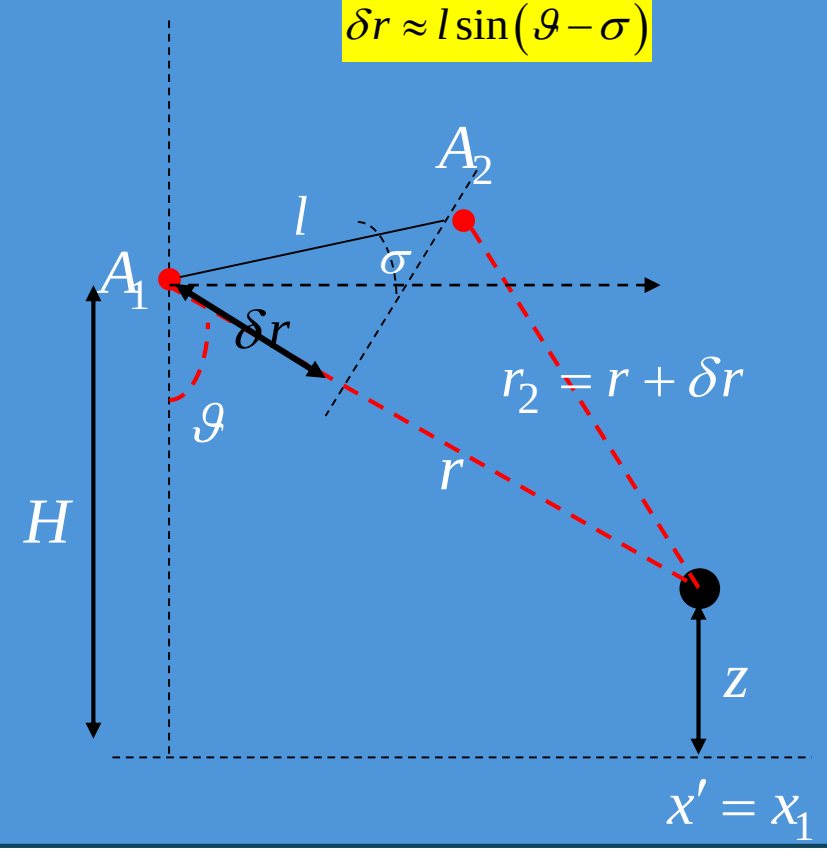

$$z = H - r\cos\vartheta \qquad \vartheta \rightarrow z$$

$$(r + \delta r)^2 = r^2 + l^2 - 2lr\sin(\vartheta - \sigma)$$

$$\begin{cases} H \\ l \\ \sigma \end{cases} + \begin{cases} r \\ r_2 = r + \delta r \end{cases} \rightarrow \vartheta \rightarrow z$$

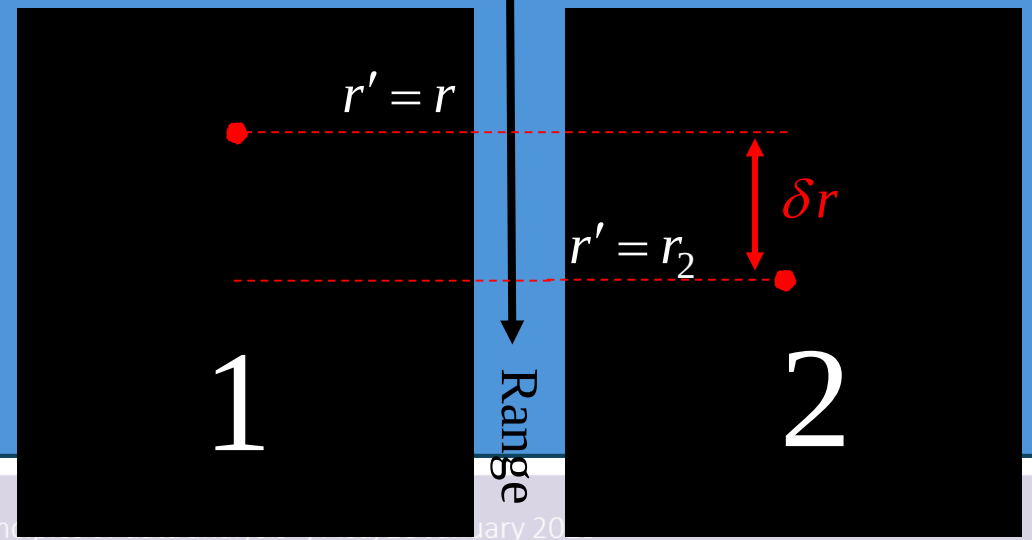

SAR Interferometry (InSAR)

Achieving the topography (z) requires knowledge of the angle θ

To this aim, we need 2 images of the same scene from two different view angles

$$\begin{cases} H \\ l \\ \sigma \end{cases} + \delta r \rightarrow \vartheta \rightarrow z$$

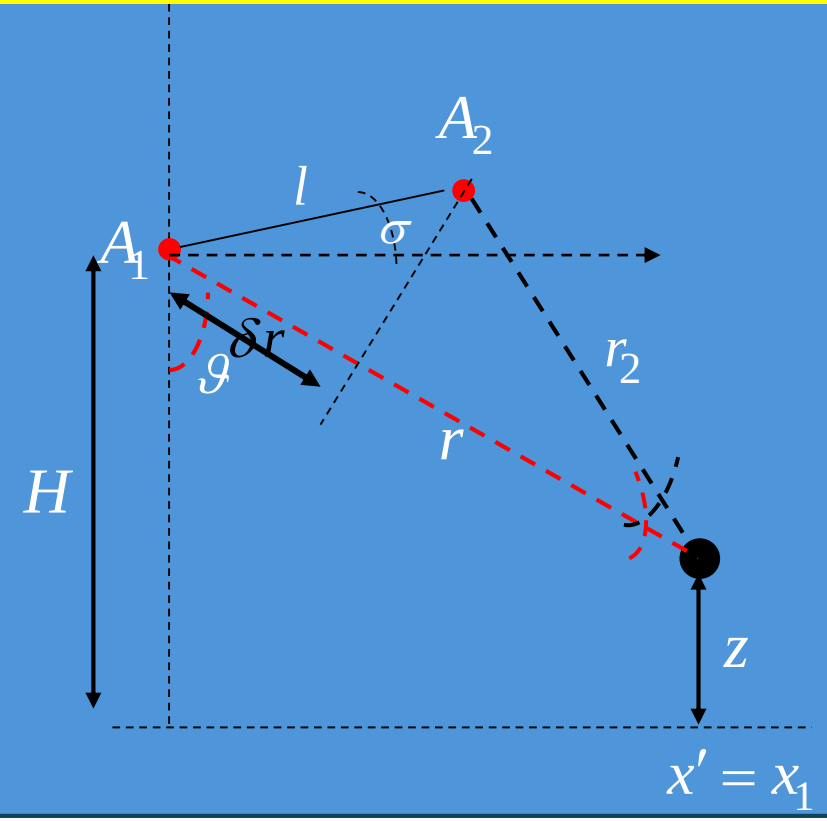

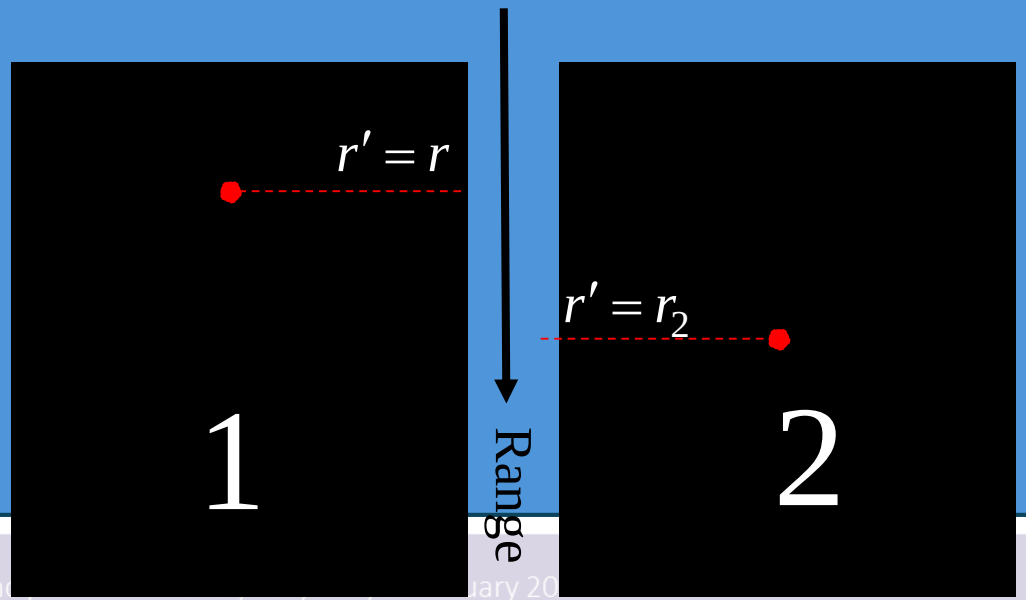

SAR Interferometry (InSAR)

The term δr can be obtained by looking for the same target in the two images …

… the achieved accuracy is on the order of the range resolution, that is, on the order of meters

SAR Interferometry (InSAR)

$$\begin{cases} z = H - r\cos\vartheta \\ \delta r \approx l\sin(\vartheta - \sigma) \end{cases}$$

$$\frac{\partial z}{\partial \delta r} = \frac{\partial z}{\partial \vartheta}\frac{\partial \vartheta}{\partial \delta r} \approx \frac{r\sin\vartheta}{l\cos(\vartheta-\sigma)} = \frac{r\sin(\vartheta)}{l_\perp}$$

$$err(z) = \frac{r\sin(\vartheta)}{l_\perp} err(\delta r)$$

Unfortunately, an upper bound exists for the baseline, over which the two images of the interferometer become completely uncorrelated

$$l_\perp < \frac{\lambda r_0}{2\mathrm{ctg}(\vartheta_0)\cdot\Delta r}$$

AIRBORNE SAR GEOMETRY

$$\begin{cases} \vartheta \approx 45^o \\ r = 10\,Km \\ l_\perp \approx 3m \end{cases} \Rightarrow \frac{r\sin(\vartheta)}{l_\perp} \approx 2300$$

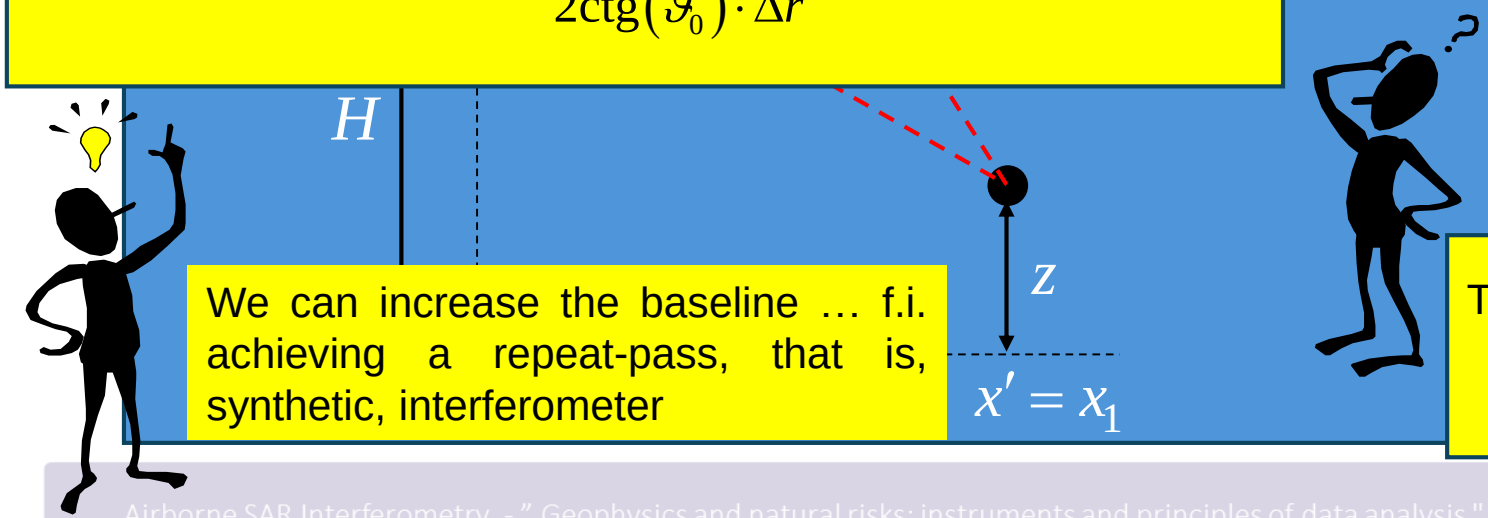

We can increase the baseline … f.i. achieving a repeat-pass, that is, synthetic, interferometer

The measurement error on δr is amplified of three orders of magnitude onto the topography measurement error

SAR Interferometry (InSAR)

Unfortunately, an upper bound exists for the baseline, over which the two images of the interferometer become completely uncorrelated

Wavelength

$$l_{\perp} < \frac{\lambda r_0}{2\mathrm{ctg}(\vartheta_0)\cdot\Delta r}$$

Range resolution of the system

SAR Interferometry (InSAR)

$$\begin{cases} z = H - r\cos\vartheta \\ \delta r \approx l\sin(\vartheta - \sigma) \end{cases}$$

$$\frac{\partial z}{\partial \delta r} = \frac{\partial z}{\partial \vartheta}\frac{\partial \vartheta}{\partial \delta r} \approx \frac{r\sin\vartheta}{l\cos(\vartheta-\sigma)} = \frac{r\sin(\vartheta)}{l_\perp}$$

$$err(z) = \frac{r\sin(\vartheta)}{l_\perp} err(\delta r)$$

Unfortunately, an upper bound exists for the baseline, over which the two images of the interferometer become completely uncorrelated

$$l_\perp < \frac{\lambda r_0}{2\mathrm{ctg}(\vartheta_0)\cdot\Delta r}$$

AIRBORNE SAR GEOMETRY

$$\begin{cases} \vartheta \approx 45^o \\ r = 10\,Km \\ l_\perp \approx 3m \end{cases} \Rightarrow \frac{r\sin(\vartheta)}{l_\perp} \approx 2300$$

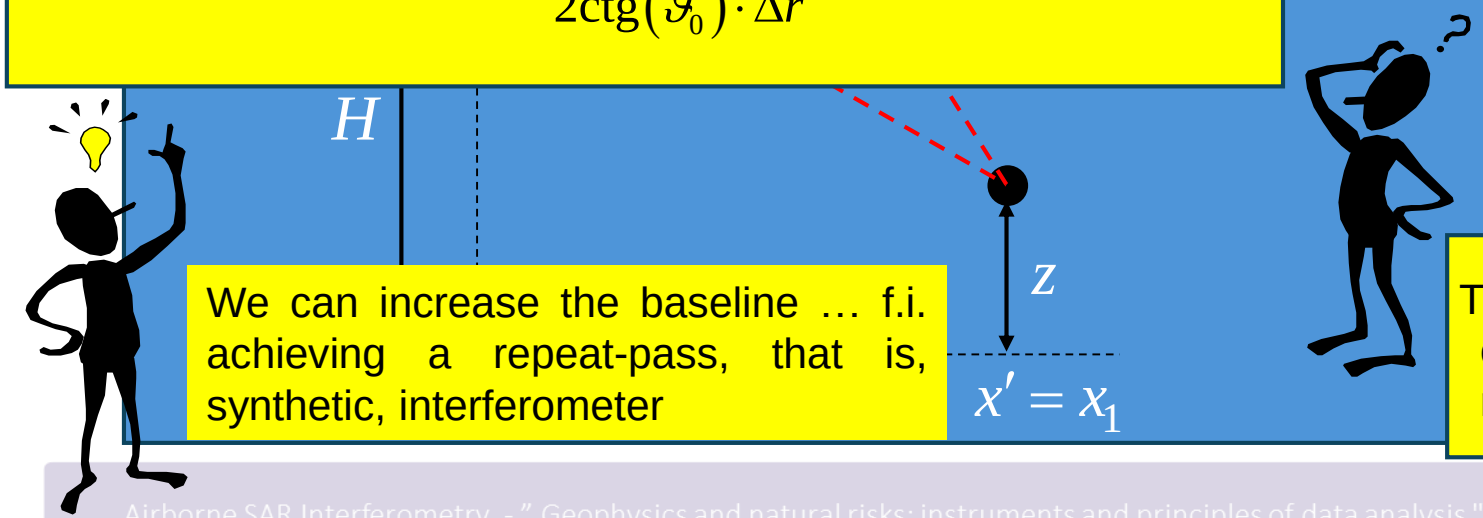

We can increase the baseline … f.i. achieving a repeat-pass, that is, synthetic, interferometer

The measurement error on δr is amplified of three orders of magnitude onto the topography measurement error

SAR Interferometry (InSAR)

$$\begin{cases} z = H - r\cos\vartheta \\ \delta r \approx l\sin(\vartheta - \sigma) \end{cases}$$

$$err(z) = \frac{r\sin(\vartheta)}{l_\perp} err(\delta r)$$

$$l_\perp < \frac{\lambda r_0}{2\,\mathrm{ctg}(\vartheta_0)\cdot\Delta r}$$

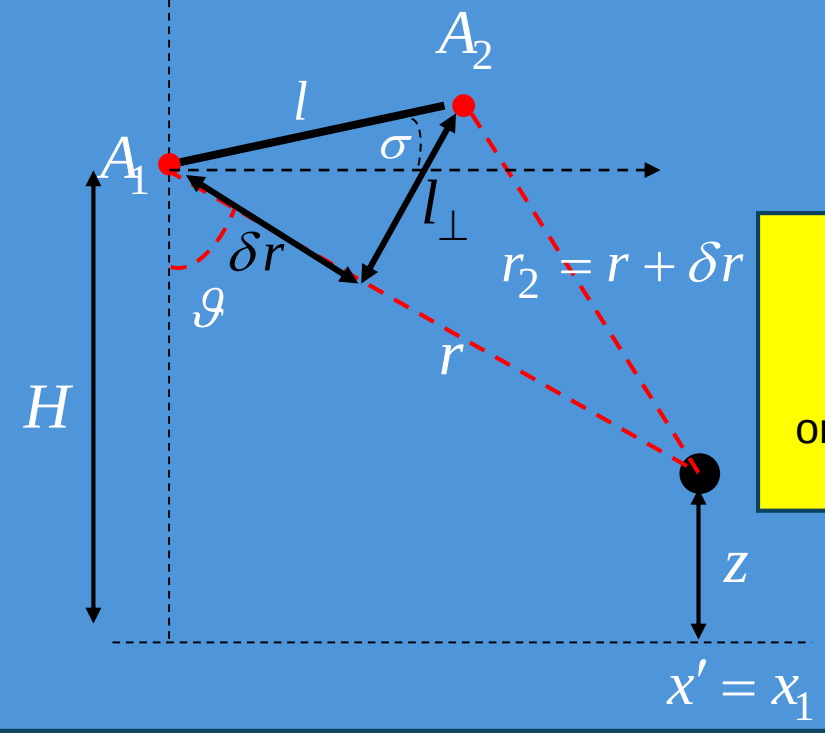

$$err(z) = \Delta r \frac{4\cos(\vartheta)}{\lambda} err(\delta r)$$

on the order of meters

on the order of centimeters

If we correctly design the interferometer, even squeezing the lemon, the measurement error on δr is in any case amplified of two orders of magnitude onto the topography measurement error

SAR Interferometry (InSAR)

$$\begin{cases} H \\ l \\ \sigma \end{cases} + \delta r \rightarrow \vartheta \rightarrow z$$

$$err(z) = \frac{r \sin(\vartheta)}{l_\perp} err(\delta r)$$

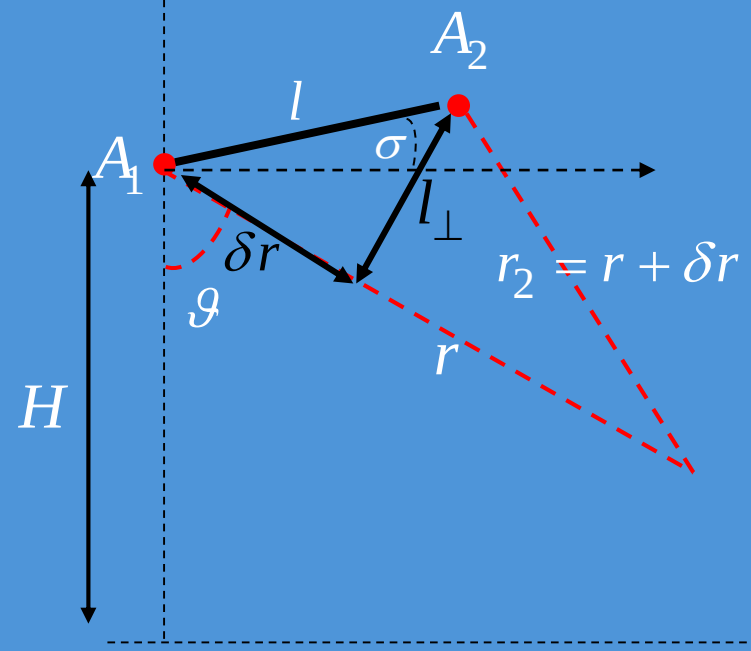

REGISTRATION

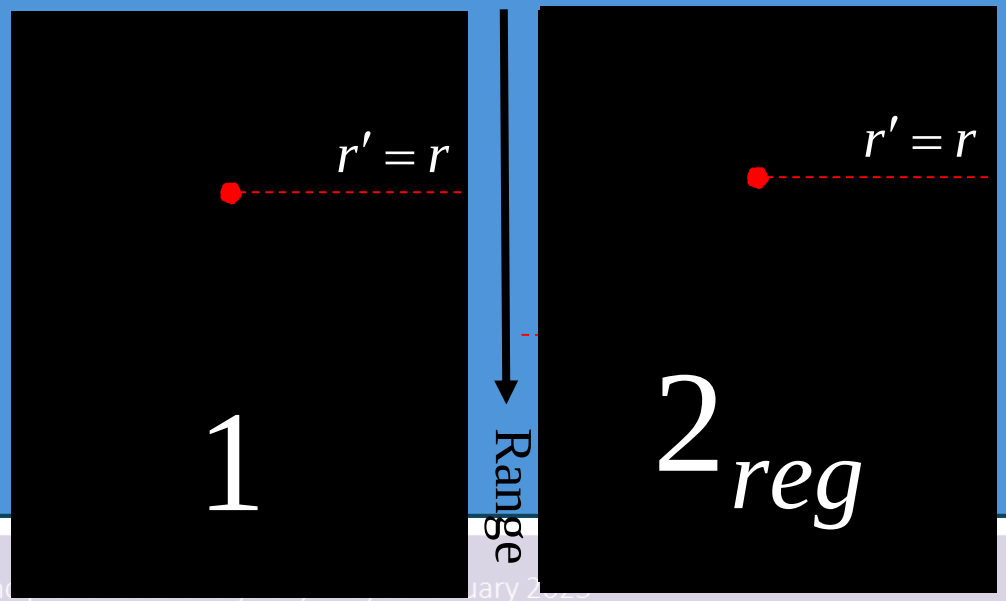

SAR Interferometry (InSAR)

$$\begin{cases} H \\ l \\ \sigma \end{cases} + \delta r \rightarrow \vartheta \rightarrow z$$

$$err(z) = \frac{r\sin(\vartheta)}{l_\perp} err(\delta r)$$

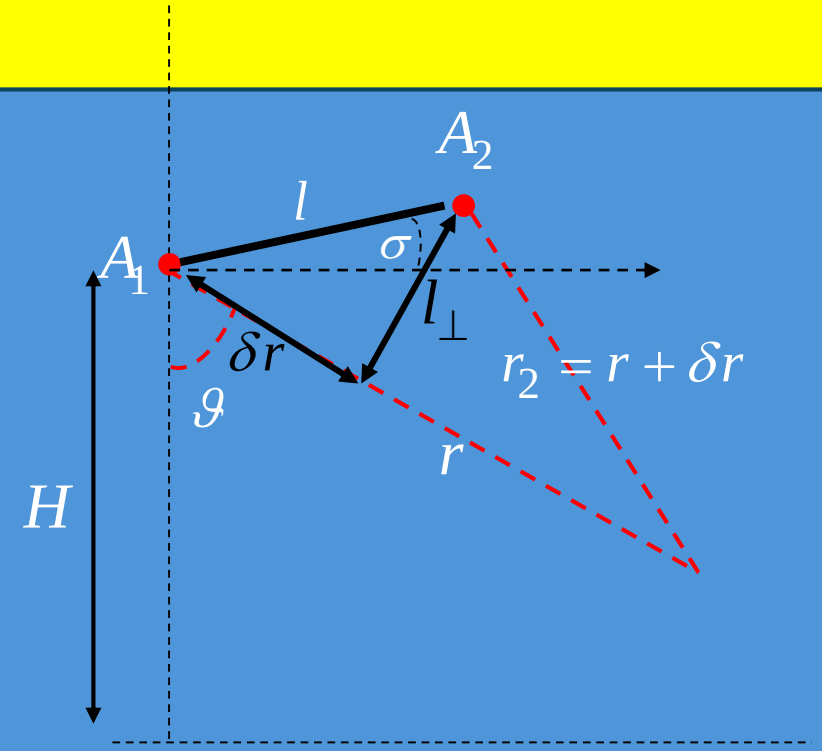

Image 1 : $\gamma(x,r)\exp\left[-j\frac{4\pi}{\lambda}r\right]$

Image 2 reg : $\gamma(x,r)\exp\left[-j\frac{4\pi}{\lambda}(r+\delta r)\right]$

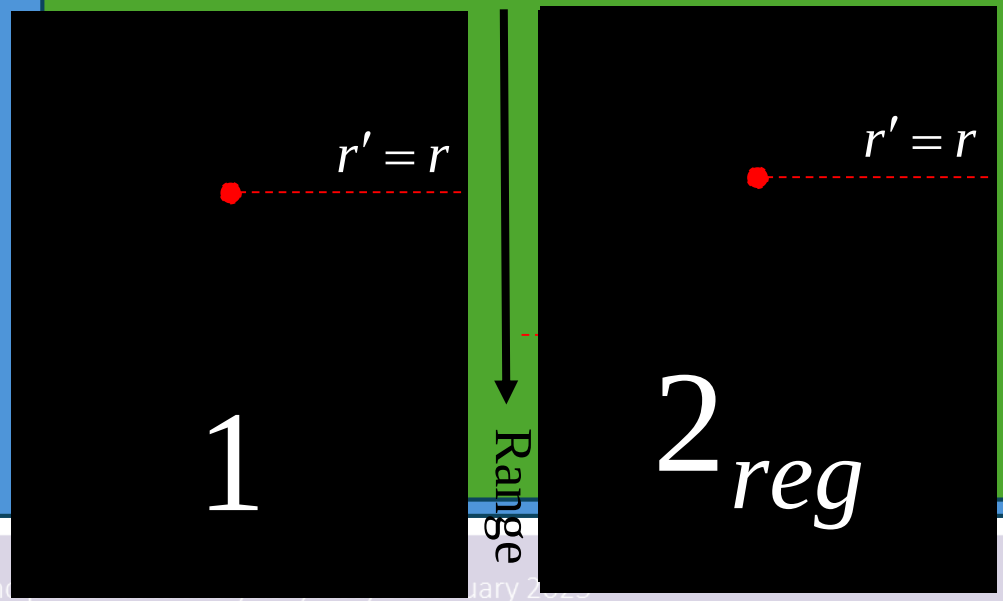

SAR Interferometry (InSAR)

$$\begin{cases} H \\ l \\ \sigma \end{cases} + \delta r \rightarrow \vartheta \rightarrow z$$

$$err(z) = \frac{r\sin(\vartheta)}{l_\perp} err(\delta r)$$

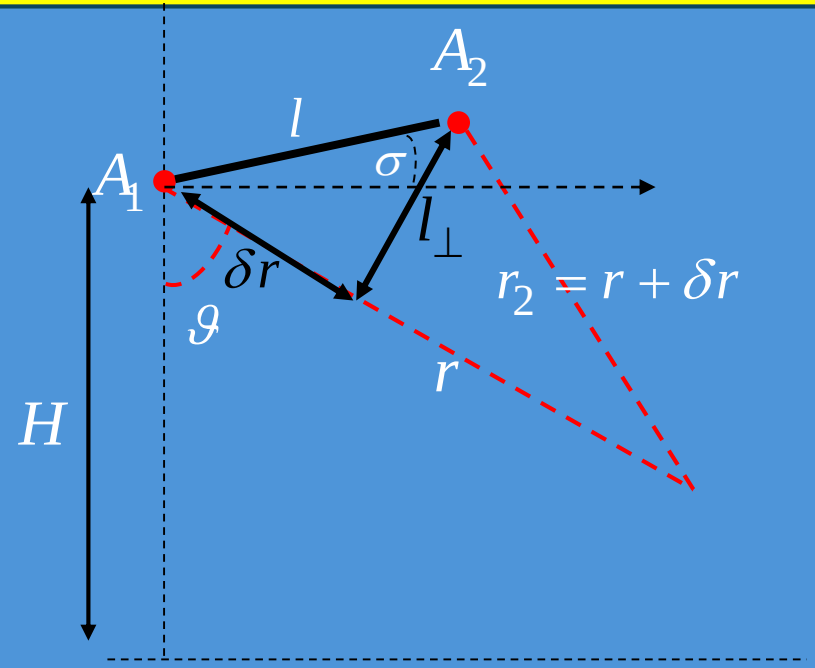

Image 1 : $\gamma(x,r)\exp\left[-j\frac{4\pi}{\lambda}r\right]$

Image 2 reg : $\gamma(x,r)\exp\left[-j\frac{4\pi}{\lambda}(r+\delta r)\right]$

(Image1) x (Image 2 reg) *

$$\varphi = \frac{4\pi}{\lambda}\delta r$$ Interferometric phase

SAR Interferometry (InSAR)

$$\begin{cases} H \\ l \\ \sigma \end{cases} + \delta r \rightarrow \vartheta \rightarrow z$$

$$err(z) = \frac{r \sin(\vartheta)}{l_{\perp}} err(\delta r)$$

$$\varphi = \frac{4\pi}{\lambda} \delta r$$

$$err(\delta r) = \frac{\lambda}{4\pi} err(\varphi)$$

In this way δr is achieved from the interferometric phase of the two images, with an accuracy on the order of fraction of wavelength, that means, centimeters or millimeters!

Image 1 : $\gamma(x,r) \exp\left[-j \frac{4\pi}{\lambda} r\right]$

Image 2 reg : $\gamma(x,r) \exp\left[-j \frac{4\pi}{\lambda} (r + \delta r)\right]$

(Image1) x (Image 2 reg) *

$$\varphi = \frac{4\pi}{\lambda} \delta r$$

Interferometric phase

SAR Interferometry (InSAR)

$$\begin{cases} H \\ l \\ \sigma \end{cases} + \delta r \rightarrow \vartheta \rightarrow z$$

$$err(z) = \frac{r \sin(\vartheta)}{l_{\perp}} err(\delta r)$$

Image 1 : $\gamma(x,r) \exp\left[-j \frac{4\pi}{\lambda} r\right]$

Image 2 reg : $\gamma(x,r) \exp\left[-j \frac{4\pi}{\lambda} (r + \delta r)\right]$

(Image1) x (Image 2 reg) *

$$\varphi = \frac{4\pi}{\lambda} \delta r$$

Interferometric phase

Spatial decorrelation: always

Temporal decorrelation: repeat-pass acquisitions

SAR Interferometry (InSAR)

Temporal decorrelation

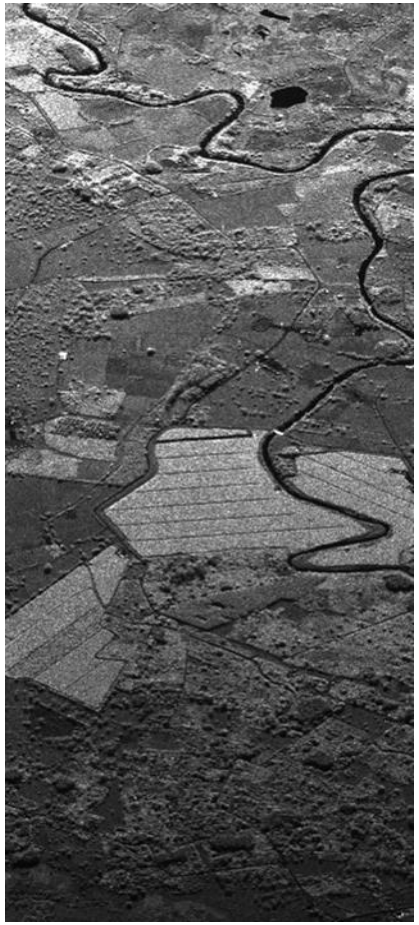

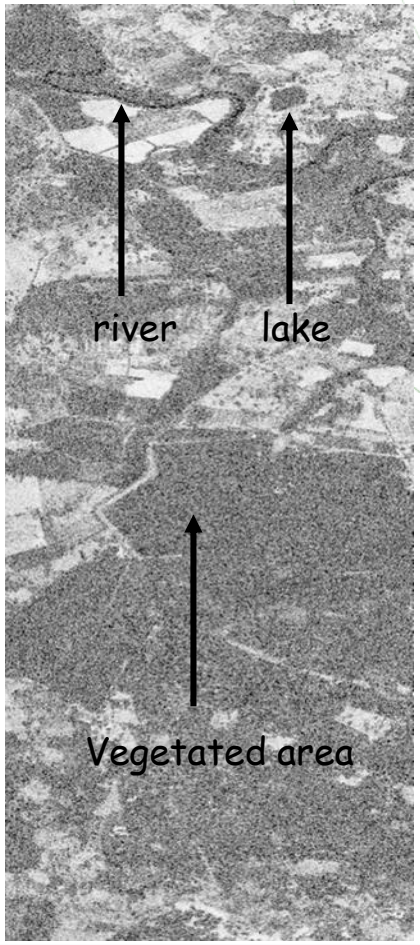

$$\frac{E\left[I_1 I_{2r}^*\right]}{\sqrt{E\left[\left|I_1\right|^2\right] E\left[\left|I_{2r}\right|^2\right]}}$$

Temporal decorrelation

Microwave frequencies for radar applications (IEEE* standard)

Band	Frequency	Wavelength
HF	3 - 30 MHz	100 - 10 m
VHF	30 - 300 MHz	10 - 1 m
P	300 - 1000 MHz	1 - 0.3 m
L	1 - 2 GHz	30 - 15 cm
S	2 - 4 GHz	15 - 7.5 cm
C	4 - 8 GHz	7.5 - 3.75 cm
X	8 - 12 GHz	3.75 - 2.5 cm
Ku	12 - 18 GHz	2.5 - 1.7 cm
K	18 - 27 GHz	1.7 - 1.1 cm
Ka	27 - 40 GHz	1.1 - 0.75 cm

Low frequencies are more robust with respect to temporal decorrelation

Most employed by SAR systems

***** **I**nstitute of **E**lectrical and **E**lectronic **E**ngineers

SAR Interferometry (InSAR)

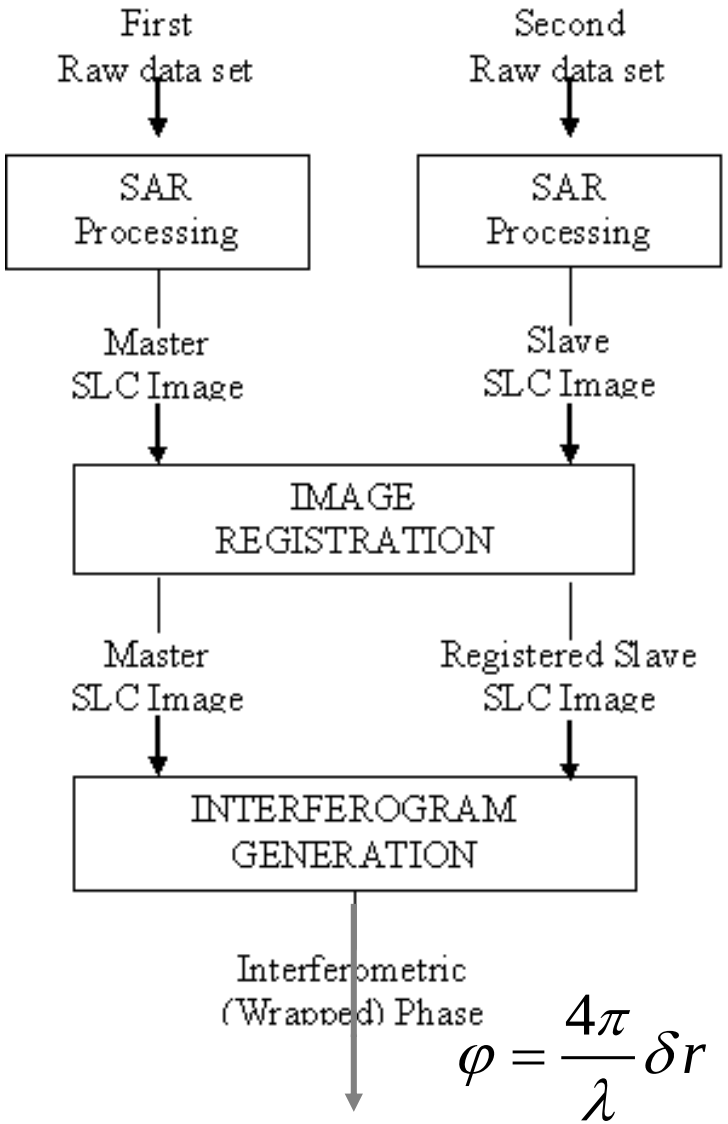

$$\varphi = \frac{4\pi}{\lambda}\delta r$$

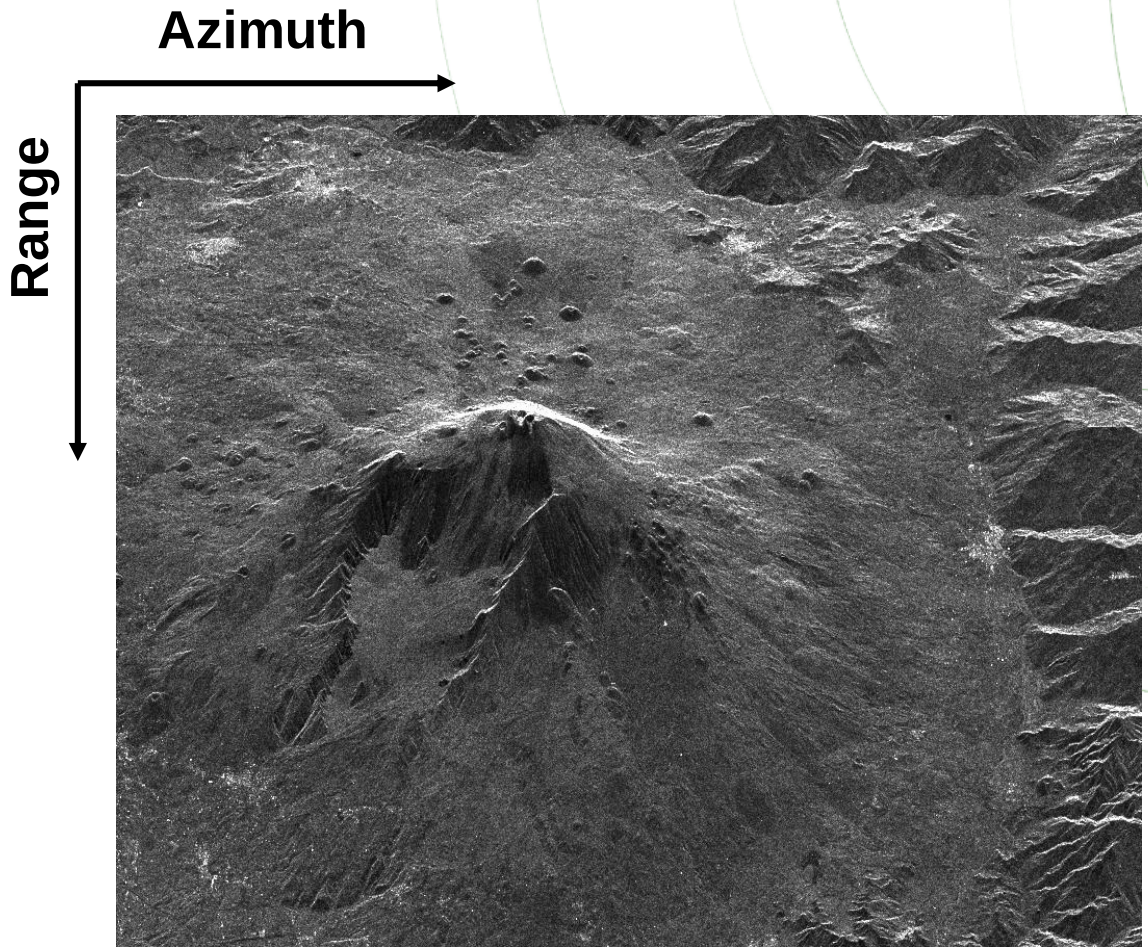

SAR Interferometry (InSAR)

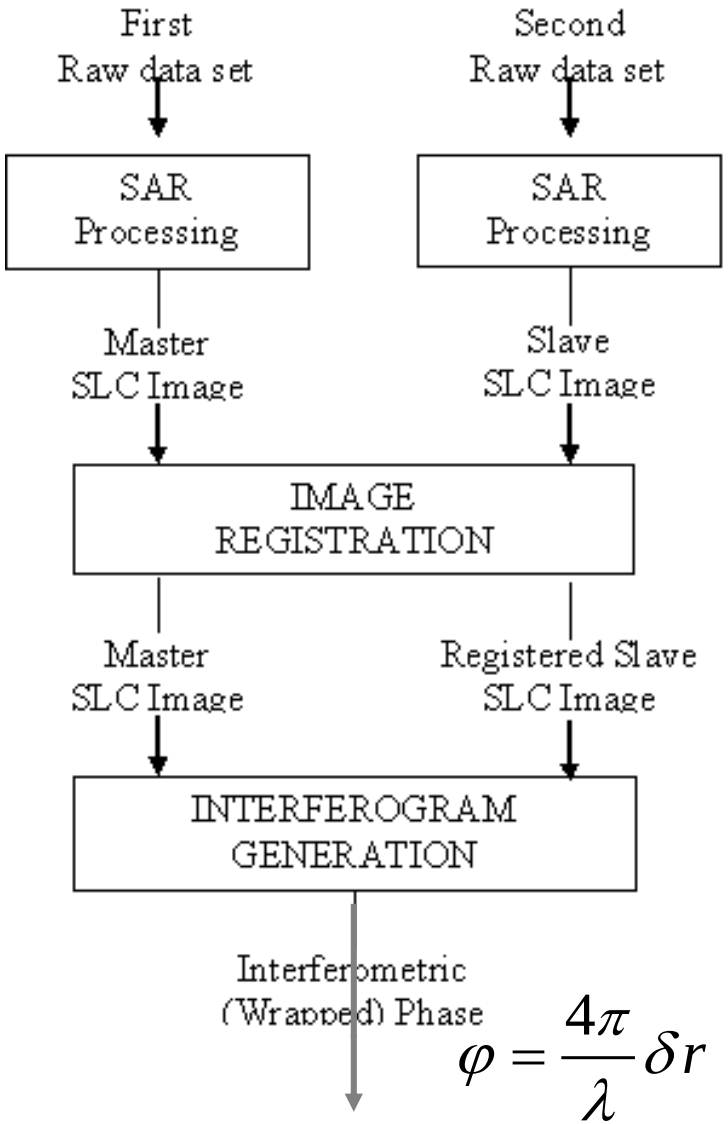

$$\varphi = \frac{4\pi}{\lambda}\delta r$$

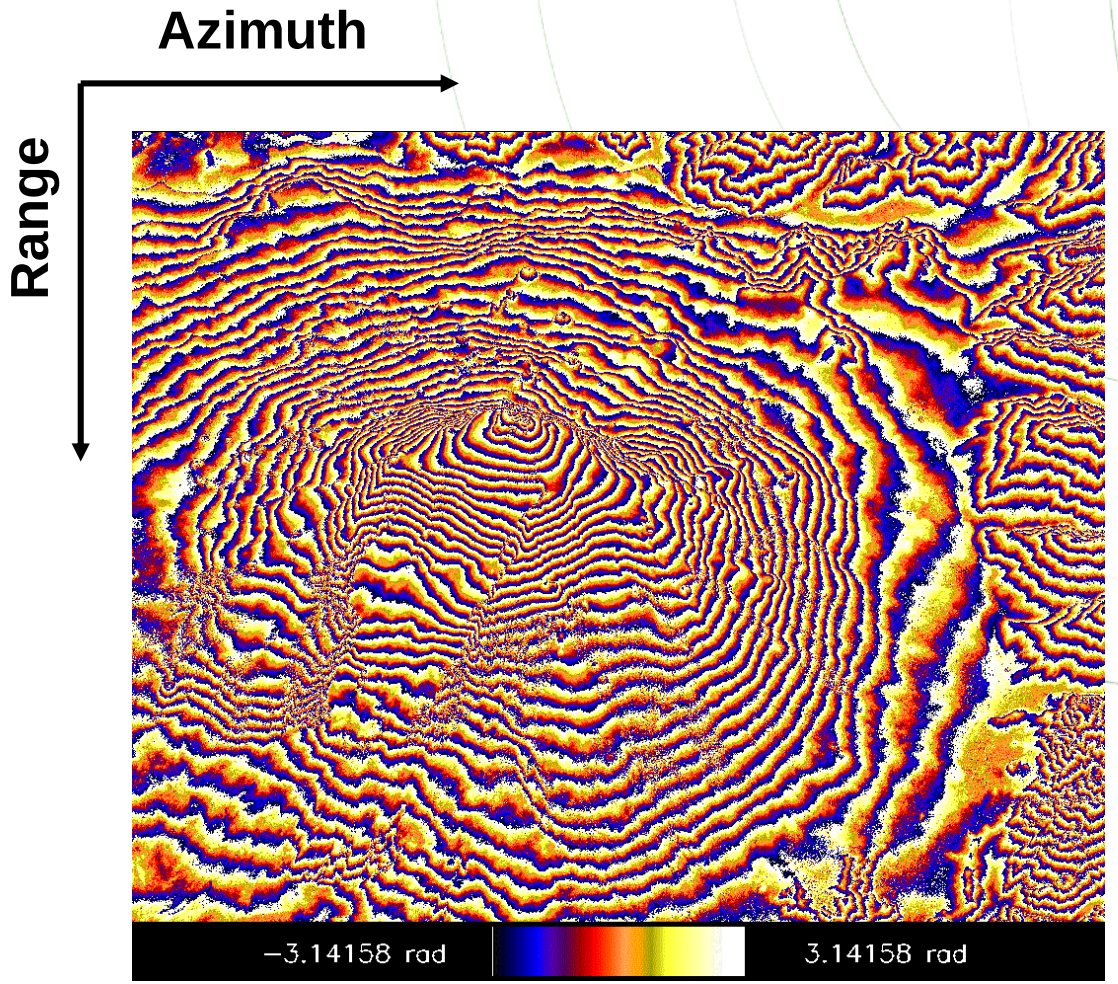

SAR Interferometry (InSAR)

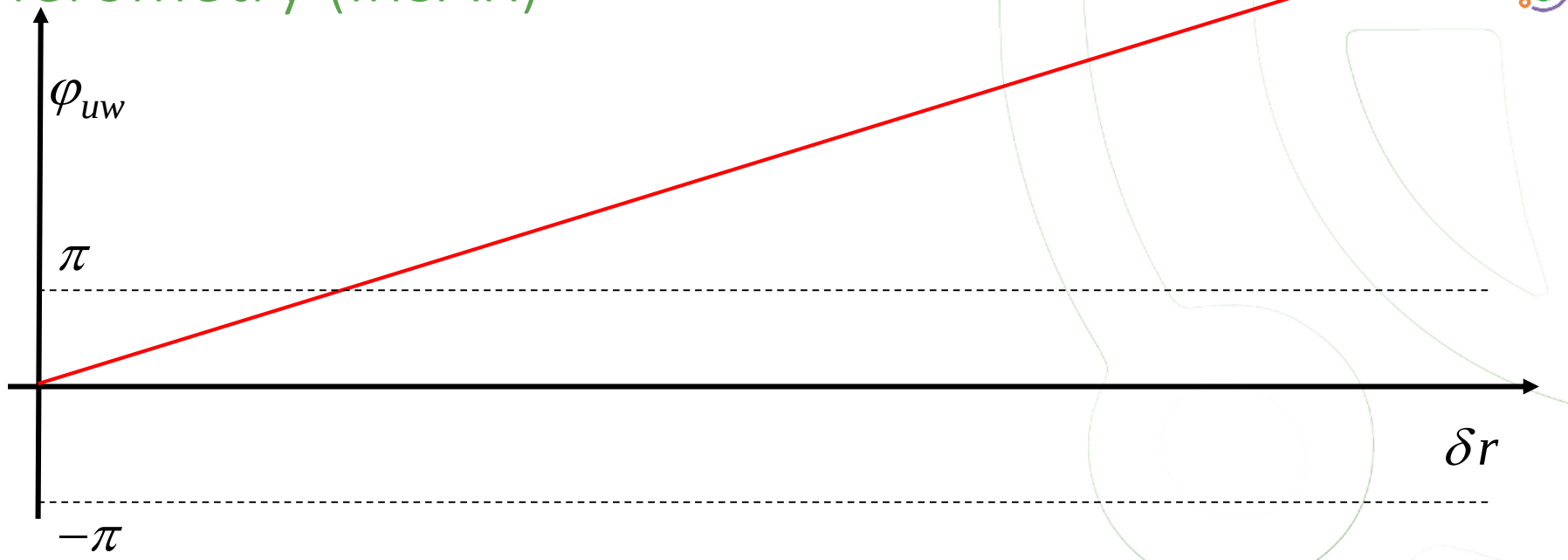

$$\varphi = \frac{4\pi}{\lambda}\delta r$$

$$\varphi_{uw} = 2N\pi + \varphi_w$$

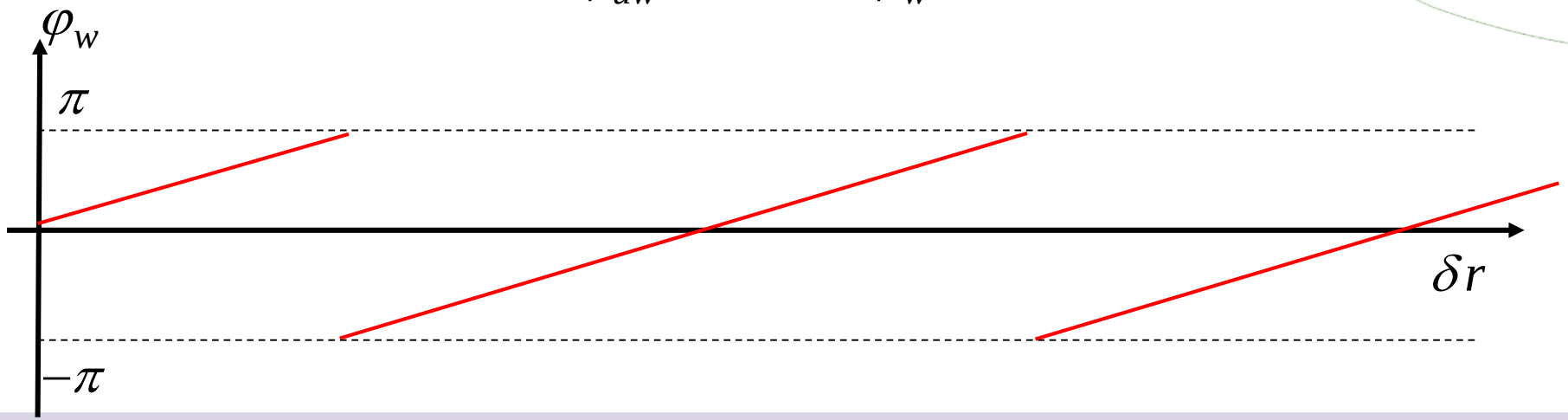

SAR Interferometry (InSAR)

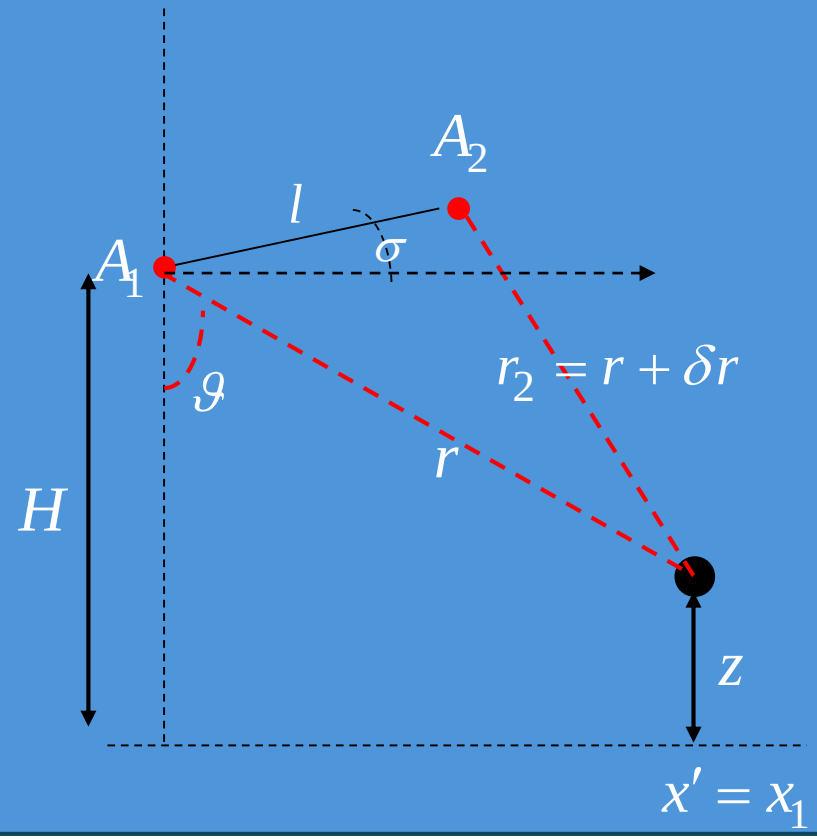

$$\varphi = \frac{4\pi}{\lambda}\delta r \qquad \varphi_{uw} = 2N\pi + \varphi_w$$

$$\lambda = 3{,}14\ cm \qquad \delta r = 1m \qquad \Rightarrow \quad \varphi_{uw} = \frac{4\pi}{\lambda}\delta r = 400$$

$$\varphi_w = -2.1239$$

$$\varphi_{uw} = 64 \times 2\pi + \varphi_w = 400$$

SAR Interferometry (InSAR)

E. Rodríguez and J. M. Martin, “Theory and design of interferometric synthetic-aperture radars,” Proc. Inst Elect. Eng., vol. 139, no. 2, pp. 147–159, 1992.

G.Franceschetti and R.Lanari; Synthetic Aperture Radar Processing, CRC PRESS, New York, 1999

D.C.Ghiglia and M.D.Pritt; Two-Dimensional Phase Unwrapping: Theory, Algorithms and Software, John Wiley and Sons New York, 1998.

SAR Interferometry (InSAR)

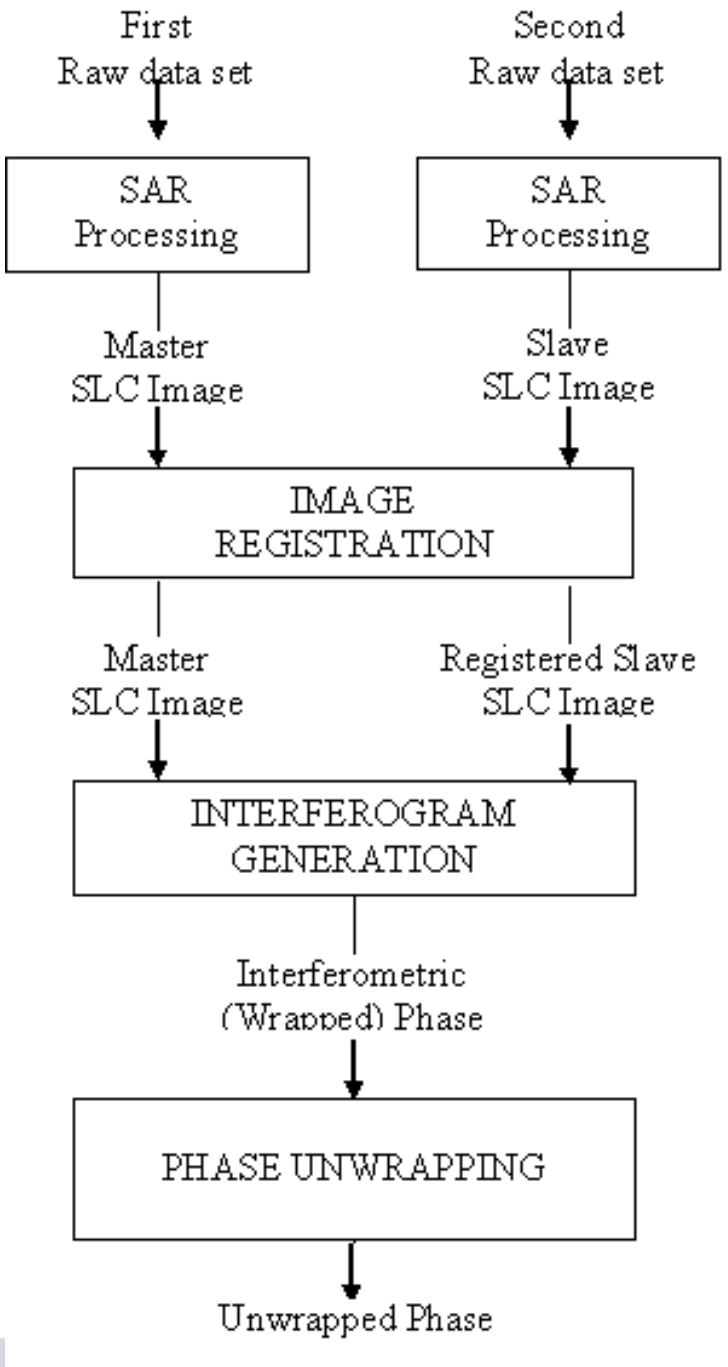

SAR Interferometry (InSAR)

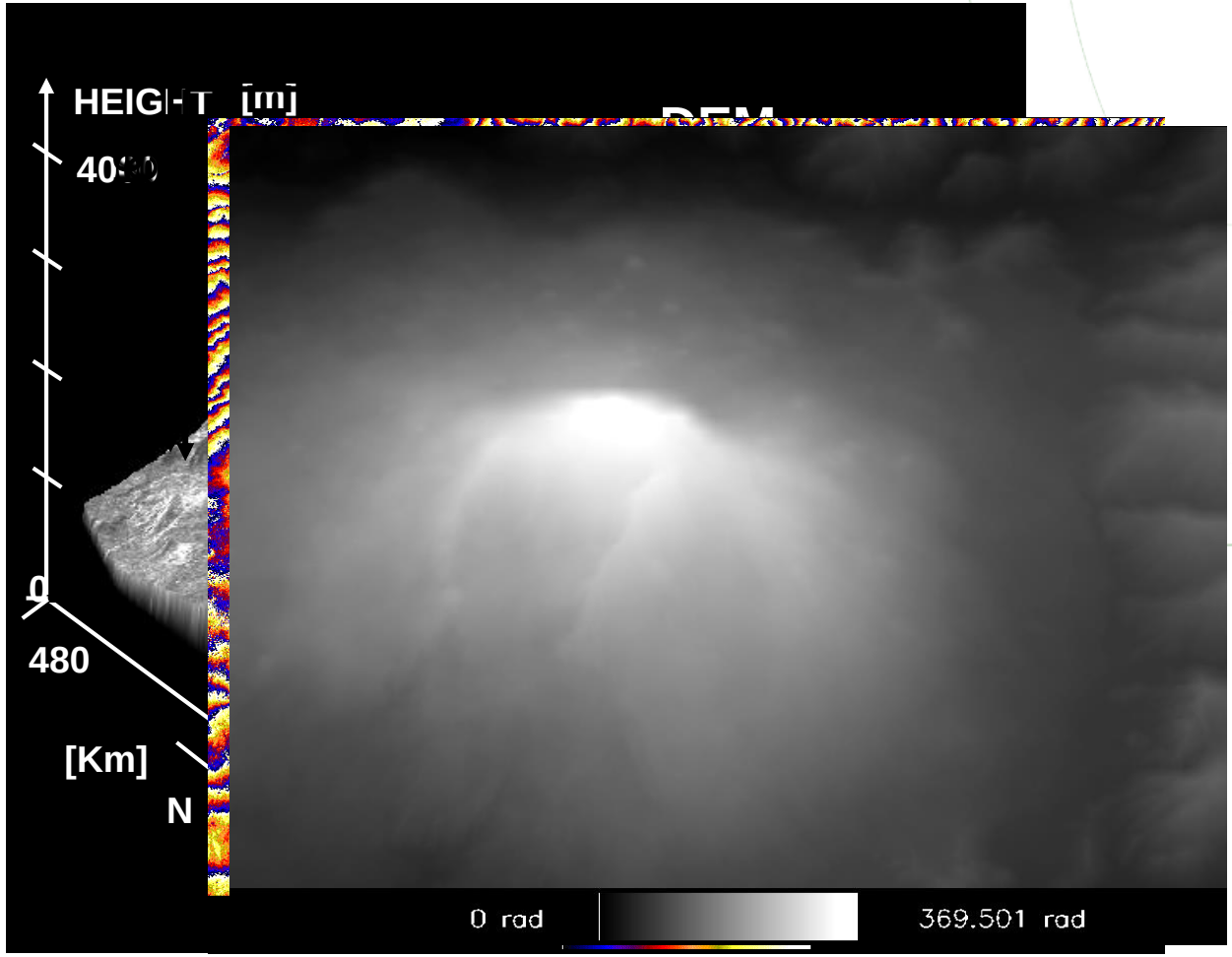

$$\beta, l$$
$$+$$
$$\delta r$$
$$\downarrow$$
$$\theta$$
$$\downarrow$$
$$z$$

SAR Interferometry (InSAR)

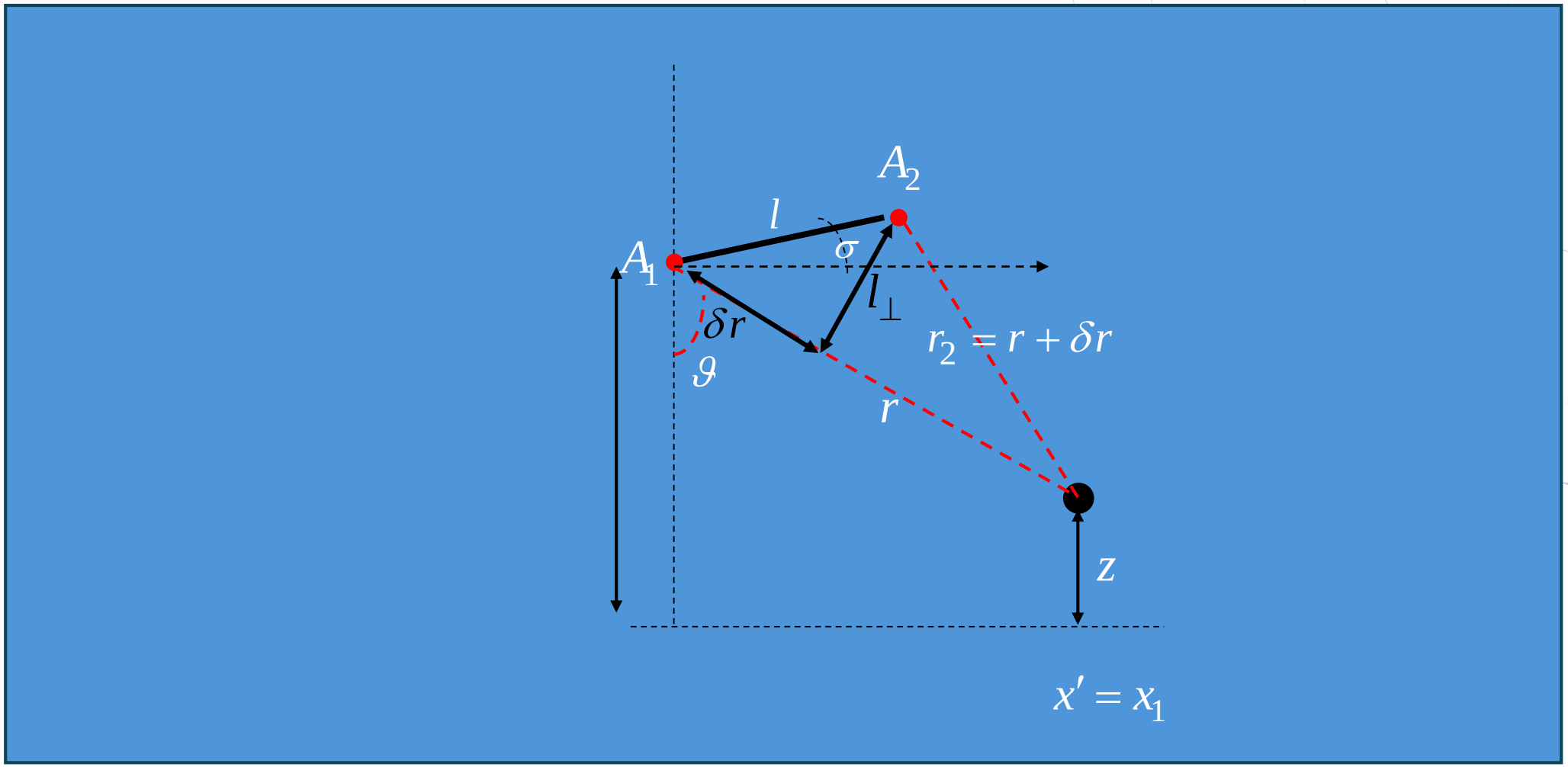

SUMMARY

Synthetic Aperture Radar (SAR)

Geometry

SAR Raw Data

Geometric Resolution

SAR focusing

SAR Interferometry (InSAR)

DInSAR

An Airborne InSAR experiment

Differential SAR Interferometry (DInSAR)

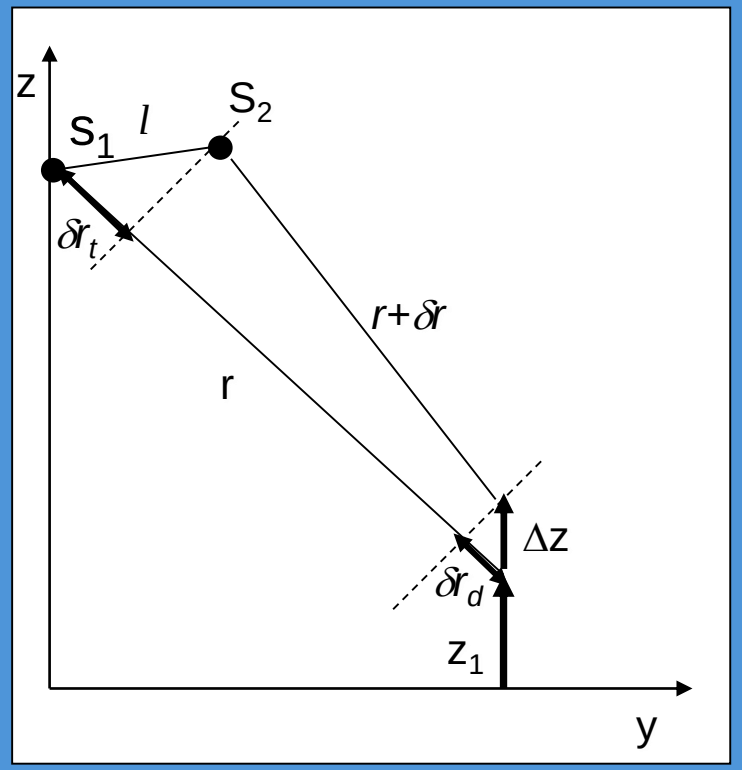

$$\delta r = \delta r_t + \delta r_d$$

SAR Interferometry (InSAR)

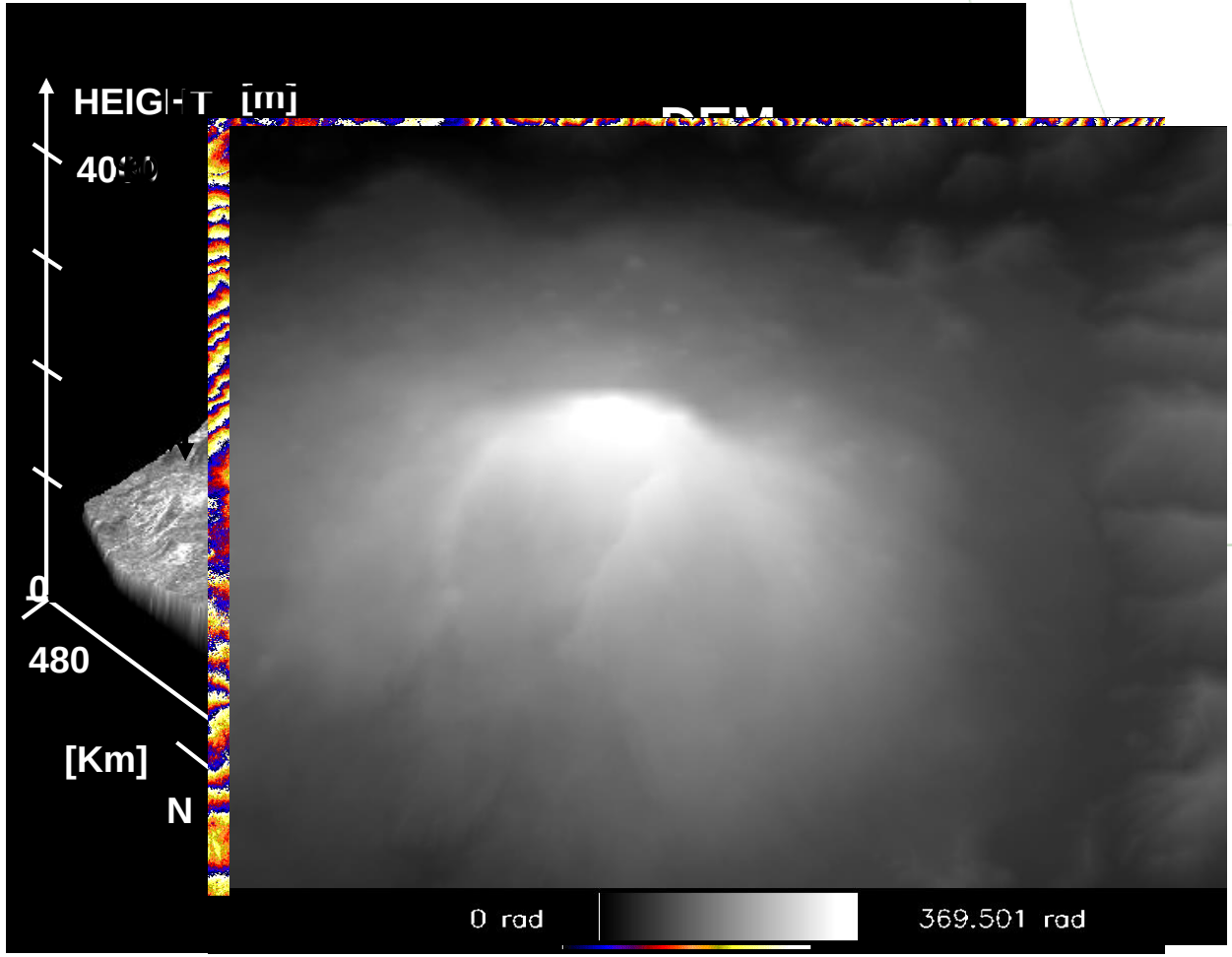

$$\sigma, l, H$$
$$+$$
$$\delta r$$
$$\theta$$
$$z$$
$$+$$
$$\sigma, l, H$$

Differential SAR Interferometry (DInSAR)

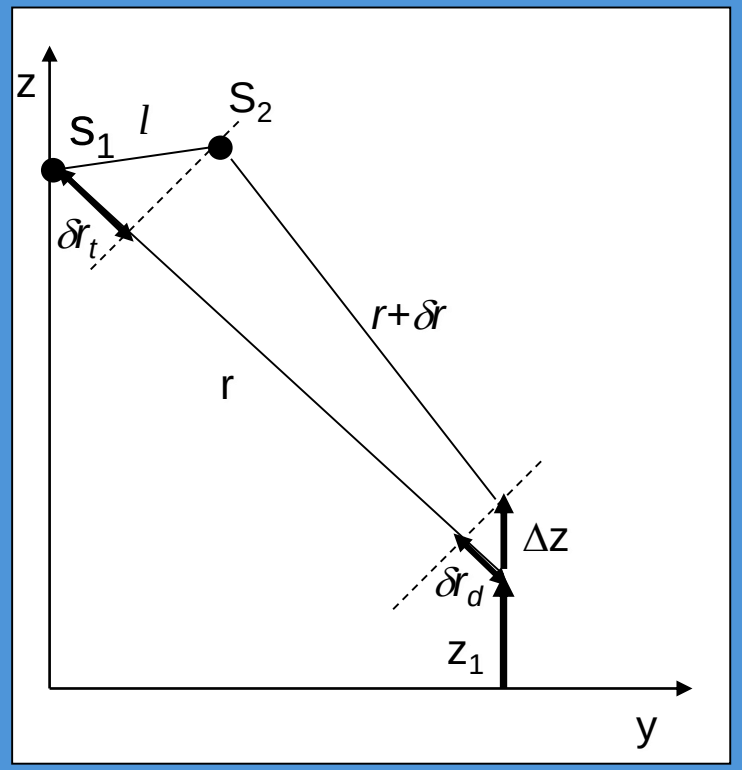

$$\delta r = \delta r_t + \delta r_d$$

$$err(z) = \frac{r\sin(\vartheta)}{l_\perp} err(\delta r)$$

$$err(\delta r) = \frac{l_\perp}{r\sin(\vartheta)} err(z)$$

Differential SAR Interferometry (DInSAR)

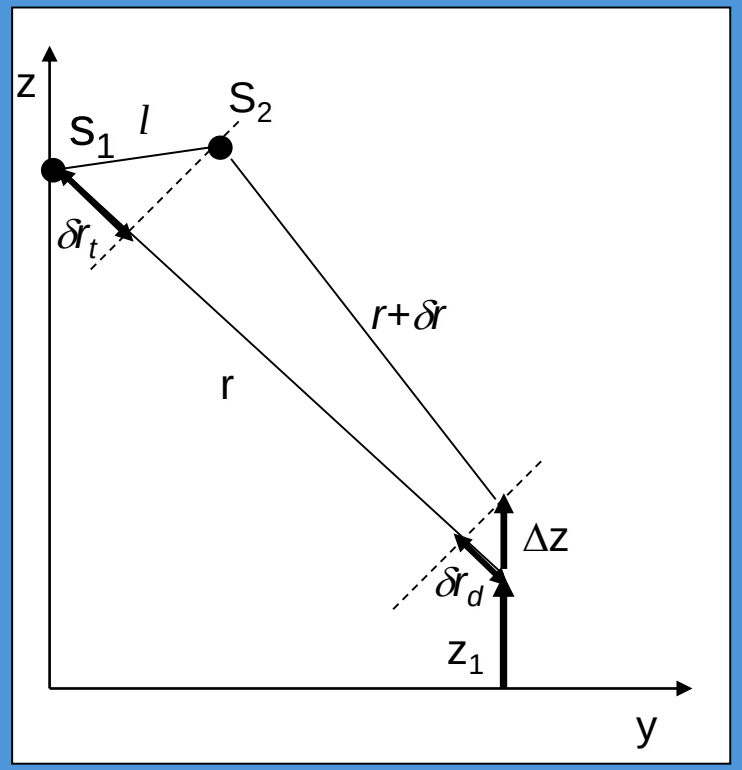

$$\delta r = \delta r_t + \delta r_d$$

$$\varphi = \frac{4\pi}{\lambda}\delta r$$

$$err(\delta r) = \frac{\lambda}{4\pi} err(\varphi)$$

In this way δr is achieved from the interferometric phase of the two images, with an accuracy on the order of fraction of wavelength, that means, centimeters or millimeters!

Differential SAR Interferometry (DInSAR)

Campi Flegrei: Vertical displacement component (Sentinel-1 : λ=5.6 cm)

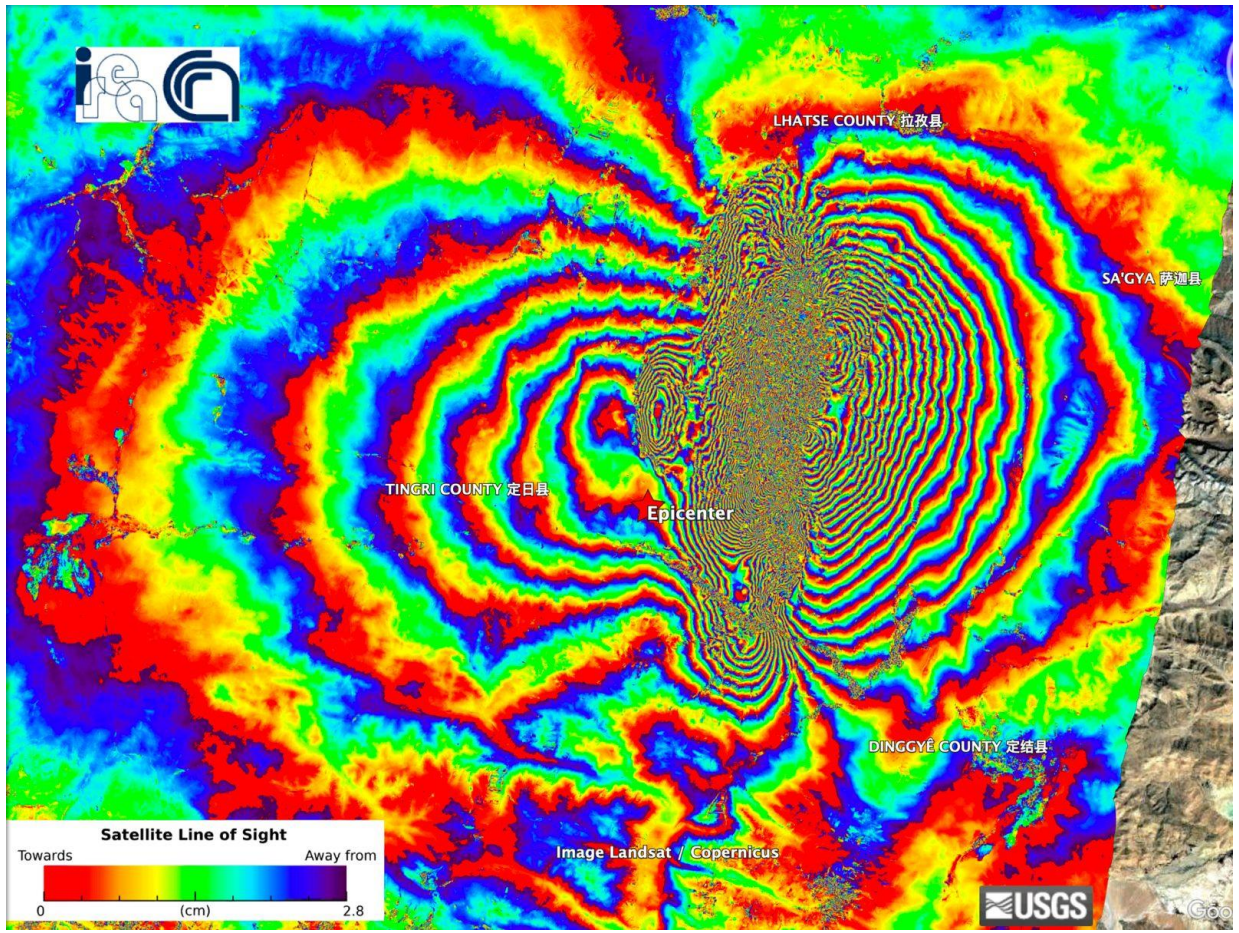

One fringe corresponds to a λ/2 displacement

$$\varphi = \frac{4\pi}{\lambda}\delta r$$

CNN World Africa Americas Asia Australia China Europe India More

World / China

Powerful earthquake rocks remote region of Tibet and parts of Nepal, killing more than 120

By Nectar Gan, Hassan Tayir, Fred He, Joyce Jiang and Esha Mitra, CNN

5 minute read · Updated 6:39 AM EST, Wed January 8, 2025

SAR Interferometry (InSAR)

D. Massonnet et al., “The displacement field of the Landers earthquake mapped by radar interferometry,” Nature, vol. 364, no. 6433, pp. 138–142, 1993, doi: 10.1038/364138a0.

A.Ferretti, C.Prati and F.Rocca; “Permanent scatterers in SAR interferometry”, IEEE Trans. Geosci. Remote Sens., 39, 1, 2001.

P.Berardino, G.Fornaro, R.Lanari and E.Sansosti; “A new Algorithm for Surface Deformation Monitoring based on Small Baseline Differential SAR Interferograms”, IEEE Trans. Geosci. Remote Sens., 40, 11, 2002.

Differential SAR Interferometry (DInSAR)

Campi Flegrei: Vertical displacement component (Sentinel-1)

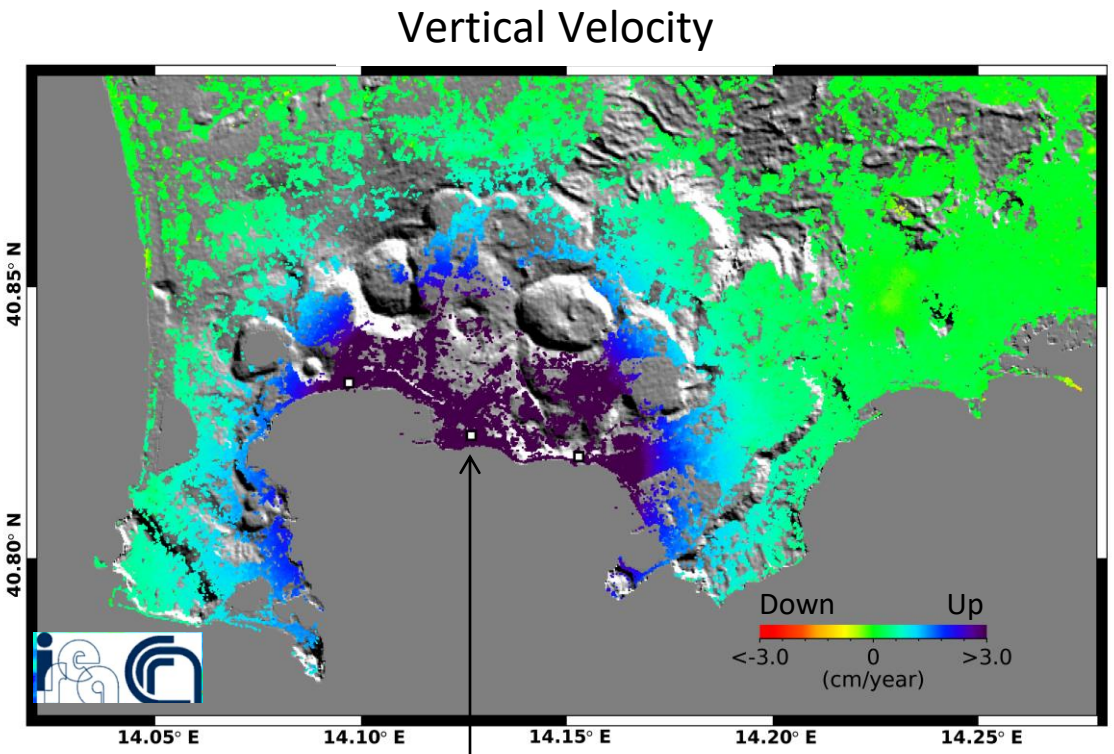

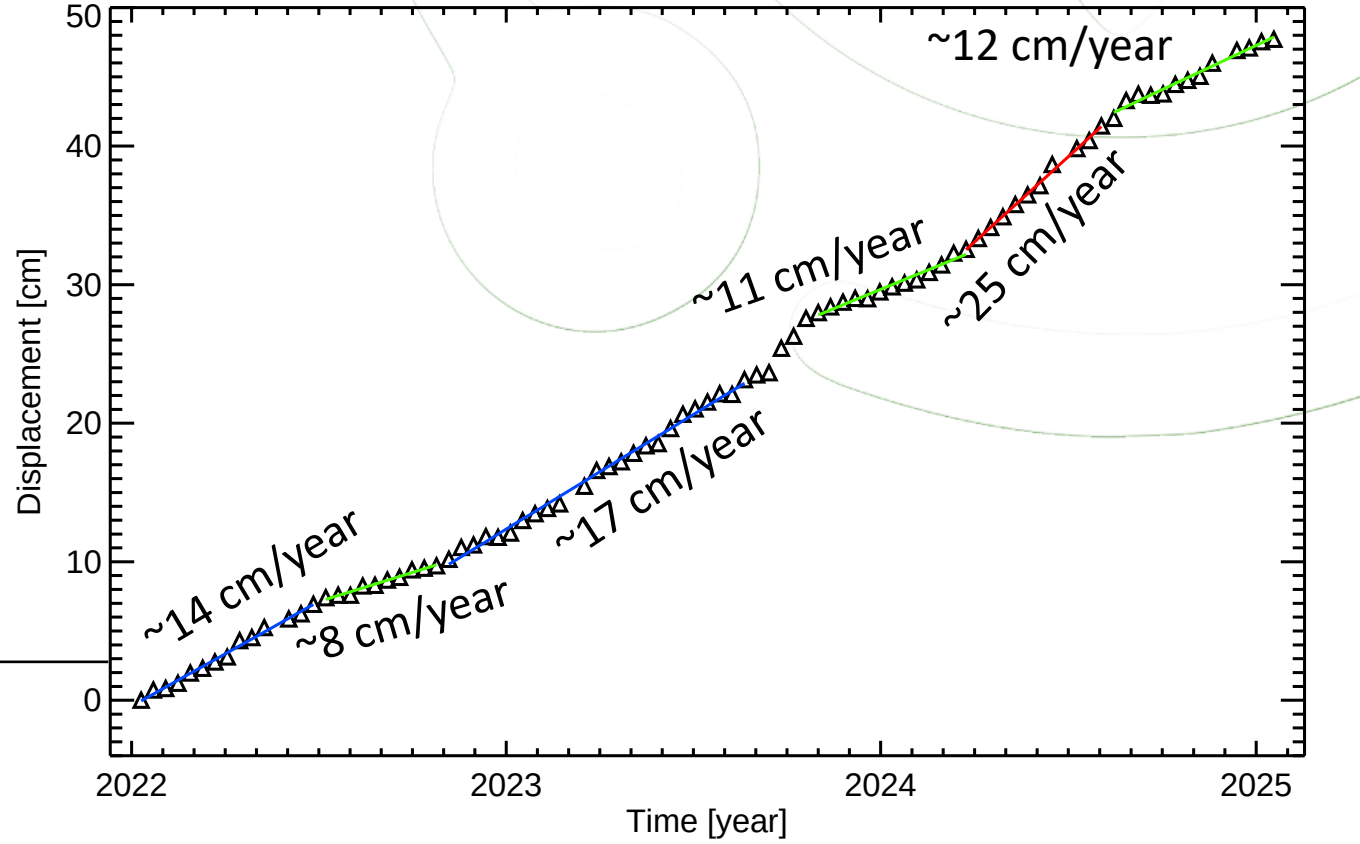

SAR Interferometry (InSAR)

InSAR vs. DInSAR

InSAR

Aim: topography reconstruction

1) Single-pass or repeat-pass

2) Orbital parameters needed

3) Baseline as large as possible (provided that the upper bound of the critical baseline is met)

DInSAR

Aim: ground deformation phenomena retrieval

1) Repeat-pass

2) Orbital parameters as well as external information on the topography needed

3) Baseline as small as possible

Airborne SAR vs. Spaceborne SAR

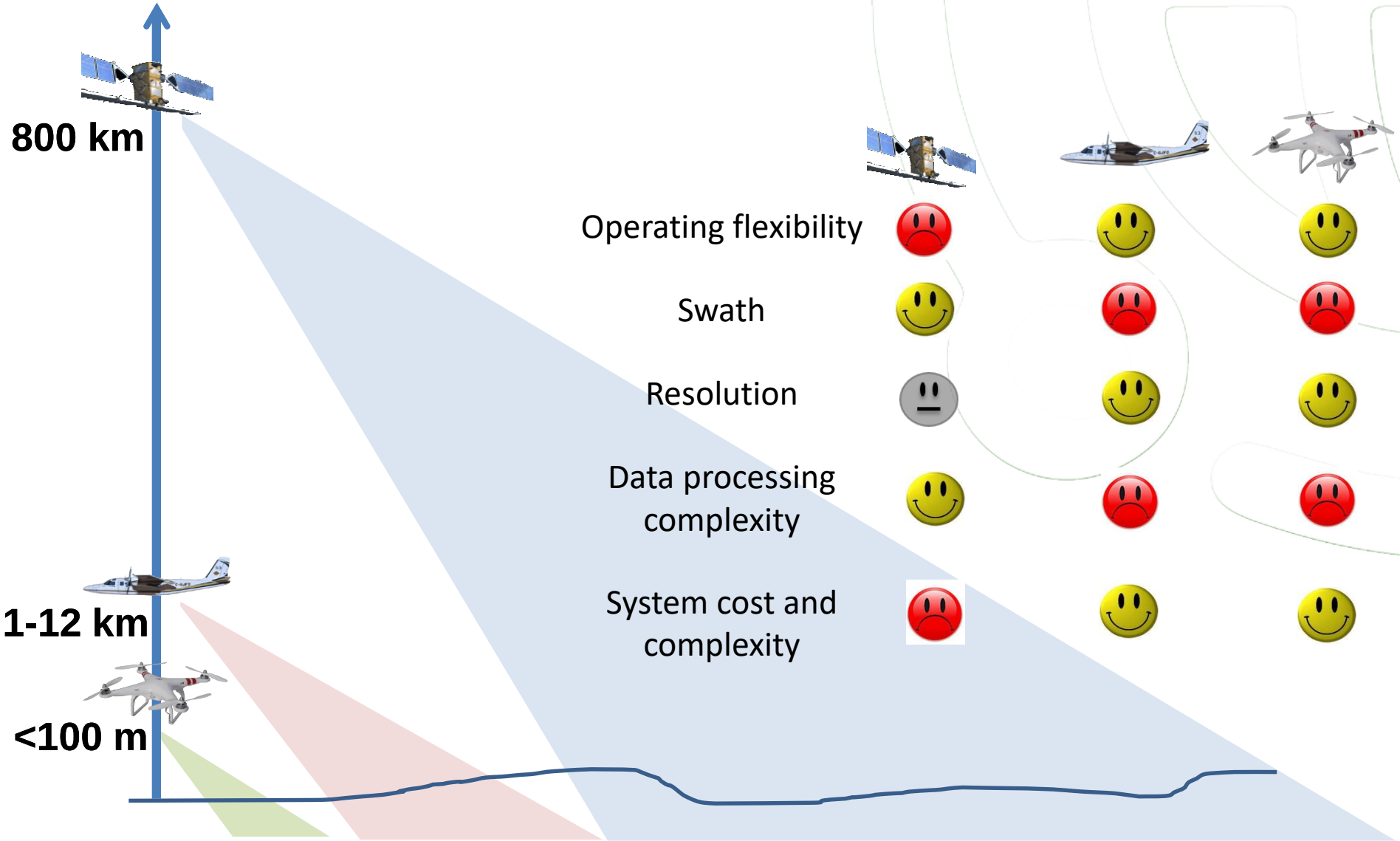

Airborne SAR vs. Spaceborne SAR

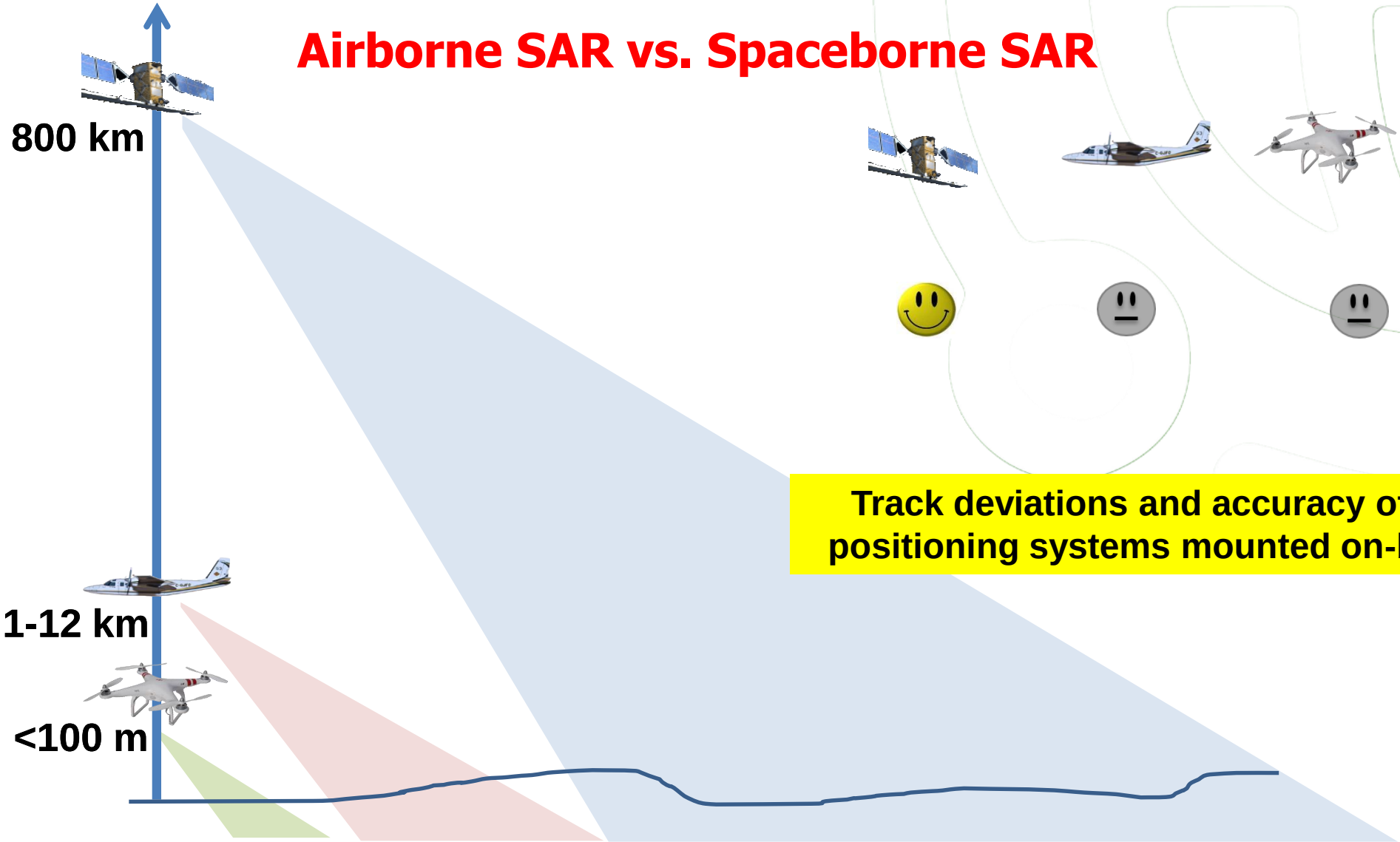

Track deviations and accuracy of the positioning systems mounted on-borad

SAR Interferometry (InSAR)

Airborne SAR vs. Spaceborne SAR

Single-pass InSAR

REDUCED TEMPORAL DECORRELATION

$$err(z) = \frac{r\sin(\vartheta)}{l_{\perp}} err(\delta r)$$

SUMMARY

Synthetic Aperture Radar (SAR)

Geometry

SAR Raw Data

Geometric Resolution

SAR focusing

SAR Interferometry (InSAR)

DInSAR

An Airborne InSAR experiment

An Airborne InSAR experiment

The airborne SAR infrastructure @IREA-CNR: flight segment

The Multiband Interferometric and Polarimetric SAR (MIPS) system

Main characteristics of the MIPS system		
Band	X	L
Technology	FMCW	
Carrier frequency [GHz]	9.55	1.35
Bandwidth [MHz]	200	125
Number of transmitting antennas (Tx)	1	1
Number of receiving antennas (Rx)	2	1
PRF [Hz]	1200	600
Antennas' sizes (azimuth × range) [cm]	24.6 x 12.6	18.5 × 18.5
Polarization	VV	Quad-Pol
Single-pass interferometry	YES	NOT

X-band RF layout

L-band RF layout

embedding the Applanix Navigation Unit

Applanix INS/GPS specifications	
Position [m]	0.05
Velocity [m/s]	0.005
Roll & Pitch [deg]	0.005
True Heading [deg]	0.008

An Airborne InSAR experiment

The airborne SAR infrastructure @IREA-CNR: ground segment

IT platform

IT platform configuration	
Operative system	openSUSE 15.4
Processor	232-core CPU (AMD EPYC 7513 2.6GHz)
Number of nodes	22
Memory size per node	2048 GB of RAM
Interconnection	25 Gb/s
Data storage	1 Petabyte

GRINT (PIR01_00013) project funded by the Italian Ministry for Universities and Research (MUR)

An Airborne InSAR experiment

The airborne SAR infrastructure @IREA-CNR: ground segment

- **Measurement of the Antenna Phase Center Position**
- **Measurament of the Antenna Patterns**

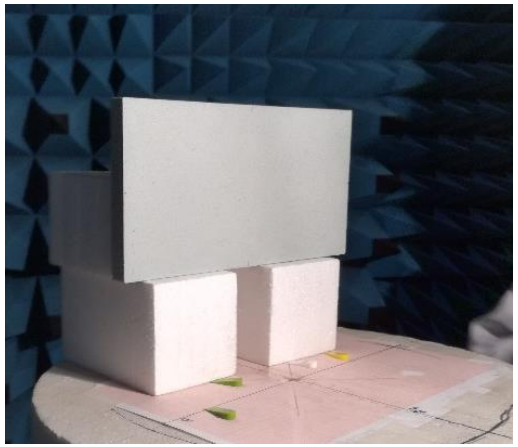

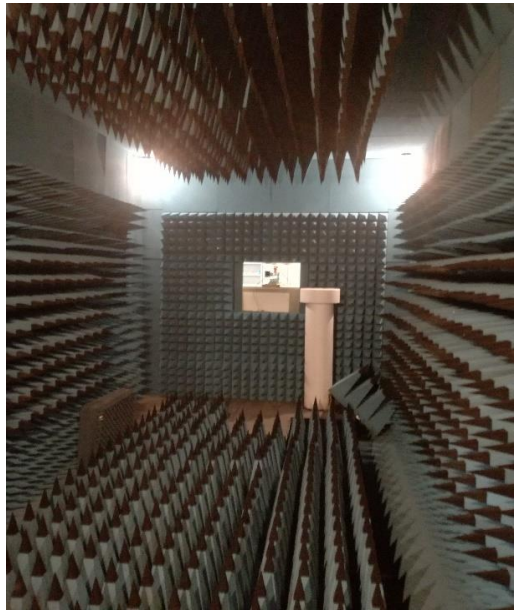

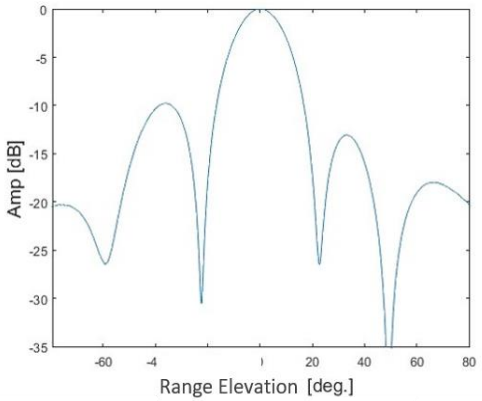

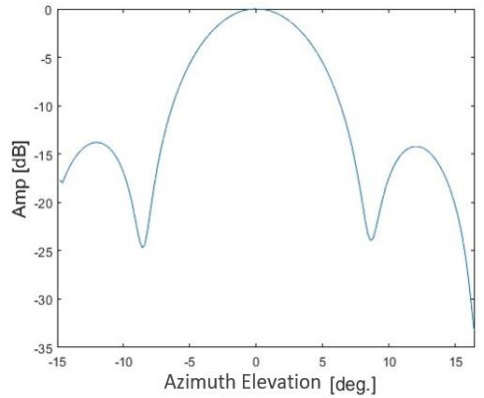

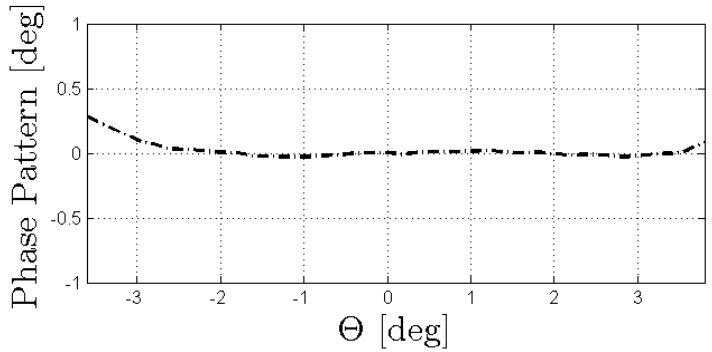

C. Esposito, A. Gifuni and S. Perna, "Measurement of the Antenna Phase Center Position in Anechoic Chamber," in IEEE Antennas and Wireless Propagation Letters, vol. 17, no. 12, pp. 2183-2187, Dec. 2018, doi: 10.1109/LAWP.2018.2870751.

An Airborne InSAR experiment

The airborne SAR infrastructure @IREA-CNR: ground segment

In-situ activities

- Assembly of the SAR sensor onboard the aircraft
- Deployment of the CRs

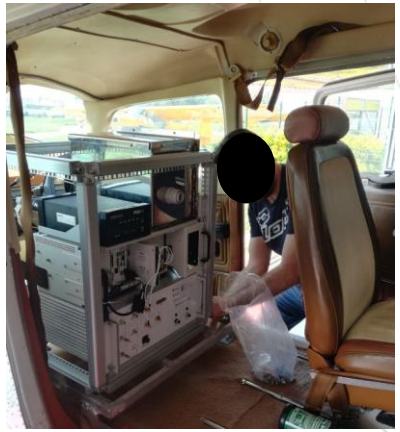

- Measurement of the CR positions
- Measurement of the antennas' lever arms

An Airborne InSAR experiment

The airborne SAR infrastructure @IREA-CNR: ground segment

Flight data processing

Detection & removal of RFI on SAR data

SAR data processing chain

An Airborne InSAR experiment

The airborne SAR infrastructure @IREA-CNR: ground segment

Flight data processing

Detection & removal of RFI on SAR data

SAR data processing chain

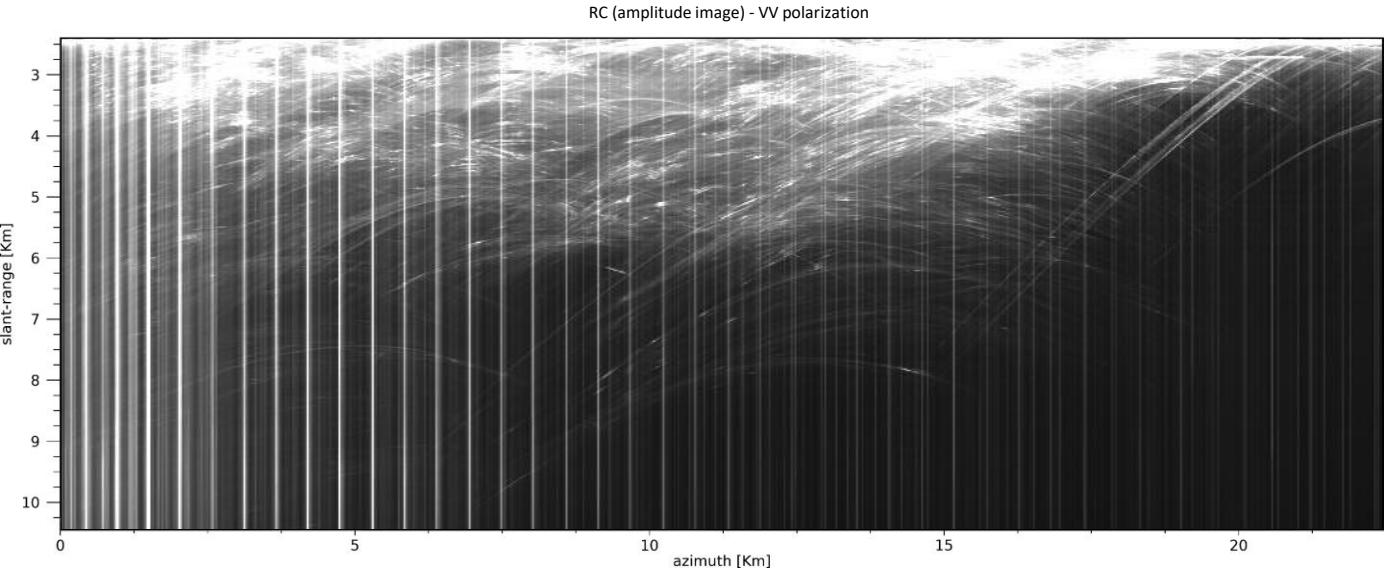

Test site: Campi Flegrei Caldera

L-Band dataset

Resolution: 2 m

Natale *et al.*, "Detection Strategies for Radio Frequency Interferences Corrupting FMCW L-Band SAR Data," in *IGARSS 2023*.

An Airborne InSAR experiment

The airborne SAR infrastructure @IREA-CNR: ground segment

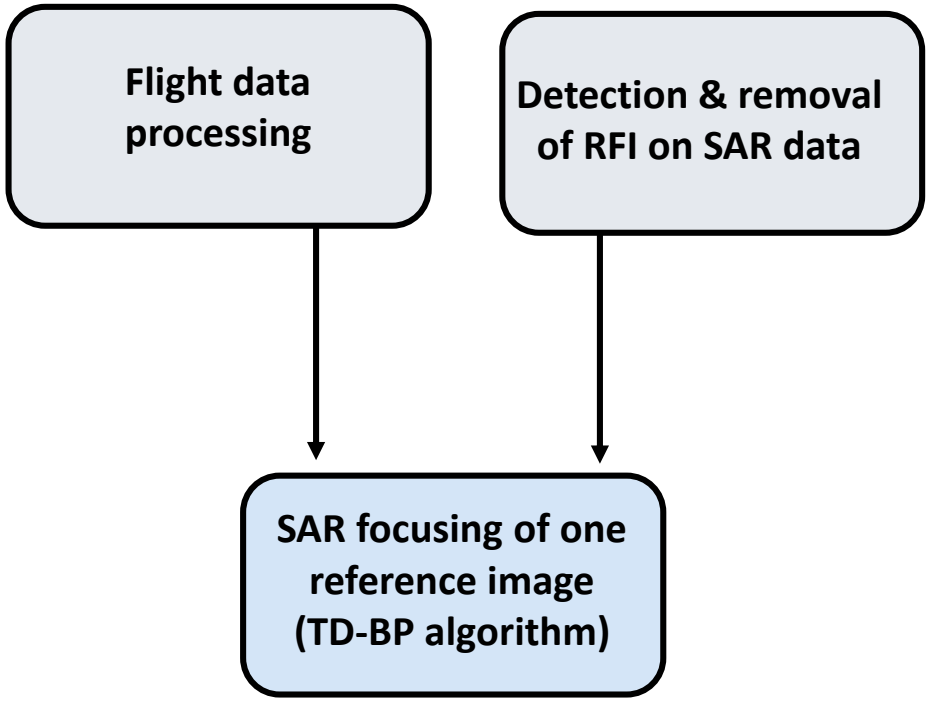

SAR data processing chain

P. Berardino, A. Natale, C. Esposito, R. Lanari and S. Perna, "On the Time-Domain Airborne SAR Focusing in the Presence of Strong Azimuth Variations of the Squint Angle," in IEEE Transactions on Geoscience and Remote Sensing, vol. 61, pp. 1-18, 2023, Art no. 5212818, doi: 10.1109/TGRS.2023.328959

An Airborne InSAR experiment

The airborne SAR infrastructure @IREA-CNR: ground segment

SAR data processing chain

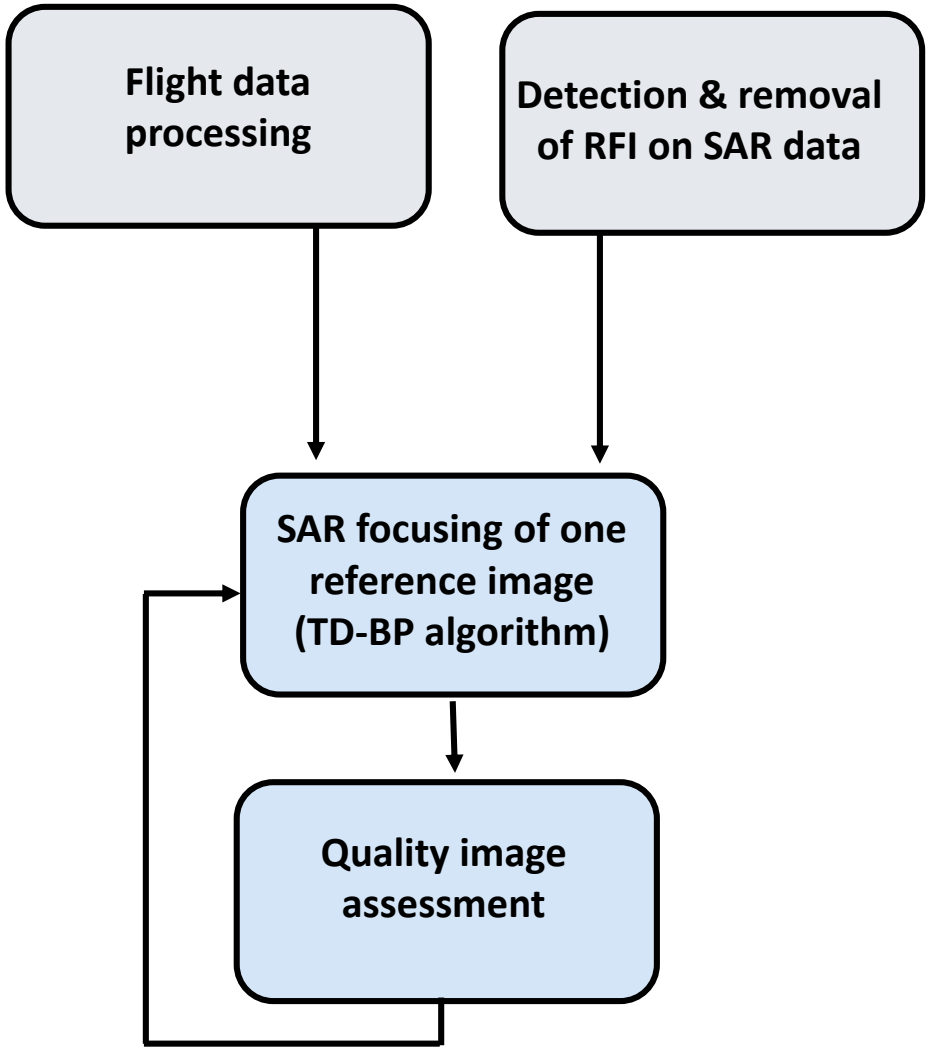

C. Esposito *et al*, "Geometric distortions in FMCW SAR images due to inaccurate knowledge of electronic radar parameters: analysis and correction by means of corner reflectors", Remote Sensing of Environment, Volume 232, October 2019, 111289, https://doi.org/10.1016/j.rse.2019.111289.

Esposito, C *et al*. On the Frequency Sweep Rate Estimation in Airborne FMCW SAR Systems. Remote Sens. 2020, 12, 3448. https://doi.org/10.3390/rs12203448

An Airborne InSAR experiment

The airborne SAR infrastructure @IREA-CNR: ground segment

SAR data processing chain

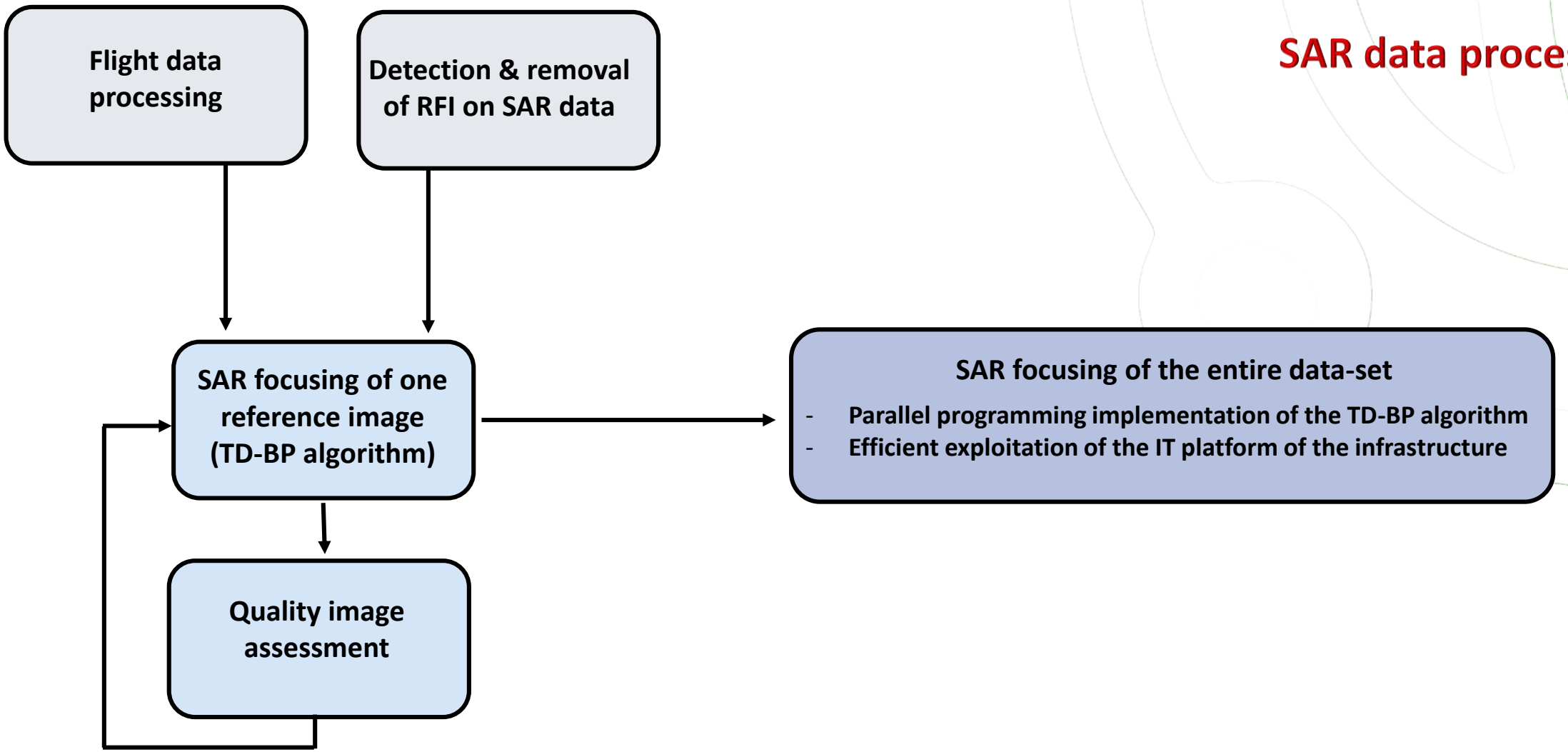

An Airborne InSAR experiment

The airborne SAR infrastructure @IREA-CNR: ground segment

Flight data processing

Detection & removal of RFI on SAR data

SAR data processing chain

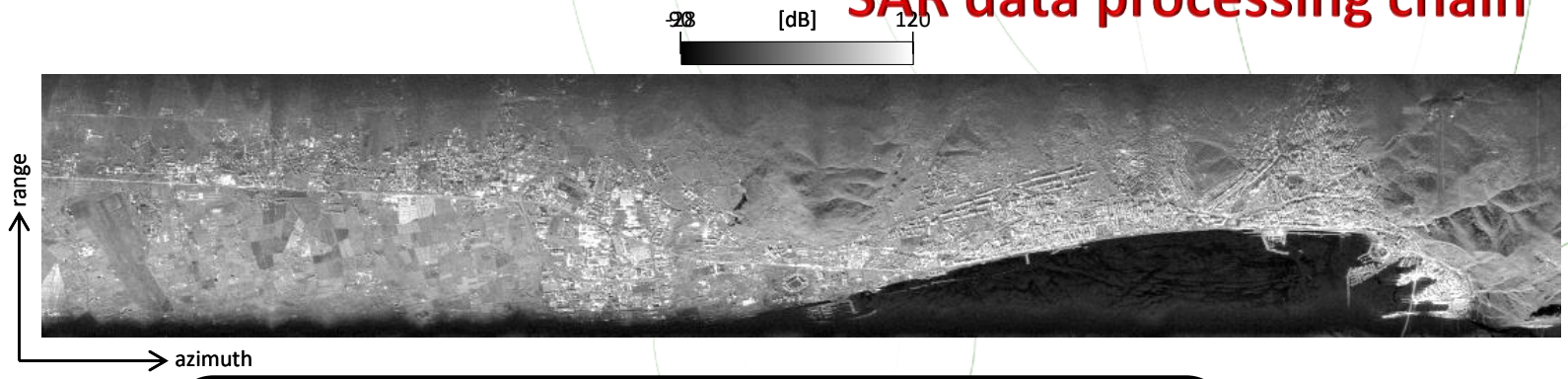

SAR focusing of one reference image (TD-BP algorithm)

Quality image assessment

Radiometric calibration

SAR focusing of the entire data-set

- Parallel programming implementation of the TD-BP algorithm
- Efficient exploitation of the IT platform of the infrastructure

Test site: Salerno, South Italy

X-Band dataset

Resolution: 2 m

An Airborne InSAR experiment

The airborne SAR infrastructure @IREA-CNR: ground segment

SAR data processing chain

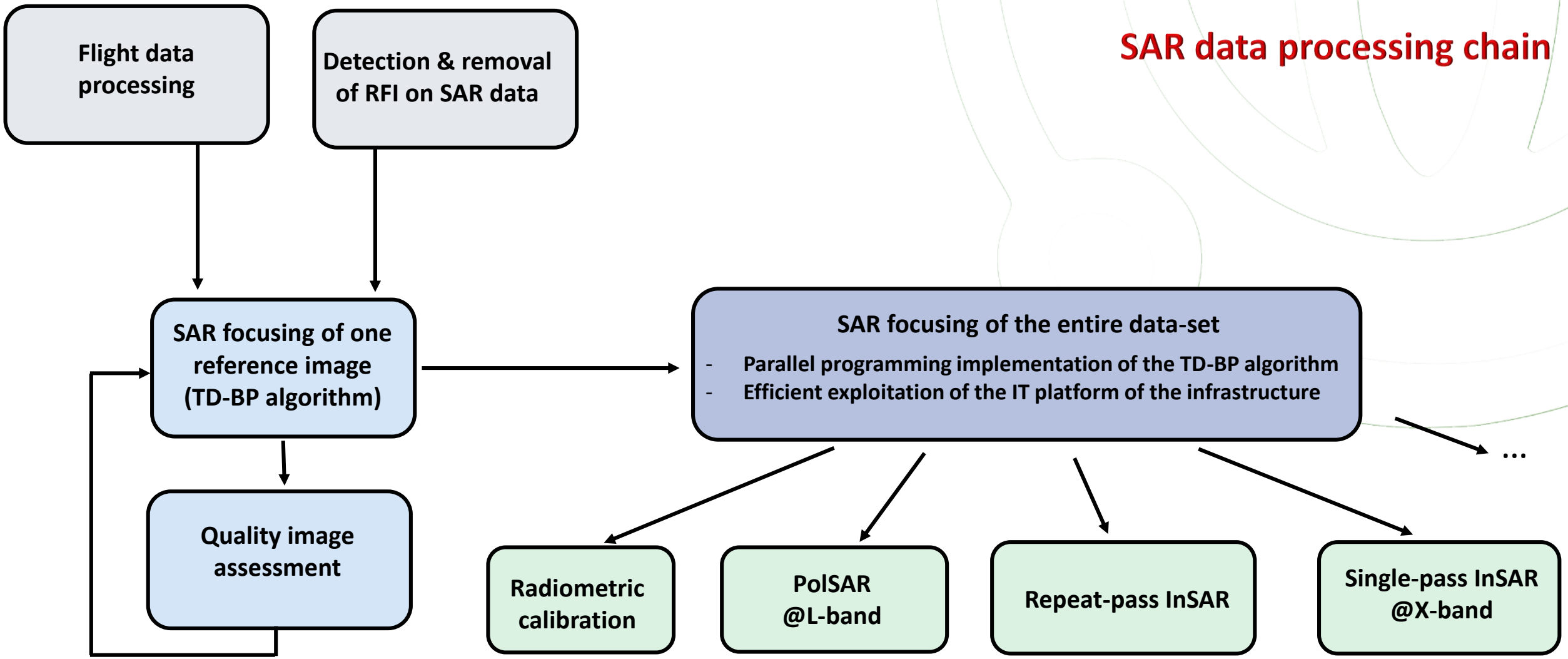

An Airborne InSAR experiment

The airborne SAR infrastructure @IREA-CNR: ground segment

SAR data processing chain

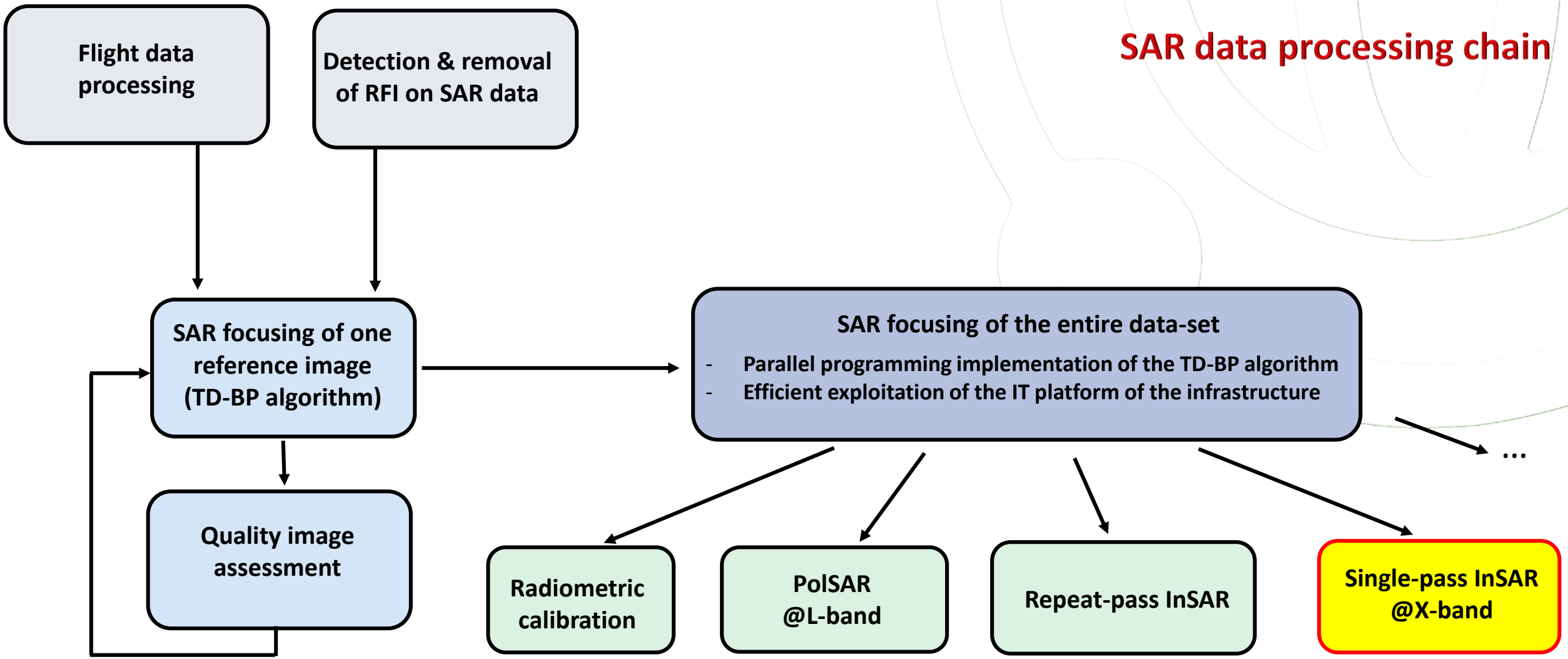

An Airborne InSAR experiment

The Stromboli case study

Agreement between IREA-CNR and the Department of Civil Protection of the Presidency of the Council of Ministers

- 7 airborne campaigns between July 2019 and October 2022

- 2 remarkable volcanic events

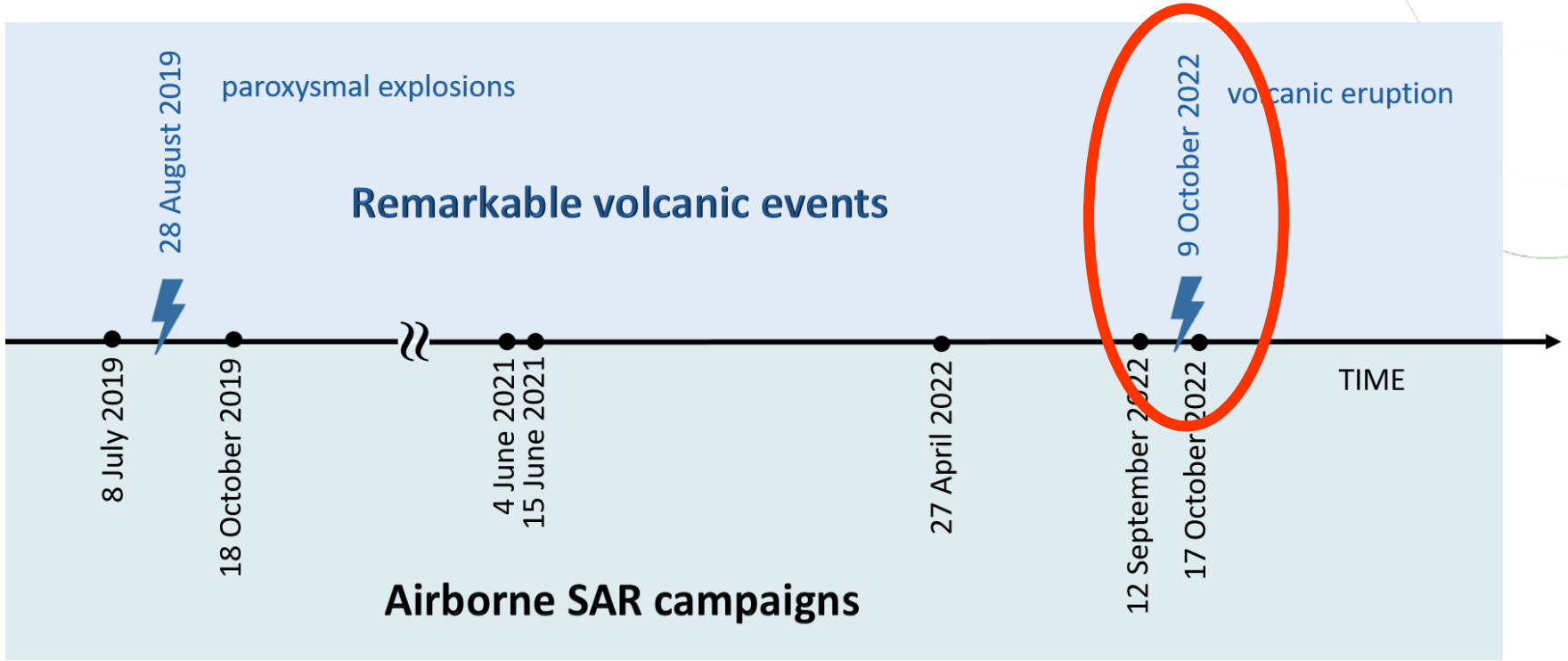

An Airborne InSAR experiment

The Stromboli case study

Abrupt loss of InSAR coherence across the event makes it impossible a co-event DInSAR analysis

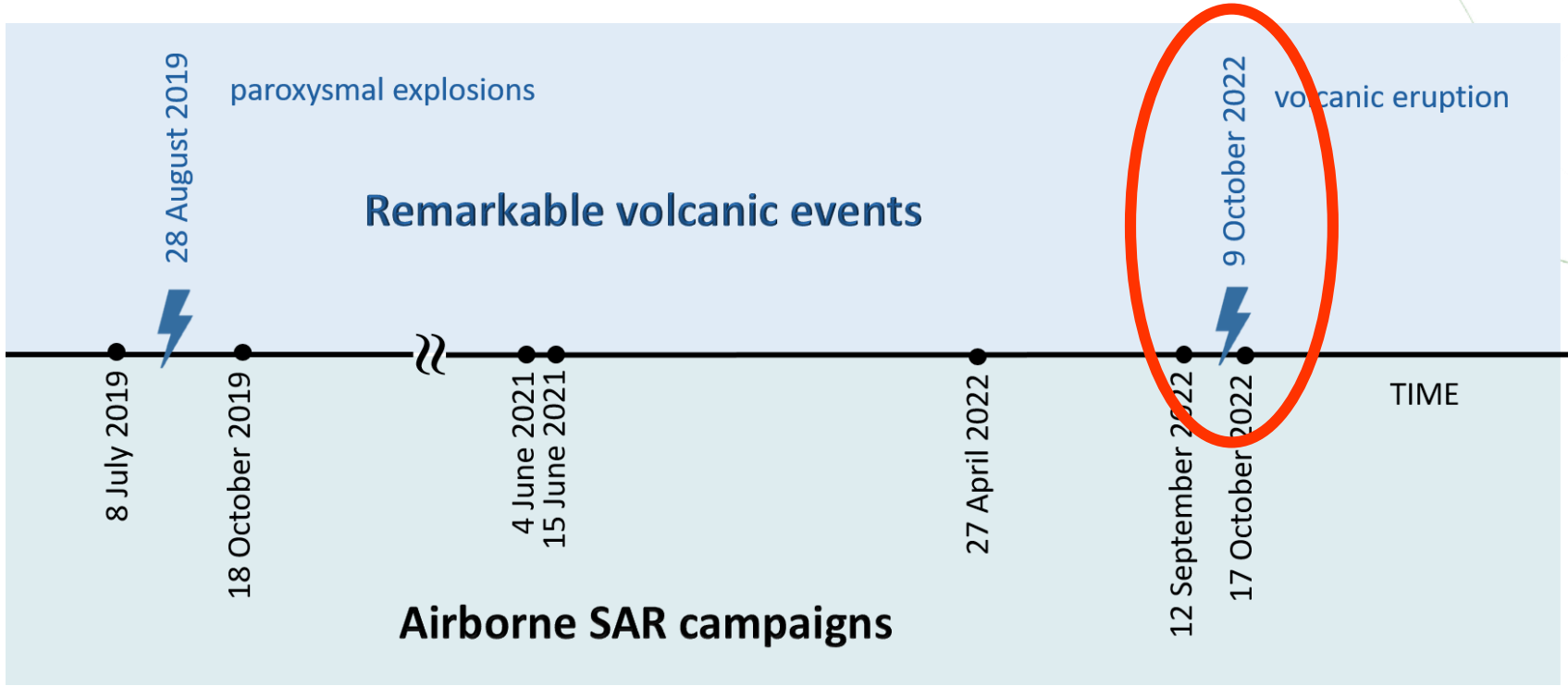

Co-event DInSAR interferogram

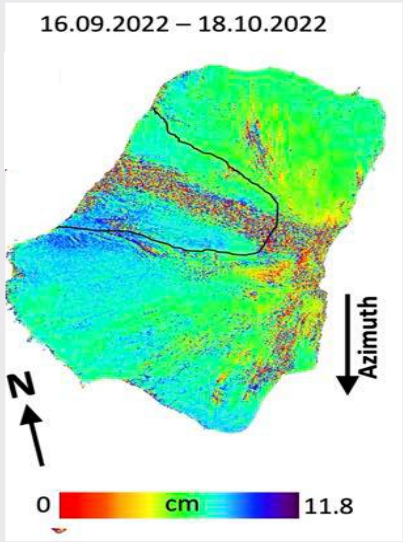

SAOCOM DATASET (L-Band)

An Airborne InSAR experiment

The Stromboli case study

Abrupt loss of InSAR coherence across the event makes it impossible a co-event DInSAR analysis

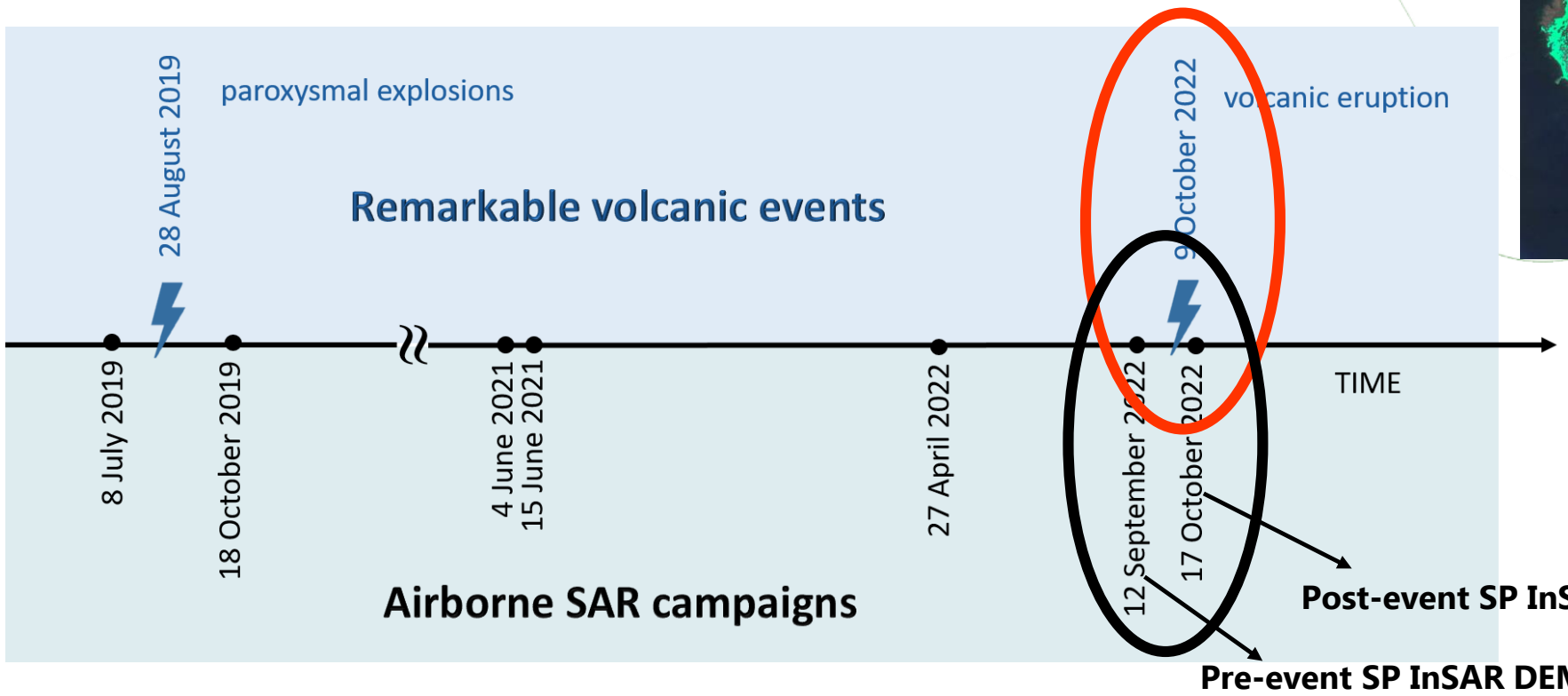

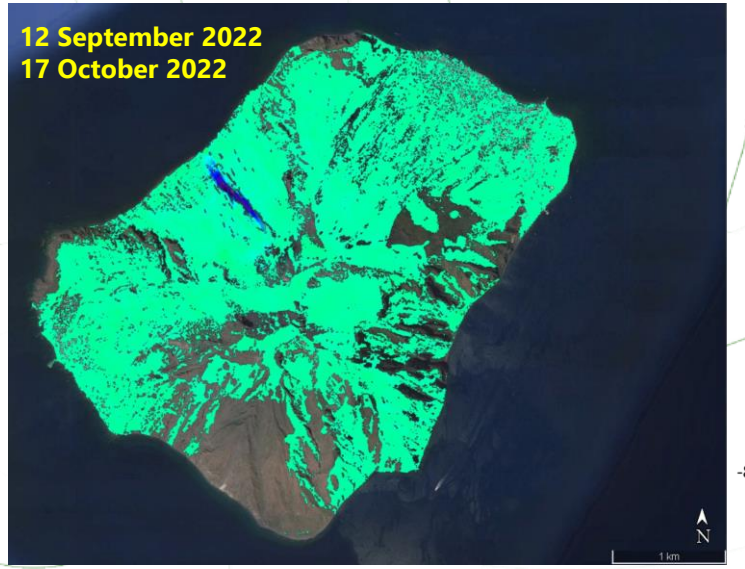

Difference of the SP InSAR DEMs

An Airborne InSAR experiment

The Stromboli case study

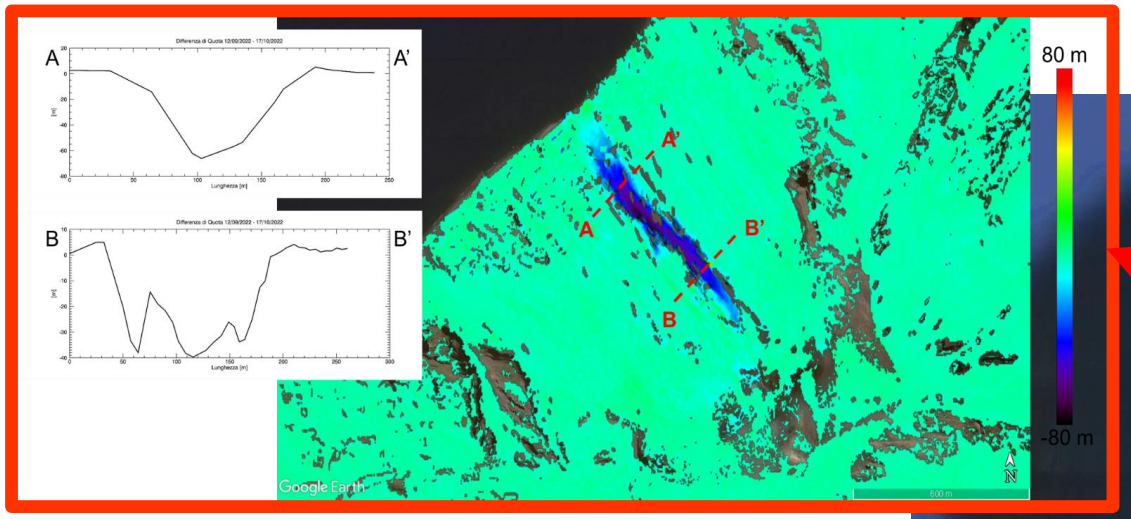

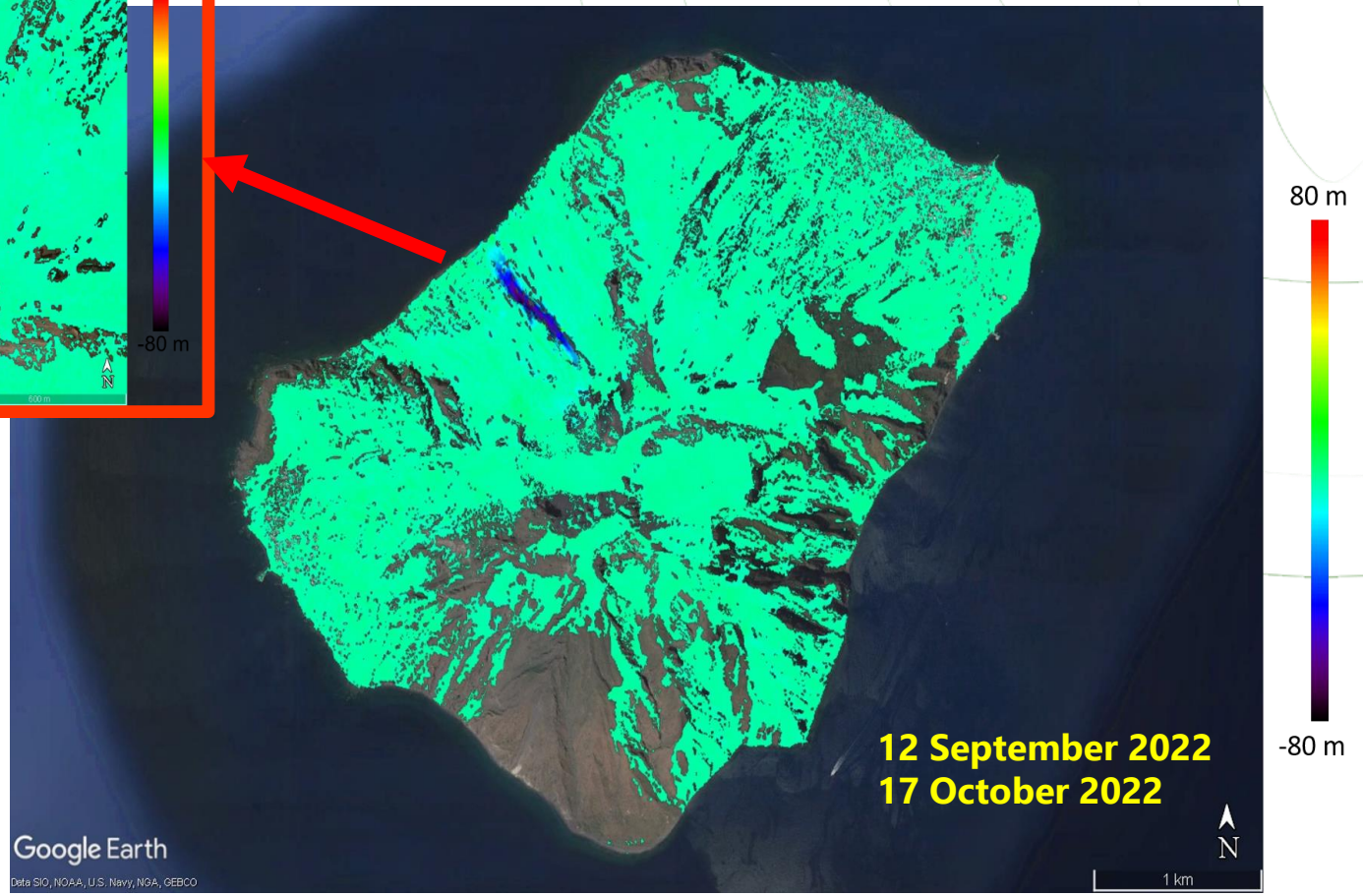

Resolution: 2 m azimuth x 1.5 m range
 # looks: 6 azimuth x 2 range

An Airborne InSAR experiment

The Stromboli case study

.. according to the Cramer Rao bound on the phase variance in:

E. Rodríguez and J. M. Martin, "Theory and design of interferometric synthetic-aperture radars," *Proc. Inst Elect. Eng.*, vol. 139, no. 2, pp. 147–159, 1992.

$$err(z) = \frac{r \sin(\vartheta)}{l_{\perp}} err(\delta r)$$

Resolution: 2 m azimuth x 1.5 m range
 # looks: 6 azimuth x 2 range

Vertical accuracy

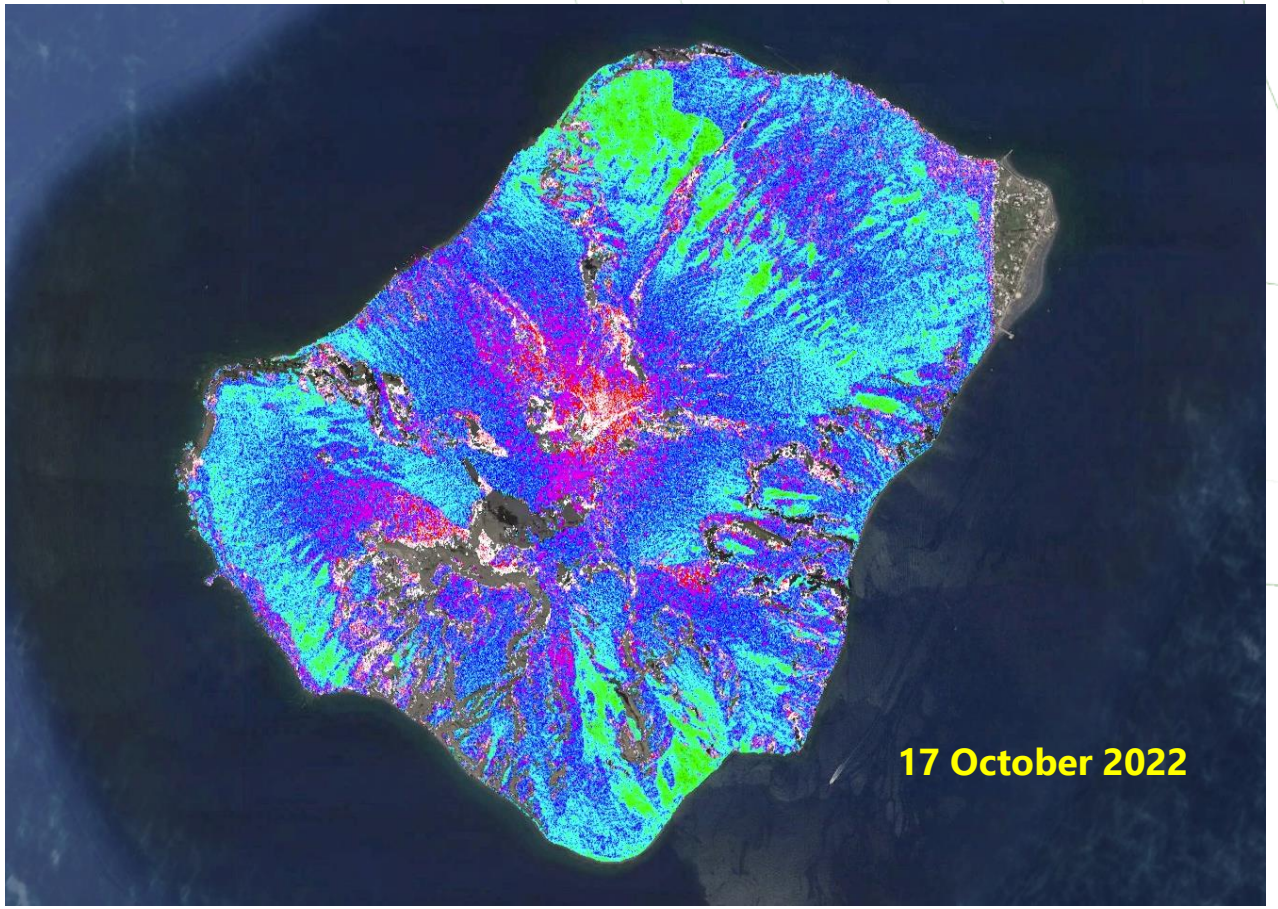

An Airborne InSAR experiment

The Stromboli case study

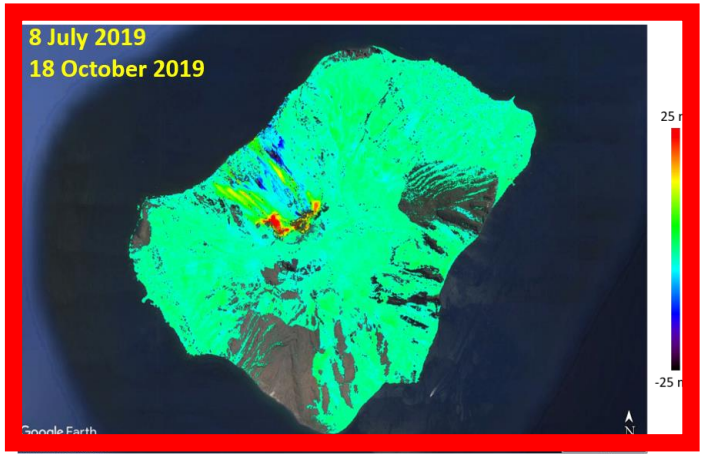

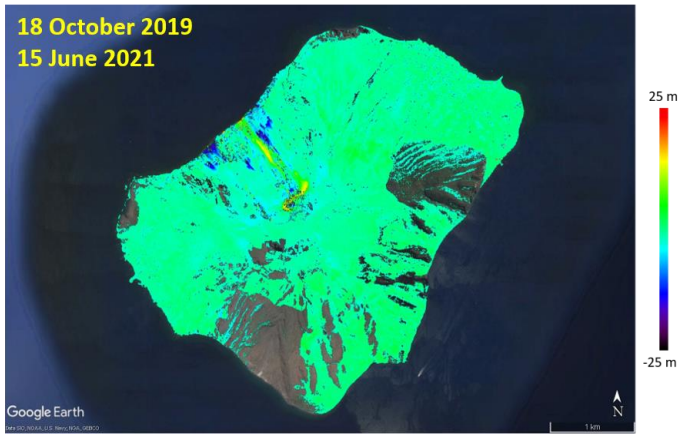

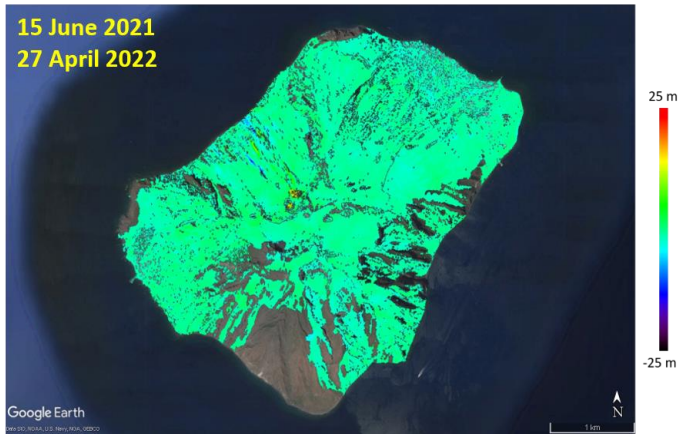

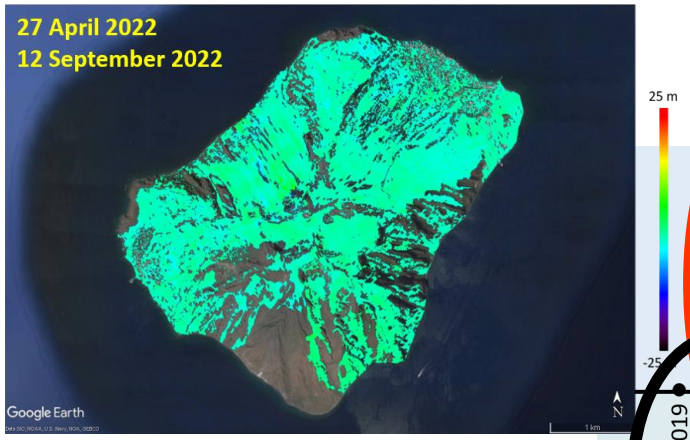

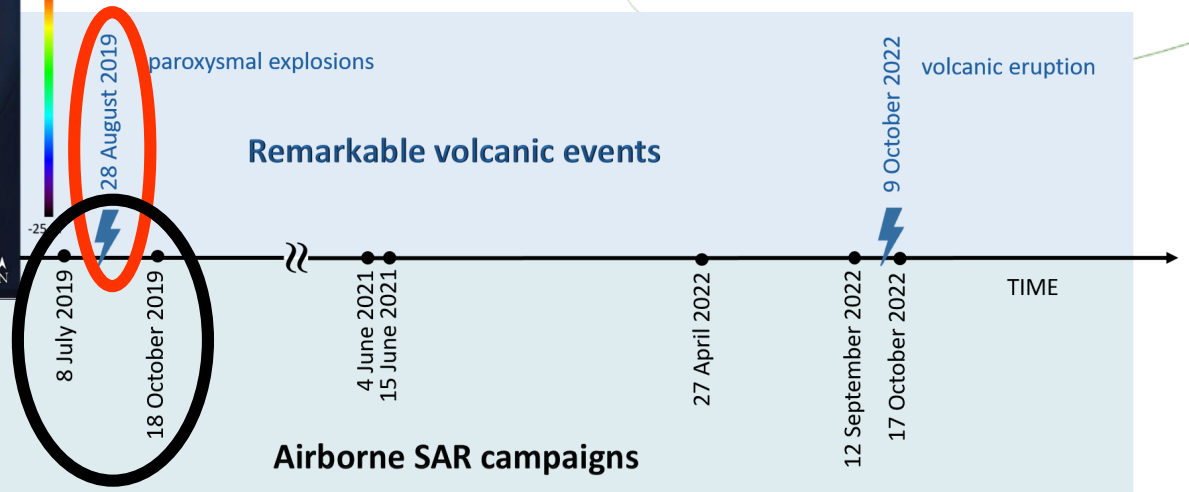

SAR Interferometry (InSAR)

Esposito, C.; Natale, A.; Lanari, R.; Berardino, P.; Perna, S. On the Capabilities of the IREA-CNR Airborne SAR Infrastructure. Remote Sens. **2024**, 16, 3704. https://doi.org/10.3390/rs16193704

THANKS!

IR0000032 – ITINERIS, Italian Integrated Environmental Research Infrastructures System
(D.D. n. 130/2022 - CUP B53C22002150006) Funded by EU - Next Generation EU PNRR-Mission 4 “Education and Research” - Component 2: “From research to business” - Investment 3.1: “Fund for the realisation of an integrated system of research and innovation infrastructures”

Finanziato dall'Unione europea NextGenerationEU
Ministero dell'Università e della Ricerca
Italiadomani